ISSN Print : 0377 - 2969
ISSN Online : 2306 - 1448
Vol. 52(2), June 2015

PROCEEDINGS

OF THE PAKISTAN ACADEMY OF SCIENCES

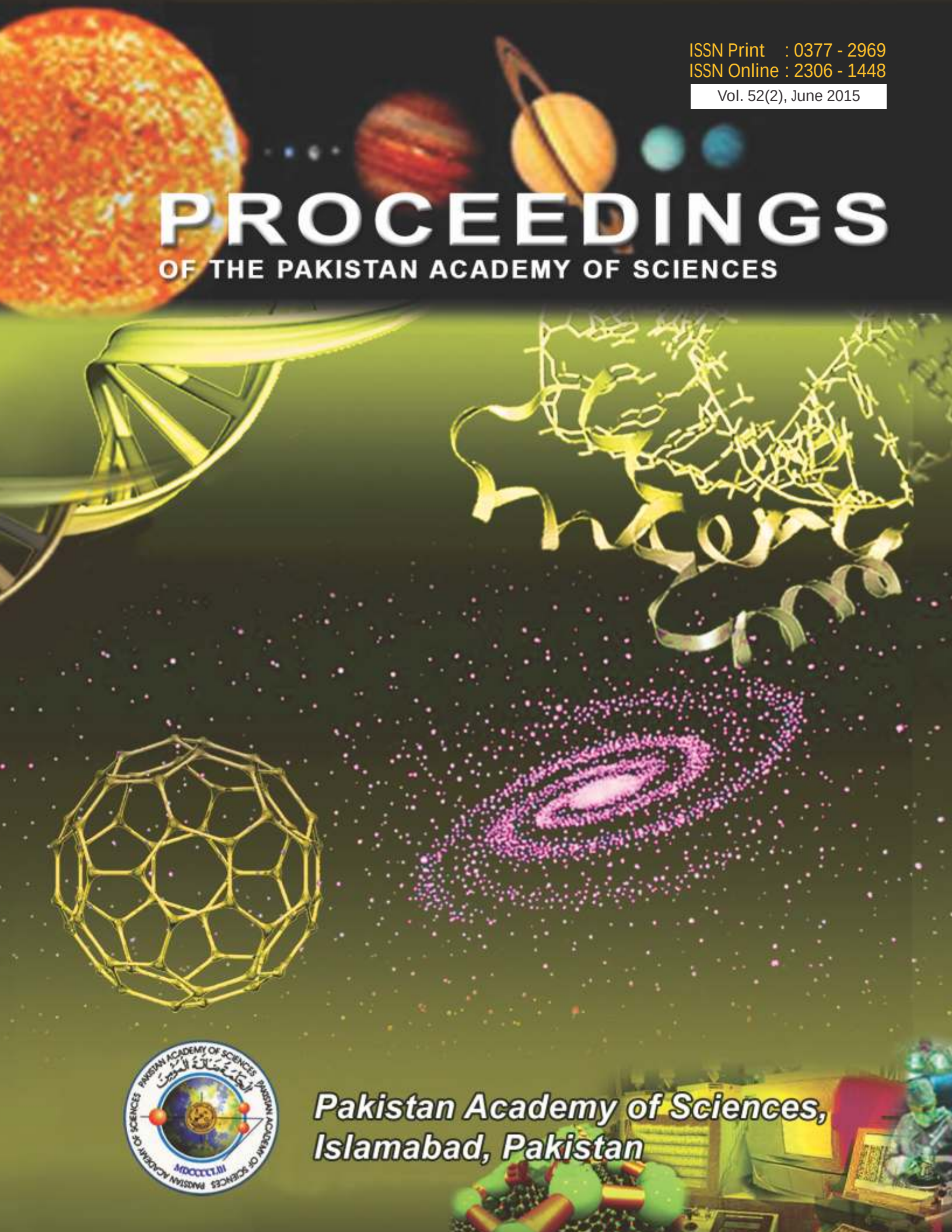

Pakistan Academy of Sciences,
Islamabad, Pakistan

PAKISTAN ACADEMY OF SCIENCES

Founded 1953

Proceedings of the Pakistan Academy of Sciences, published since 1964, is quarterly journal of the Academy. It publishes original research papers and reviews in basic and applied sciences. All papers are peer reviewed. Authors are not required to be Fellows or Members of the Academy, or citizens of Pakistan.

Annual Subscription: **Pakistan:** Institutions, Rupees 2000/- ; Individuals, Rupees 1000/-
Other Countries: US$ 100.00 (includes air-lifted overseas delivery)

HEC Recognized, Category X; PM&DC Recognized

Published by **Pakistan Academy of Sciences**, 3 Constitution Avenue, G-5/2, Islamabad, Pakistan
Tel: 92-5 1-9207140 & 9215478; **Fax:** 92-51-9206770; **Website: www.paspk.org**

Printed at **PanGraphics (Pvt) Ltd.,** No. 1, I & T Centre, G-7/l, Islamabad, Pakistan
Tel: 92-51-2202272, 2202449 Fax: 92-51-2202450 E-mail: pangraph@isb.comsats.net.pk

Proceedings
OF THE PAKISTAN ACADEMY OF SCIENCES

CONTENTS

Volume 52, No. 2, June 2015 **Page**

Submission of Manuscripts: Manuscripts may be submitted online at www.paspk.org or as E-mail attachment. Authors must consult the ***Instructions for Authors*** at the end of this issue and at the Website: www.paspk.org

Proceedings of the Pakistan Academy of Sciences 52 (2): 91–102 (2015)

ISSN: 0377 - 2969 (print), 2306 - 1448 (online)

Pakistan Academy of Sciences

Research Article

A Computational Framework for Unified Biological Databank to Overcome Heterogeneity of Biological Data Format

Muhammad Usman Ghani Khan, Sana Amanat, Abdul Nasir, Razi Iqbal, and Muhammad Idrees

Bioinformatics Lab, Al-Khwarizmi Institute of Computer Science,
Department of Computer Science and Engineering,
University of Engineering and Technology,
Lahore, Pakistan

Abstract: Building block of life is DNA which produces RNA and protein sequences; all these molecular blocks lie in the category of biological data. Biological data which comprises various organisms like animals, plants, viruses, bacteria and humans,throughout the globe has heterogeneous nature. This heterogeneity is caused by different parameters such as storage mechanism, information representation and content format. The abundance of heterogeneity creates a havoc towards optimized exploitation, integration, storage and retrieval of existing biological data. This work introduces a computational framework for achieving a unified format for biological data, which can accommodate different formats of storage; and data presentation. An information retrieval system for biological data has been developed which sheds light on different recompenses gained by this unified format of the biological data.

Keywords: Biological data, heterogeneous format, unified format, integration, parser

1. INTRODUCTION

Biological information is electronically available in the form of databanks under certain categories of organisms such as Homo sapiens, plants, virus, bacteria and animals [1]. These databanks have towering versatility of biological data formats as compared to other information [2]. These biological data are available in scrappy form under certain molecular categorization like DNA, RNA and protein sequences.

There are multiple sources of molecular databases, e.g., DNA Databank of Japan (DDBJ) [3], National Centre for Biotechnology Information (NCBI) [4], European Molecular Biology Laboratory-European Bioinformatics Institute (EMBL-EBI) and some others [4, 5]. These databanks provide heterogeneous [6] biological data under certain formats. It is observed that this heterogeneity leads to numerous hurdles towards the storage, retrieval, data mining [2], semantic search, integration [7], discovery and optimized utilization of existing biological data [8].

Upon critical inspection of different databanks, i.e., GenBank, DDBJ and EMBL-EBI, we formalize three levels of heterogeneity in relation to biological data which are storage mechanism, content format and information representation format. Storage mechanism: leads to the storage techniques used to store molecular information physically such as txt, dat, seq and web pages. Content format: expresses the methodology to store a sequence such as FASTA [9], GenBank, and EMBL. Information Representation: depicts the format in which biological information is presented to the user, e.g., as text and images. Table 1 shows three levels of heterogeneity for existing biological databanks, i.e. storage, presentation and content.

Received, April 2014; Accepted, April 2015
*Corresponding author: Muhammad Usman Ghani Khan; Email: usman.ghani@uet.edu.pk

Table 1. Three levels of biological data format heterogeneity.

Molecule type	Data bank	Storage format	Presentation	Content format
DNA	DDBJ	Dat, Seq, Fasta	Text	Fasta, GenBank
	ENA	Seq	Text	EBML
	NCBI	A, Fasta	Text	Fasta, GenBank
Human Genes	GeneCards	Web Page	Text, Image	-

So far, it seems as if there is no such versatile databank with unified format that can accommodate all levels of heterogeneity, with respect to biological data. It is important to note that it is not a complete list of available formats across the globe, but it provides the most common list of biological databanks with their format information. To cope with heterogeneity, we propose a unified format which is capable to accommodate all levels of heterogeneity.

1.1 Contributions and Goals

Development of unified biological databank with unified format has following goals and contributions:

1. To provide unified biological repository.
2. To provide unified format for heterogeneous biological data formats.
3. Integration of all molecular data at a single point.
4. Generation of a biological databank service in Pakistan.
5. 24/7 Retrieval of unified biological databank.
6. Availability of updated biological information.
7. Download services for databank.
8. Addition of molecular data discovered at wet labs for sharing with the public.
9. Provide an efficient, authorized and scalable hub for biological research purposes.

2. MATERIALS AND METHODS

This section covers the physical arrangement of databank, which is composed of various modules and processes such as data acquisition process, computational modules (download server, biological data processing engine, data server and reporting server), security mechanism of databank and interface for internal and external communication. Furthermore, the conversion from heterogeneous to unified format is also discussed in this section.

2.1 Enactment of Unified Biological Databank

Physically unified biological databank [10] is based on four core components. Fig.1 shows the abstract overview of unified biological databank.

2.1.1 Data Acquisition Process

There are various sources of biological data such as wet lab and dry lab [11]. By considering dry lab, the data are available in diverse forms i.e. web pages, images, videos and text files. In the context of text file format there are various existing databanks which provide molecular information for different organisms like *Homosapiens*, *Musmusculus*, *Rattusnorvegicus*, *Oryzasativa* and others [12]. These databanks provide information to the public for further utilization per requirements. In this work we have downloaded various data sets for numerous molecules and organisms. Some of the considered data sources for our work are given below:

1. DDBJ : ftp://ftp.ddbj.nig.ac.jp/ddbj_database/
2. ENA: ftp://ftp.ebi.ac.uk/pub/databases/embl/cds/
3. NCBI: ftp://ftp.ncbi.nlm.nih.gov/blast/db/FASTA/
4. Ensemble: ftp://ftp.ensembl.org/pub/release72/fasta/homo_sapiens/dna/
5. Vector Base: https://www.vectorbase.org/downloads
6. RNAfam: ftp://ftp.sanger.ac.uk/pub/databases/Rfam

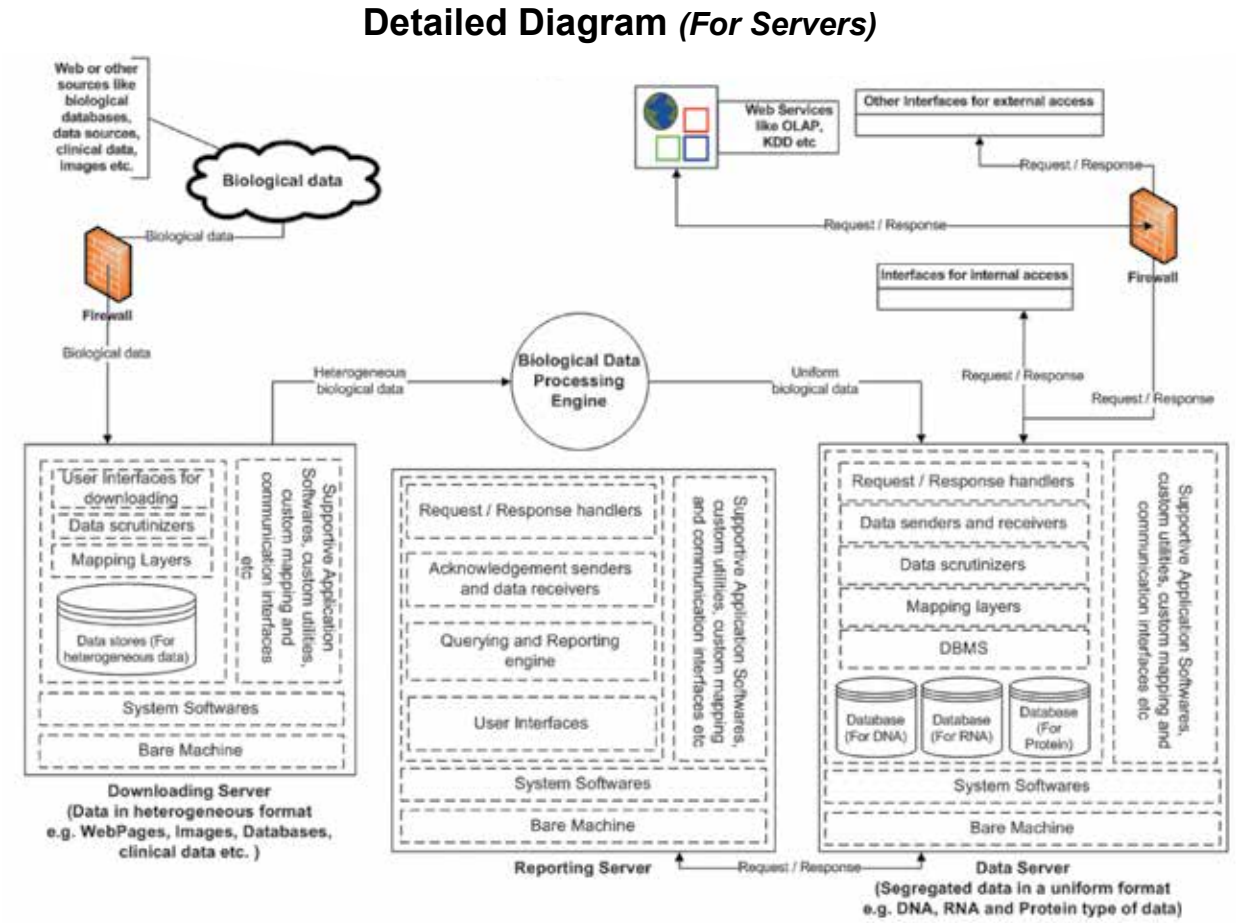

Fig. 1. Proposed framework for unified biological databank.

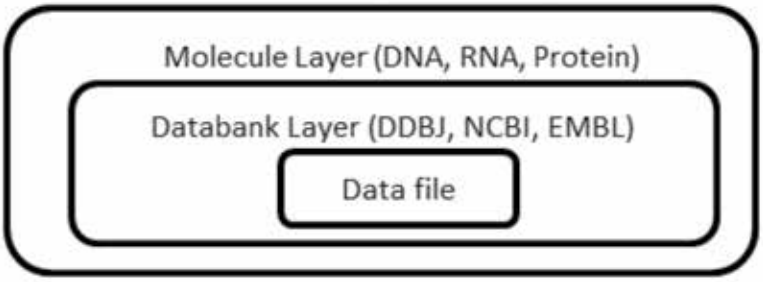

Fig. 2. Abstract view of data mapping layers.

7. miRbase: ftp://mirbase.org/pub/mirbase/CURRENT/

The above list consists of the most common but not all databanks which are publically available.

2.1.2 Download Server

The outcome of data acquisition process is the data source links through which we can download our required data on our download server. These data source links are stored into local index file and a request is send to these links one by one under file transfer protocol. On the behalf of request, a response is generated by the server [13] for the links which communicate with the download server and firewall to make the internet traffic more secure. After negotiating the protocol destination file server provides a list of all those files which exist on that link.

Firstly, download server sends a request to the data source link under file transfer protocol to start the communication. In response to the sent request, data source file acknowledges and negotiates the underlying protocol to start the transfer of data. As soon as download server receives the acknowledgement from download server, it starts receiving the list of all those files which exist on that link. This transfer continues till the end of last file. Next step of this process is to read the content of those files which exist in the list of those files received from particular data source link.

Local index file which contains the list of all those files which exists on a particular data source link is read out. The first index of local index file is the name of the file which exists at index 0 on that data source link. After getting the first index from local index file it is searched on download server that either this file already exists or not, if that file does not exist then a new file is created in the name of 0^{th} index file. Next step is to read the file content from source server and write that content into newly created file at download server. This process goes on till the end of the file.

Other than text files, biological information which is available on web pages is also gathered using the hypertext transfer protocol (HTTP) [14]. To gather the interested set of biological information, a request is sent to the particular web server under http and the response is generated by the web server which permits the download server to receive the requested data. Download server has several parsers which read the content of that particular web page.

Since there exist a lot of other information in addition to biological information, so utilities to scrutinize the data are applied for filtering, sorting [15], trimming [16] and examining the required biological information from the web pages. At the end of this process the content and data source files are stored on download server on underlying mapping layers which determines the hierarchy in which data has to be stored physically as shown in Fig. 2.

Some of the download utilities interact with the underlying system software throughout the process from request to the storage of data on particular memory location of data server. System software interacts with the bare machine to accomplish the task of storage.

2.1.3 Biological Data Processing Engine

The main purpose of this databank is to provide biotic information in unified form using some standards and rules. This engine takes heterogeneous data which is in FASTA, GenBank and EBI format from data server and on the behalf of incoming format it chooses an appropriate parser that converts it into unified format.

Rule 1: If incoming stream has FASTA format then extracted identifier, organism and sequence are to be converted into unified format.

Rule 2: If incoming stream has DDBJ format the command is to extract all tags which are in upper case for conversion into unified format.

Rule 3: If incoming stream has EBI format, it

commands to extract all tags such as ID, XX, and SQ to convert those into unified format.

2.1.3.1 Data server: The outcome of biological data processing engine is the unified data which has to be stored on data server. To start the storage on data server biological data processing sends a request to the data server using request handler. After getting the response from data server it receives the data from biological data processing engine and starts receiving the data. On this received unified data, scrutinizer algorithms are applied using utilities which examine the type of molecule, databank and organism. After examining the incoming data, mapping layer communicates with the underlying database management system which defines the rules to store the unified biological data under certain molecule categories such as DNA, RNA and protein. System software interacts with bare hardware to make possible the storage of unified biological data on data server. Rules which are applied to store the unified data are as under:

Rule 1: If incoming data has DNA molecule and organism is animal then store it into DNA repository under "wildlife" category.

Rule 2: If incoming data has DNA molecule and organism is Homo sapiens then store it into DNA repository under "human" category.

Rule 3: If incoming data has Protein molecule and organism is animal then store it into protein repository under wildlife category.

Rule 4: If incoming data has RNA molecule and organism is animal then store it into RNA repository under wildlife category

2.1.3.2 Report server: To make sure the availability of unified biological databank a user interface, i.e., web page is provided via report server. A user can give input and sends request to generate the desired report using a secured channel such as firewall to control the incoming and outgoing network traffic. The process from user input to the generation of report is as follows:

Whenever user provides the input a request handler of report server sends a request to the data server to enable the communication for data exchange. Data server sends an acknowledgement using response handler indicating a ready state for data transfer. After negotiating the communication protocols the query analyzer performs the examination on requested query.

The user's query and input parameters are provided to the query engine which executes the incoming query and communicates with the data server to fetch the required data from unified database. At this stage report server and data server simultaneously communicate with each other using message passing to execute the query and transfer of data. Data server transfers the requested data which is received on report server to generate the reports.

2.1.3.3 Options: To generate report there are many options available such as:

1. *Generate report on web page:* If the users avails this option then generated report has to be showed on the web page and user can easily approach it.
2. *Generate report which is downloadable:* In this option if the user does not want to receive the report of web page and is desirous to download this report for later use, then pdf based reports be provided to facilitate the user.
3. *Sends the generated report via email:* If user wants to receive its generated report into mail box then the user has to provide his valid email address.

2.1.3.4 Levels: There are many users of this databank and every user wants the information on report according to his level and requirements. There are some of the levels of report content such as:

(a) Biologists, pathologists: These users require more detailed report because they deal with the

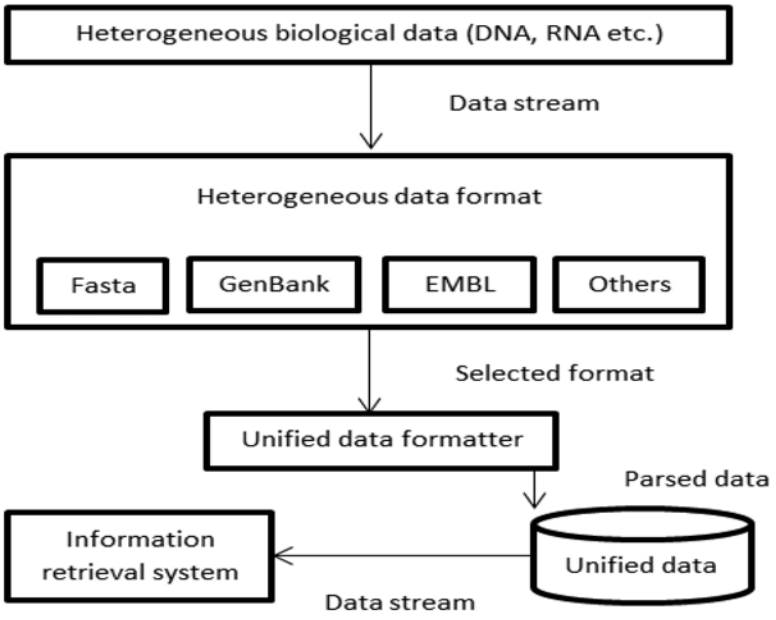

Fig. 3. Conversion steps from heterogeneous to unified format.

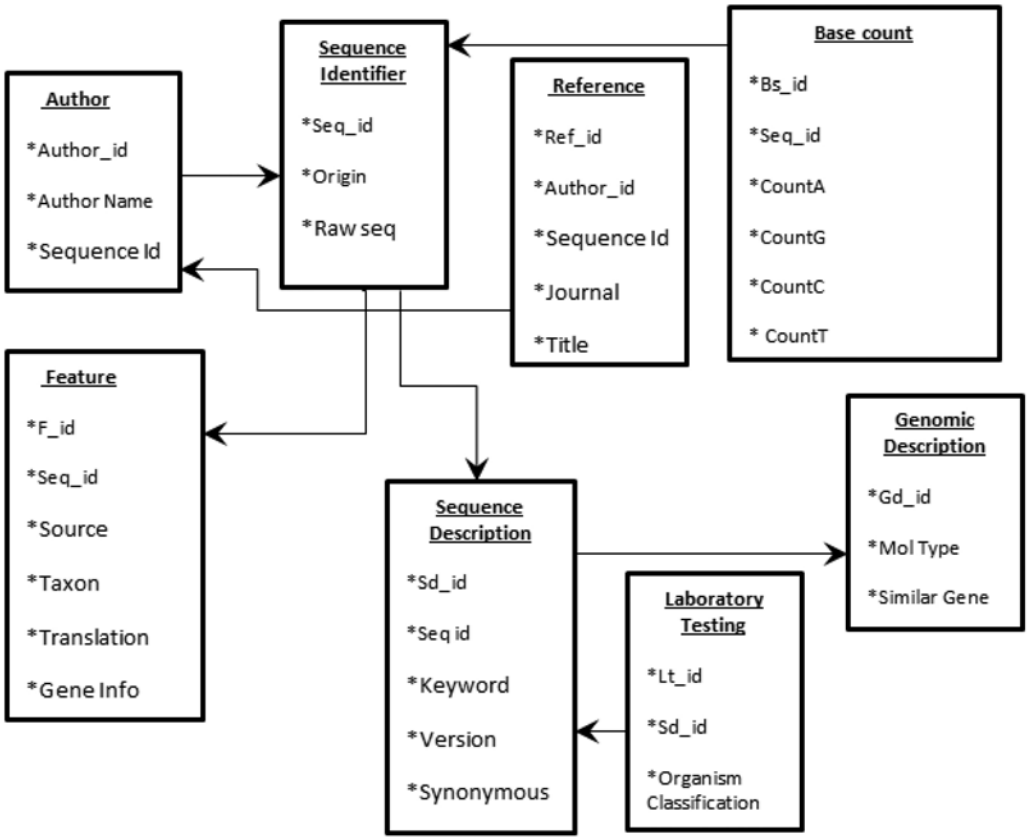

Fig. 4. Physical structure of unified format.

invention, diagnose, repairing and treatment of molecular level substance.

(b) *Researchers:* They deal with the invention and research of biological data at molecular level for all organisms. So they required report which contains the more information about taxonomy.

(c) *Layman, newbies:* They use this databank for studies, for DNA matching and for learning purpose.

2.2 Exertion of Unified Format

To convert the heterogeneous format into unified format for biological data a framework is proposed which receives heterogeneous biological data, analyze it, selects a particular parser, converts it into unified format and stores it into unified databank. Framework of unified format is shown in Fig. 3. For internal processing of unified formatter, we designed numerous parsers for each type of incoming format based on heterogeneous data stream. Upon careful inspection of input data stream of heterogonous nature, a particular parser is selected by the unified formatter that automatically converts and accommodates all the fields into unified format to overcome three levels heterogeneity. Outcome of this unified data formatter is the unified biological data without any kind of heterogeneity treated as unified data set. This data set is accessible via information and retrieval system using different searching parameters. Detail of this framework is as follows:

2.2.1 Heterogeneous Data Format

Biological data is available in heterogeneous formats such as FASTA, GenBank and EMBL. Some formats are less descriptive like FASTA and other formats provides sequence related information in details, most common features of formats are identifier, organism and raw sequence.

2.2.2 Unified Data Formatter

Working of data formatter is as follows:

Downloading of Heterogeneous biological data: According to Table 2 all downloading links of various databanks are maintained in a file and files are downloaded on our down server using the following algorithm.

2.2.2.1 Download files: Get file list form the link by sending request to the ftp server.

Step1- > IF: File does not exist or time; start download.
Else: Goto Step2

Step2-> IF: Time or date of file that exist in our system is less than time on the ftp server. Delete the file and start download again.
Else: Goto Step3

Step3- > IF: Size of the file that exists on our system, is less then size on the ftp server. Delete the file and start download again.
Else: Goto next iteration of loop (Goto next file.)
It is important to store the files in some layered fashion physically. We maintained this approach using the following algorithm.

2.2.2.2 Hierarchy maintenance: Read all the databanks from the file databank.txt

Table 2. Various attributes of existing heterogeneous format.

Format	Fields
FASTA	Definition line, sequence
GenBank	Accession, Version, Reference, Author, Origin, Reference, Keywords, Source, Title, Journal,Remark,CommentFeatures,Basecount,Consortium
EMBL	Accession, Project, Date, Keyword, Organism classification, Organelle, Reference Number, Reference Position, Reference Comment, reference cross-reference, Reference Group, Reference Author, Reference Title, Reference Location, Third Party Annotation, Feature Header, Feature Table

Step1-> IF: Folder of the databank in the databank. txt, present. Go to Step2.
Else: Create the Folder and its txt file for databanks and Go to Step2.Checking for all databanks in the .txt file of the particular databank using threads. For each Data bank of databank in threads= number of banks of a particular databank.

Step2-> IF: Data bank folder exist then
Go to Step3
Else: Create Folder and Go to step 3.

Step3- > Read links from the .txt file of the databanks and then start to download files.

Upon careful inspection of these downloaded data files it can be argued that these files contains most common formats such as FATSA, EBML and GenBank format and has these following fields which are shown in Table 2.

2.2.3 Unified Format

Unified format holds all the fields of heterogeneous formats as mentioned in Table 2 and some of the additional fields. Unified format contains all the fields of FASTA, GenBank and EMBL format. Detail of all fields of unified format with physical structure is as shown in Fig. 4.

All these tables are linked via a sequence identifier which plays a role as primary field and all other fields are considered to be the secondary fields because they provide data related to the primary field. This schema contains various tables such as author table which contains information of author and sequence identifier. Sequence table stores the information about sequence only such as raw sequence which is a combination of nitrogen bases, its original unique identifier and the identifier which we used to store this sequence in our database.

Other tables contains the information of base pairs of raw sequence, definition, organism name, molecule type and the information of publication with respect to author, journal title, sequence. Furthermore the additional information in form of annotation is also stored in feature table and header table format. Detail of some of the extra fields in unified format is as below:

2.2.4 Secondary Identifier

This is the unique identifier which is assigned to every record which has to be entered into our databank. Format of this field is as: name of original data bank, name of organism, actual unique identifier. Actual identifier could be strain, accession number, genome identifier or any unique property that can distinguish every record, i.e.:

"Name of reference databank + name of organ/ organism+ uniquely identified feature e.g. DDBJ_ HomosapienDNA_AB1001"

CountA: Contains total count of adenine base in a sequence.

CountG: Contains total count of guanine base in a sequence.

CountC: Contains total count of cytosine base in a sequence.

CountT: Contains total count of thymine base in a sequence.

2.2.5 Parser Rule

There are certain rules which are followed while converting heterogeneous format into unified format.

Rule 1: Tag matching for GenBank format: If data stream has any tag locus, accession, version, keyword then split the stream and store the chunk of stream from current Index+1 to the length of stream. If data stream does not have any tag then concatenates it with the previous stream.

Rule 2: Tag matching for FASTA format; If data stream starts with > symbol then split the stream by special letters and store each splitting region from current Index to the length of stream by the increment of 1.

Rule 3: Tag matching for EMBL format. If data stream has any tag ID, OS, FT, PA, SQ then split the stream and store the chunk of stream from current Index+1 to the

length of stream: If data stream does not have any tag then concatenates it with the previous stream.

2.2.6 Unified Dataset

Outcome of the parsing is the unified biological data which is stored in a repository under molecule category such as DNA, RNA and protein sequence. This unified dataset is actually known as unified biological databank.

2.2.7 Information Retrieval Tools

Unified biological databank is made accessible via information retrieval engine. Where users can input any query such as accession number, raw sequence, author name, organism, specie and other parameters. Against these parameters information retrieval engine searched the repository and show the results to the user.

2.2.8. Demo

We have developed a prototype of unified biological databank, which will be deployed at the link http://kics.edu.pk/edanbioinformatics/home.html. Currently, the web page indicates the objectives and main milestones of the project, while the link and accessibility to the utilization of software/databases will be provided to public at the completion of the project**.** This application initially downloads existing heterogeneous biological data at download server and converts it into unified format using biological processing. Unified biological data is stored on our data server, from which user can download unified data and generate reports. Initially searching criteria from unified biological repository is accession number, which can be enhanced in the upcoming versions.

In order to use this application, the user has to enter the accession number of a sequence as input to our system. In addition to input, the user has to select the target database from which the search will be carried out. After providing input the result will be shown on the screen consisting of accession, organism and sequence as shown in Fig. 5.

3. RESULTS AND DISCUSSION

There are multiple formats of biological data and it is analyzed that FASTA, GenBank and EMBL formats are fiasco to accommodate all types of molecule information by compensating all levels of heterogeneity. It is clear that unified format is more versatile which has enough capability to accommodate variety of formats without losing any useful information. It accommodates all fields of heterogeneous formats, all formats of files such as seq, fa, fasta, xls, txt and others using parsing rules. So we can argue that unified format tackles all issues of heterogeneity.

3.1 Evaluation

To validate this unified format, we store various datasets of FASTA, GenBank and EMBL format in unified format by using numerous parsers. This unified repository is accessible via information retrieval system. Information retrieval system takes input which is passed to the information retrieval engine to perform analysis. Searching criteria is extracted from the input query for processing and the required data is fetched based on provided searching criteria.

The output of query processor displays on graphical user interface in a unified manner.

3.2 Demonstration

Initially, we used a single parameter; accession number as searching criteria keeping in mind the fact that every record has an accession number. On the behalf of provided input retrieval system provides the name of author, sequence ID and author ID. This result is purely based on user end, which fields or information they want in return. We will extend the searching criteria in next versions. Fig. 5 shows the sample of output based on unified format.

To evaluate the performance of this tool, a task based evaluation strategy was planned, where an end user is asked to search and retrieve some specific record according to his requirement.

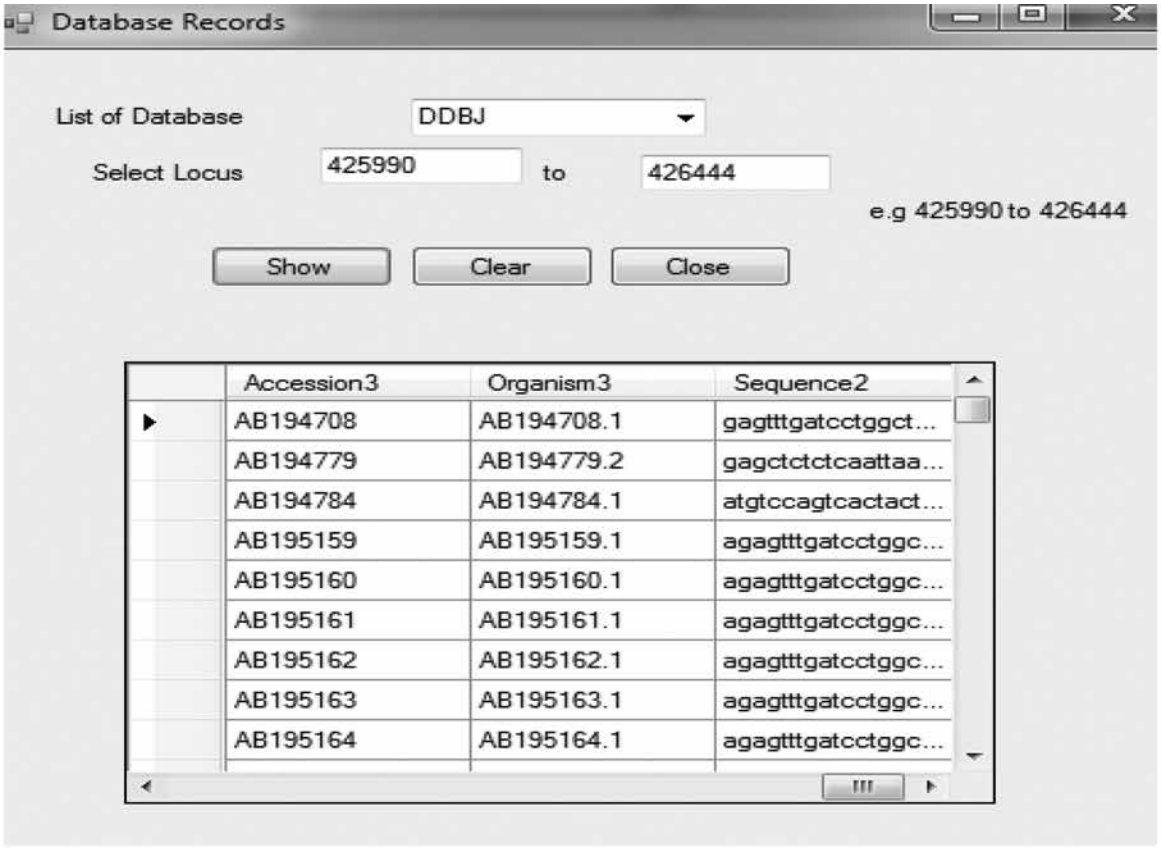

Fig. 5. Sample screen of the developed software.

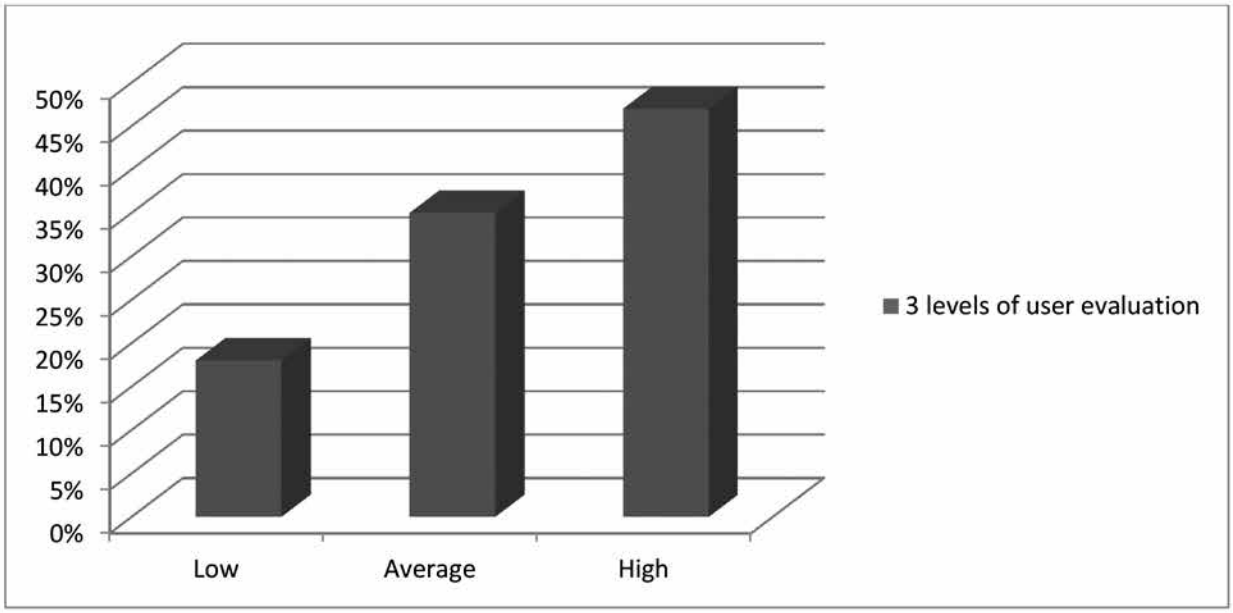

Fig. 6. Evaluation of information retrieval system based on various queries provided by the user.

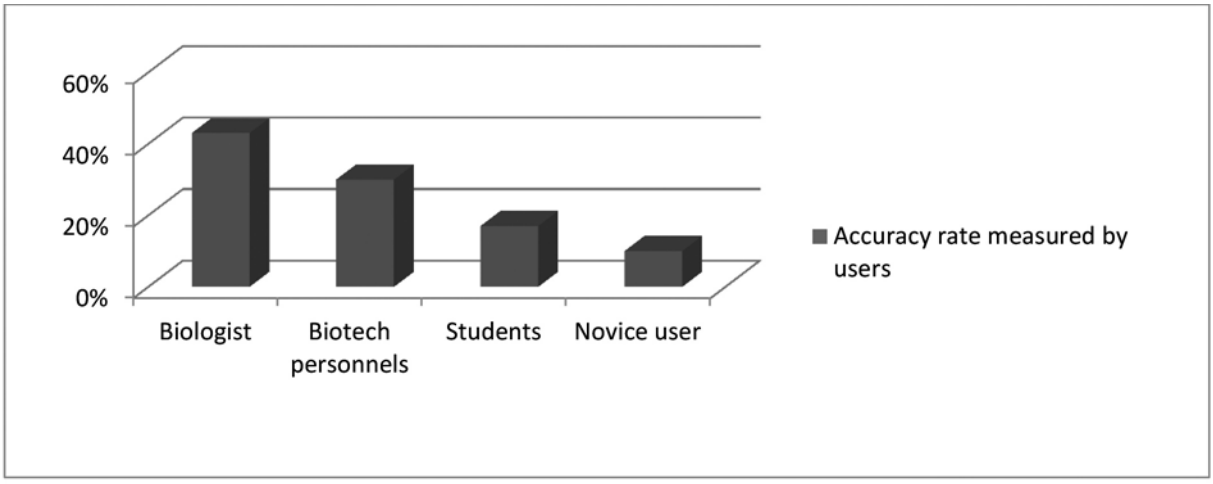

Fig. 7. Role-based evaluation.

3.2.1 Task Based Evaluation

A group of testers used this tool according to their role some and evaluate the performance of this tool as showed in Fig 6.

3.2.2 Relevance of Searching Criteria

This evaluation was performed to find the relevance of retrieved information. Users were given a questionnaire with the following three questions.

i. Retrieved information is highly relevant.
ii. Retrieved information is relevant.
iii. Retrieved information is not relevant.

In this type of evaluation the searching result was tested. There are certain levels of relevance such as highly similar, average and low showed the degree of searching result as per desire and searching criteria. Fig.7 shows the overall degree of relevance of search result.

To tackle certain issues of heterogeneity, we proposed a unified format, which holds all the fields of heterogeneous format, which is enough adept to accommodate data of all file formats.

There are many heterogeneous biological databanks and sequence alignment tools such as NCBI, DDBJ and BLAST, respectively. The major drawback in these databanks is that these are providing heterogonous biological data which is a major issue in integration and semantic search. These databanks are confined to specific organism sequences only [6, 13]. Furthermore, BLAST analysis has become a ubiquitous method of interrogating new sequence data, but these are the major limitation to using BLAST alone as a discriminating tool and its output is often skewed [16].

This project will basically deal with the establishment of a biological databank for the purpose of serving the community because in Pakistan such type of databank does not exist as yet. The need of this project urged due to some of the factors, i.e., economic stability, employment opportunity for undergrads and graduates, distance learning, agricultural and forensic science development. Setting up a new laboratory with equipment and trained staff for research purpose is highly costly job, by using this databank scientist can take access biological data efficiently and effectively. Newbies in bioinformatics and biotechnology can use this databank for study and research work. Even some pharmaceutical companies can sue it for drug discovery and their experimental work. This project can also help in detection of dengue, polio and other viruses which directly attacks human DNA structure [17– 20].

4. CONCLUSIONS

Globally, biological information is available in

segregated form with heterogeneous flavor and in Pakistan a unified biological databank is not available. Heterogeneity nature of biological data is a main hindrance towards the semantic searching and integration of various biological data sets. To address these issues, a unified format might be proposed which holds all the fields of heterogeneous format, which is enough adept to accommodate data of all file formats. As an implementation we provide unified biological databank which is composed of four processing machine e.g. download server, data server, reports server and biological data processing engine. Firstly, heterogeneous data is acquired and stored on data server, which is further provided to the engine to convert it into unified form. This unified data is stored on data server which communicates with the reports server to generate reports on the behalf of user's input. To make available this unified biological databank an interface is provided which receives the input from user and displays the result.

5. REFERENCES

1. Coral, D.V., H.G. Karl & S. Sandor. cDNA2Genome: A tool for mapping and annotation cDNAs. *BMC Bioinformatics* 4(1): 1471-2105 (2003).
2. Min-Huang, H., Y.S. Chang, M.C. Cheng, L. Kuang-Li & S.M. Yuan. *A Unified, Adjustable, and Extractable Biological Data Mining-Broker* (Springer) 2690(1): 773-777 (2003).
3. Kosuge, T., M. Jun, K. Yuichi, F. Takatomo, K. Eli, O. Osama, K. Okubo, T. Takagi & N. Yasukaza. DDBJ progress report: a new submission system for leading to a correct annotation. *Nucleic Acids Research* 42(D1): 44-49 (2014).
4. Wollbrett, J., P. Larmande, F.D. Lamotte & M. Ruiz. Clever generation of rich SPARQL queries from annotated relational schema: application to Semantic Web Service creation for biological databases. *BMC Bioinformatics* 14(1): 14-126 (2013).
5. Amir, E.D., K.L. Davis, M.D. Tadmore, F.S. Erin, H.L. Jacob, C.B. Sean, K.S. Daniel, K. Smita, P.N. Garry & P. Dana. viSNE enables visualization of high dimensional single-cell data and reveals phenotypic heterogeneity of leukemia. *Nature Biotechnology* 31(6): 545-554 (2013).
6. Cao, S.L., L.H. Qin, W.Z. Zhong, Y.Y. Zhu & Y.X. Li. Semantic Search among Heterogeneous Biological Databases Based on Gene Ontology. *Acta Biochimica et Biophysica Sinica* 36(5): 365–370 (2004).
7. Alison, C., T.J. Cruz & M. Dumontier. Ontology-based querying with Bio2RDF's linked open data. *Journal of Biomedical Semantics* 4 (Suppl 1): 115-127 (2013).
8. David, S.W. J. Timothy, A.C. Guuo, M. Wilson, C. Knox, Y. Liu, D. Yanninck, R. Mandal, F. Aziat, E. Dong, S. Bouatara, S. Igor, A. David, J. Xia, P. Liu, F. Yallou, B. Trent, P.P. Rolando, R. Eisner, F. Allen, V. Neveu, G. Russ & S. Augustin. HMDB 3.0 — the human metabolome database in 2013. *Nucleic Acids Research* 1065: 801-807 (2013).
9. Rose, P.W., B. Bojan, C. Bi, W.F. Bluhm, D. Dimitris, S.G. David, A. Prlic, Q. Martha, G.B. Quinn, D.W. John, Y. Jasmene, Y. Benjamin, Z. Christine, M.B. Helen & E.B. Philip. The RCSB protein data bank: Redesigned web site and web services. *Nucleic Acids Research* 39 (Suppl 1): 392-401 (2011).
10. David, B.K. DNA Microarrays in the undergraduate microbiology lab: Experimentation and handling large datasets in as few as six weeks. *Journal of Microbiology & Biology Education* 8.1:3-12 (2007).
11. Dennis, A., I. Benson, M. Karsch, J. David, J.O. Lipman & L.W. David. GenBank. *Nucleic Acids Research* 41.D1: 36–48 (2013).
12. Walker, G.K. & K. Gordon. Responding to hypertext transfer protocol (http) requests. *U.S. Patent Application* 13/838,744.
13. Block, M., M. Strenge, C. Mohr, G. Boris & F. Franz. Integrated Application Server and Data Server Processes with Matching Data Formats. *U.S. Patent Application:* 13/919,921.
14. Chen, B.P. A quick sorting algorithm adaptive to massive data with high repetition rate. *Advanced Materials Research* 834: 1002-1005 (2014).
15. Shrestha, R.K., B. Lubinsky, V.B. Bansode, M.B. Moinz, G.P. McCormack & S.A. Travers, QTrim: A novel tool for the quality trimming of sequence reads generated using the Roche/454 sequencing platform. *BMC Bioinformatics* 15(1): 1-6 (2014).
16. David, A., S.A. Garry & R. Jacques. Visualization of comparative genomic analyses by BLAST score ratio. *BMC Bioinformatics* 6(2): 1-7 (2005).
17. Shah, A. & S. Ahsan. Problems and issues in managing biological data. In: *International Symposium on Bio-Inspired Computing 2005 (BIC 05)*, Johor, Malaysia. Sept 6-10, 2005 (2005).
18. Idrees, M. & M. Khan. SMGCD: Metrics for biological sequence data. *Nucleus* 51(1): 125-131(2014).
19. Idrees, M., M. Khan & A. Shah. Unified Data Model for Biological Data. *Mehran University Research Journal of Engineering & Technology* 3(3): 261-277 (2014).
20. Ghani, M.U., P.I. Khan, K.H. Asif, A. Nasir, M.J. Arshad & S. Amanat. An Agent-based CBIR system for medical images. *Journal of Faculty of Engineering & Technology* 21(2): 39-45 (2014).

Proceedings of the Pakistan Academy of Sciences 52 (2): 103–107 (2015)

ISSN: 0377 - 2969 (print), 2306 - 1448 (online)

Pakistan Academy of Sciences

Research Article

Convective Drying of Chilies Using a Concentrating Solar Collector

M. Hanif[1*], M. K. Khattak[1], M. Rahman[1], M. Aamir[1], M. Ramzan, M. Amin, M. Khan[2], and S. Shiekh[1]

[1]Department of Agricultural Mechanization, Faculty of Crop Production Sciences, University of Agriculture, Peshawar, Pakistan
[2]Nuclear Institute for Food and Agriculture (NIFA), Peshawar, Pakistan

Abstract: A concentrating solar collector was developed for convective drying of green chilies by providing optimum drying environment. A temperature in the range of 45-65°C and relative humidity of less than 10% was observed during the drying period provided by the solar collector from 9.00 am to 5.00 pm. Different levels of drying temperature and air mass flow rates were tested to find their effect on drying time of the chilies. The experiment was laid out as a randomized complete block design with a factorial arrangement of the treatments consisting of 3 levels of temperature and 3 levels of air mass flow rate, replicated 3 times. Drying temperature and air mass flow rates effected the drying time significantly. The means comparison showed that minimum drying time of 17.96 h was recorded at high temperature of 65°C followed by a drying time of 20.27 and 21.43 h at temperatures of 55 and 45°C. The means of air mass flow rates showed that minimum drying time of 18.49 h was noted at high air mass flow rate of 3.50 kg min^{-1} followed by 20.32 and 20.86 h at air mass flow rates of 1.5 and 2.30 kg min^{-1}. Chilies dried at temperature of 65°C and air mass flow rate of 3.5 kg min^{-1} showed an average drying rate of 0.02 $g_{(H_2O)}$ hr^{-1} cm^{-2} as compared to the slow drying rates at 55 and 45°C. It was concluded that chilies must be dried at high temperature and high air mass flow rates to get on time quality dried chilies.

Keywords: Concentrating solar collector, green chilies, drying rate

1. INTRODUCTION

Solar drying of condiments is most famous and ancient technique for preserving food. This technique is very economical as we save energy and preserve food as well. Most of the condiments were dried with the help of the sun drying method. If chilies were dried in open sun, then there would be chances of microbial infestation and the products would be spoiled quickly. For this purpose development of solar drier which provides controlled drying conditions in a scientific way is the best option [1-2].

Chili (*Capsicum sp.)* is the main ingredients for making condiments as it adds flavor and spiciness in our food. Chilies in the form of dried powder can compliment any dish with better taste. They can enhance our gastronomic experience with a mild heat. The chili powder gives your recipe a distinctive flavor and a unique culinary flair [3]. During drying, chilies must be dried at a temperature of 50 to 60°C and air mass flow rates of more than 3.0 kg min^{-1}. It is due to a reason that drying rate is directly proportional to the air temperature and air mass flow rates. Thus the increase in both temperature and the air mass flow rate will accelerate the drying mechanism. Drying time is minimized when a drying rate is accelerated. So drying must be accomplished at high temperatures and air mass flow rates. The upper limit for drying chilies is 60 °C and air mass flow rate of 3.5 kg min^{-1} [4].

Received, December 2014; Accepted, February 2015
*Corresponding author: M. Hanif; Email: hanif_mechanization@aup.edu.pk

The present research study was on solar drying of green chilies using a concentrating solar collector to get good quality dried chilies. After drying, the chiles were ground to make powder. Different parameters studied were drying conditions of drying chamber, moisture lost in each hour by chilies on wet and dry basis. The objective of the study was to find the effect of different levels of drying temperatures and air mass flow rates on the drying time and drying rate of chilies.

2. MATERIALS AND METHODS

2.1. Site Selection

The collector was tilted on the rooftop of the Department of Agricultural Mechanization, The university of Agriculture Peshawar, Pakistan located between the longitudes 71.0.15^{o} and 72.0.45^{o} East and Latitudes 33. 0. 45^{o} and 34. 0. 01^{o}.

2.2 Description of the Concentrating Solar Collector Assembly

The concentrating solar collector assembly consists of two parts (Fig. 1).

2.2.1 The Concentrating Solar Collector

The dish solar collector was composed of a concentrating reflector. The reflector was basically a mirror which concentrates the solar radiation on the Absorber. The absorber consists of two black painted steel pipes having a diameter of 0.05 m. Both the pipes are covered by a glass to minimize heat loss. The pipes receive air from outside environment which was heated here and then this hot air was delivered to the drying chamber.

2.2.2 Drying Chamber

The drying chamber was made of steel, fully insulated from inside with the help of polystyrene foam. The chamber was 1.0 m high and 0.55 m wide and 0.57 m long. The chamber was divided internally into two compartments in which upper compartment was provided for drying while the lower compartment was filled with rocks for solar energy storage. This stored energy in the rocks was used when there was no sunlight available or after sunset. There are three exhaust fans each having a diameter of 0.054 meters is fixed to each outlet which sucked hot air from the absorber inside the drying chamber. The flow rate of each fan was 3.56 kg.min^{-1}. These fans run on a solar panel during day time. The total volume of the drying chamber was 0.3135 m^{3}. The total air flow of three fans is 10.5 kg.min^{-1}. There was an outlet fixed at the top of the

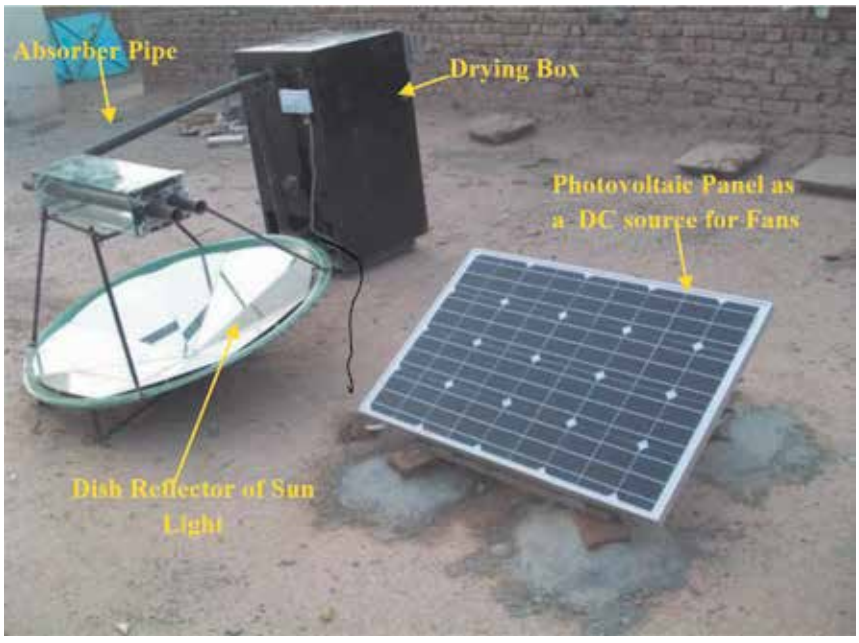

Fig. 1 The concentrating solar collector assembly showing different parts of the collector.

drying chamber having a diameter of 0.02 m for emission of humid air.

2.3 Relative Humidity and Temperature of air pumping through the collector

Relative humidity and temperature data were recorded with the help of digital thermo-hygrometer after each hour during drying of chilies.

Moisture content of green chilies was determined after each hour of drying. The products were dried down to 5% moisture content to minimize mold, insects and bacterial attacks. The initial moisture content was determined by the oven method while the moisture loss after each hour in drying on wet basis was determined by using equation 1 [5].

$$\text{M.C.} = \frac{\text{Wi} - \text{Wf}}{Wi} \; x \; 100 \quad \ldots\ldots\ldots\ldots\ldots\ldots \quad (1)$$

Where M.C. is moisture content (%), W_i is the intial weight of each sample before drying (g) and W_f is the finalweight of sample after each hour of drying (g).

2.4 Determining Drying Rate

Similarly moisture loss on dry basis was calculated using equation 2 [6].

$$\text{Dr} = \frac{M.L}{t\,XA} \quad \ldots\ldots\ldots\ldots\ldots\ldots \quad (2)$$

Where Dr is the drying rate of samples ($g_{(H2O).}$ $hr^{-1}.cm^{-2}$), M.L is the moisture lost per hour of drying (g), t is drying time (hr) and A is area of the product (cm^{-2}).

Chilies were considered dried when their moisture content reached to less than 10%. Drying time was noted as soon as the chilies were placed on the trays in the dryer till the required level of moisture was achieved.

2.5 Experimental Procedure

Only good quality and disease free chilies were used in this experiment. About 4.0 kg of fresh chilies were dried, without any chemical pre-treatment, until the required final moisture content was attained. The fresh chiles were loaded over the trays of the dryer. The initial moisture content was calculated by the oven method by taking three different samples. Then the fan switched on and the air flow rate through the collector was adjusted to 1.5 kg min^{-1}. The velocity of air at the inlet of the tray was measured with the help of Digital anemometer. Solar intensity was measured using pyranometer. Temperatures at the inlet and outlet of the solar collector and drying chamber were measured at one hour intervals. During idle conditions, the chiles were covered with polyethylene sheet to avoid re-absorption of moisture. All the experimental observations were made after the drier attained the required drying condition. The experiments were repeated thrice and an average value was considered. The drying characteristics of chilies such as moisture content, drying rate, and drier thermal efficiency were determined [4, 8].

2.6 Experimental Design and Treatment Applications

The experiment was laid out as a randomized complete block design. Both the Temperature and air mass flow rates were consisting of 3 levels. The data were replicated three times, resulting in a total of 27 treatments. Factors and their treatment levels are given as below

Temperature

T1 = 45°C

T2 = 55°C

T3 = 65°C

Air mass Flow Rates

F1 = 1.50 kg min^{-1}

F2 = 2.30 kg min^{-1}

F3=3.50 kg min^{-1}

3. RESULTS AND DISCUSSIONS

3.1 Drying Conditions for Chilies

Chilies were dried at a temperature of 50°C and humidity of less than 10%. Chilies took almost 26

hours of drying in the drying chamber to reduce moisture from 76% at initial to 5% when fully dried, as Brewer et al [8] reported that moisture content less than 10% in any product increases its shelf life and also attack of mycoflora, bacteria and other pathogens are minimized.

3.2 Drying Time Taken by Chilies

The initial moisture content of chilies was 76% and was dried until the final moisture content reached to less than 10%. It is due the fact that pathogen attack was minimized when chilies have a moisture content less than 10%. Drying temperature, air mass flow rate and their interaction have significant ($P \leq 0.01$) effect on the drying time of chilies. Minimum drying time of 17.96 h was recorded at high temperature of 65°C followed by a drying time of 20.27 h and 21.43 hr at temperatures of 55°C and 45°C. The means of air mass flow rates revealed minimum drying time of 18.49 h, which was noted at high air mass flow rate of 3.50 kg min^{-1} followed by 20.32 and 20.86 h at air mass flow rates of 1.5 and 2.30 kg min^{-1}. These results are in accordance with the findings of Mohanraj & Chandrasekar [7], Brewer *et al* [8] and Morison [9] and Santos et al [3] and Mahmood et al [4] also found significant effects of mass flow rates and temperature on drying time of chilies.

3.3 Moisture Loss in Each Hour

Chilies were dried at an average temperature of 50°C and a humidity of 5%. Chilies took almost 26 hours of drying period (Fig. 2) in the drying chamber to be dried. The initial moisture content of chilies was 75%, which was reduced up to 5% in the 26 hours of drying period, these results are in argument with the findings of Brewer et al [8]. Chilies showed a very slow drying rate (Fig. 3) of 0.003 $g_{(H_2O).}$ $hr^{-1}.cm^{-2}$ at first four hours of drying, which was constant rate drying, which was then decreased to 0.0015 $g_{(H_2O).}$ $hr^{-1}.cm^{-2}$ after 13 hours of drying because 50% reduction in the moisture content of the chilies. The drying rate becomes at falling rate and slower at the end of drying chilies which were about 0.0010 $g_{(H_2O).}$ $hr^{-1}.cm^{-2}$ because

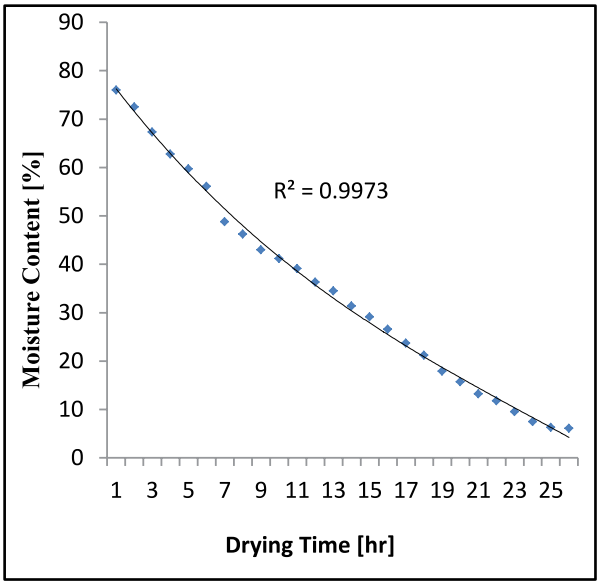

Fig. 2 Moisture loss on wet basis by chilies.

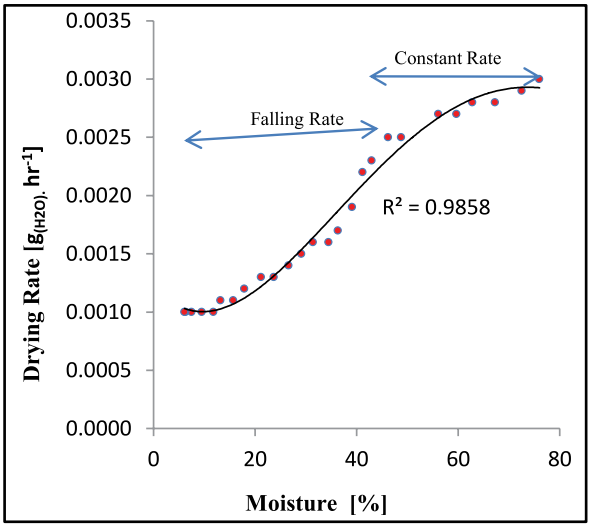

Fig. 3 Moisture loss on dry basis by chilies.

chilies were having less moisture of 15%, which was difficult to be dehydrated from chilies by the hot convective air. These results are in accordance with the findings of Santos *et al* [3], Morison [9], Ahmad [10], Henderson and Perry [11] and Masit et al [12].

4. CONCLUSIONS

It was concluded that concentrating solar drier provided optimum drying conditions for drying of green chilies. Chilies must be dried at high temperature and high air mass flow rates to get minimum time for drying. Solar drying of green

chilies using a concentrating solar collector is time saving, economical and the product dried were safe from pathogen attack. It is recommended that to get good quality and valuable dried green chilies they must be dried at a temperature of 60°C and high air mass flow rate of 3.5 kg min^{-1} to get spicy and valuable dried green chilies to be ground easily to powder for taste in food.

5. ACKNOWLEDGMENTS

The Author acknowledges the help provided by Mr. Muhammad Aamir in the construction and installation of the concentrating solar collector.

6. REFERENCES

1. Wilcke, W.F. *Low Temperature Solar Grain Drying Handbook*. Midwest Plane Press, University of Illinois, USA (1980).
2. Karim, A.M. & M.N.A. Hawlader. Development of Solar Air Collectors for drying applications. *Journal of Energy Conservation and Management* 45(3): 329-344 (2003).
3. Santos, B.M., R. Quiroz & T.P. Borges. A Solar Collector Design Procedure for Crop Drying. *Brazilian Journal of. Chemical Engineering* 22 (1): 104-132 (2005).
4. Mahmood, Z., K. Mazzullah, A. Masood & M. Asif. Design and development of a gable type solar dryer for drying fruit and vegetables. *Sarhad journal of Agriculture* 21(4): 525-529 (2005).
5. Ehiem. J.C., S.V. Irtwange & S.E. Obetta. Design and development of an industrial fruit and vegetable dryer. *Journal of Applied Science, Engineering and Technology* 1(2): 44-53 (2009).
6. Hanif. M., M. Ramzan & M. Aamir. Drying of grapes using a concentrating solar air heater. *Journal of Agricultural Research* 50 (3): 487–496 (2012).
7. Mohanraj, M. & P. Chandrasekar. Performance of a forced convection solar drier integrated with gravel as heat storage material for chili drying. *Journal of Engineering Science and Technology* 4(3): 305-314 (2009).
8. Brewer, N. R., A.F.J. Clifford, S.T. Elwynn, L.K. Joe & W. Morris. *Solar Applications in Agriculture*. The Franklin Institute Press. Auburn University, Auburn, Alabama, USA (1981).
9. Morrison, D. *Agricultural Solar Design Booklet*. Cooperative Extension Services Press, Agricultural University of Illinois, USA (1981).
10. Ahmed, A.G. Design and construction of a solar drying system with a cylindrical section and it's analysis of the performance of the thermal drying system. *African Journal of Agricultural Research* 6 (4): 343-351 (2011).
11. Henderson, S.M. & R.L. Perry. *Agricultural Process Engineering. Engineering*. University of California, AVI Press California, USA (1976).
12. Masit, L., A.E. Fossdal, K.M. Broch & B. Erisksen. *Renewable Energy*. The Center for Renewable Energy, Norwegian University of Science and Technology, Norway (2007).

Proceedings of the Pakistan Academy of Sciences 52 (2): 109–116 (2015)

ISSN: 0377 - 2969 (print), 2306 - 1448 (online)

Pakistan Academy of Sciences

Research Article

Influence of Situational Constraints and Public Transport Incentives on Acceptability of Car Use Restrictions in Lahore, Pakistan

Muhammad A. Javid

Department of Civil Engineering,
National University of Computer and Emerging Sciences, Faisal Town, Lahore, Pakistan

Abstract: The rapid increase in private car ownership and its usage has resulted in traffic congestion on road infrastructure in Lahore city. It is very important to explore the potential of some travel demand management policies under local socio-economic context. This paper aims to explore the influence of situational constraints and public transport incentives on acceptability of car use restrictions. A questionnaire survey was conducted in Lahore city to obtain the required data. Data was analyzed using structural equation modeling technique. Results revealed that situational constraints and public transport incentives have significant influence on people's travel behavior and acceptability of mobility restrictions on car use. The findings of this study would be useful for local planners in making decision regarding transit improvements and implementing car use reduction measures.

Keywords: Travel demand management (TDM), structural equation modeling (SEM), situational constraints, traffic congestion, public transport

1. INTRODUCTION

The rapid increase in private vehicle ownership and its usage has resulted in traffic congestions on road infrastructure in most of the developing countries. The traffic jams tend to increase social cost in terms of increase in energy congestion and air pollution, increase in travel time and cost, and increase in accidents. Building more road infrastructure results inequitable solutions for the reduction of traffic congestion because it just facilitates the private vehicle users. It does not provide any appropriate mobility options for the poor people such as non-motorized and public transport modes users. Moreover, such supply side measures encourage more private vehicle ownership and its usage, and tend to increase social cost. In developing countries, the main focus is on supply side measures in order to reduce the gap between demand and supply. However, lack of financial, technical and institutional resources and environment sustainability related problems argue from planners and policy makers to look for demand side solutions with supply side measures. In this perspective, travel demand management (TDM) strategies are considered as effective tools in reducing the traffic congestion and its related social and environmental problems. The TDM strategies tend to influence the individual's travel behavior for the reduction of traffic congestion and have impact on reduction in travel time and cost, and convenience of travel options [1]. Garling and Schuitema [2] believe that it is vital to promote such policies that should reduce the advantage of car use and increase benefits of public transport usage. The TDM strategies are mainly classified into two types such as push or disincentive measures aiming to reduce the advantages of car use (e.g., increase in fuel and road taxes), and pull or incentive measures where alternative travel choices are provided (e.g., improved public transport, van pooling, HOVs lanes) [3]. Another classification includes hard measures such as road pricing, parking charges,

Received, December 2014; Accepted, April 2015
*Corresponding author: M.A. Javid; Email: ma.javid@hotmail.com

new public transport service and soft measures such as workplace travel plans, personalized travel planning, public transport marketing and travel awareness campaigns [4].

According to Meyer [5], it is required to manage travel demand efficiently for commuting and non-commuting trips and for recurring and non-recurring congestion events in order to optimize the performance of existing transportation system. It is argued that those TDM strategies will be effective in developing countries which offer cheaper travel alternative to the majority of the residents [6]. The TDM measures such as support for ridesharing, public transport improvements and implementation of land use policies can reduce the private vehicle trips. Implementation of parking control measures, and support for pedestrians and cyclists can also be effective in altering the travel demand and pattern [7]. Faiz et al [8] argue that imposing vehicle ownership and other usage related taxes like road tax and parking charges may discourage both car ownership and usage. It is very important to evaluate the public acceptability for the specific TDM strategies before implementing [9] because commuter's behavior will be key factor in their success and effectiveness. In some studies, push measures like road pricing and parking charges perceived low acceptance from public compared with pull measures like public transport improvements [10-11]. However, it is believed that commuters normally perceive pull measures to be more suitable; though push measures are often believed to influence car use reduction to a greater extent [12, 3]. In addition, the acceptability of a measure is important if its objectives have to be achieved [9, 13].

Different factors can influence the acceptability of TDM policies. These factors include individual's socio-economic demographics (SED), lifestyle, attitudes and intentions [3, 12, 17-18]. It is vital to explore the influence of such factors on acceptability of TDM strategies in the local context. Therefore, the objective of this paper is to diagnose the influence of situational constraints or coupling constraints and public transport incentives on acceptability of car use restrictions. The findings of this study are based on results of a questionnaire survey and structural equation modeling. This paper organized in the following manner. Section 2 describes the characteristics of study area and data collection methods. Section 3 presents the results and analysis part and last section summarize the key findings of this study.

2. STUDY AREA AND DATA COLLECTION

In this study, Lahore city selected for case study. It is the second largest city of Pakistan after Karachi and largest one of Punjab Province. The population of Lahore city is almost 8.65 million and area about 1792 km^2 [14]. The urban population growth rate is almost 3% per annum [14]. It is concentrated with educational, economic and medical facilities. The people from other parts of the country travel to Lahore in order to enjoy the culture and better living facilities. The presence of such facilities attracts many people from suburban areas and generates huge travel demand. The number of trips generated is very high from the inner zones of the city due to high density development. Population density varies from 450 persons per hectare in the inner zone to 100 persons per hectare in the outer zone and almost 80% of population is living within a radius of 7-8 km from the city centre [14]. Considering the number of trips generated and attracted due to this high density development in the inner zone and concentration of facilities, it can be argued that Lahore city has high potential for mass transit development. On the other hand, the rapidly growing population and traffic demand has resulted persistent traffic congestion on roads despite significant supply of related infrastructure in the last decade. The ownership of private vehicles is increasing at an alarming rate of 17 % per annum [14]. Insufficient and inefficient existing public transport system is one of the main reasons for this increase. Other main elements in the rapid increase of car ownership and usage are banking leasing policy to own a car, changing lifestyles, status symbol and low ownership and usage cost. It

is believed that motorized traffic also threatens the safety of non-motorized modes users in the busy urban areas [15]. The increased social costs due to heavy traffic congestion in terms of increase in travel time and cost increase in energy consumption and air pollution demands the provision of sustainable travel options. In the context of these stated issues it is required to consider and implement demand management measures in order to solve the congestion oriented problems, and ensure the sustainability of the city.

A questionnaire survey was conducted in Lahore to obtain the required data in order to accomplish the study objectives. A comprehensive questionnaire was designed consisting of following two parts. Part one included only personal and trip information of the respondents i.e. gender, marital status, age, income, education, occupation, vehicle ownership, possesses driving license or not, etc. In part two of the questionnaire respondents were requested to state their behavioral intentions for the use of improved public transport under some situational constraints, mobility restrictions on car use, and public transport incentives. A five point Likert scale was used in this part to evaluate the respondents stated intentions, i.e., never (1), almost never (2), sometimes (3), almost every time (4) and every time/always (5). There were fourteen conditional statements as presented in Table 2 and respondents needed to show their intentions for the use of public transport against each statement using five point Likert scales as mentioned above. The respondents were asked to show their preferences to use public transport under different situational constraints such as travelling alone, travelling with family members or friends, and travelling with elder family members. Some incentives were given to the respondents on public transport usage such as reliable service, direct access to important destinations along transit route, low travel cost and less travel time as compared to private car. Some mobility restrictions on car use were included such as limited car parking space at destination; parking is very far from the destination, imposition of road tax and heavy parking fees on car use, and entry restrictions on car in public transport service area.

This questionnaire survey was conducted in the various private and civil organizations and educational institutions located in Lahore city. The survey locations were selected keeping in view the target groups of respondents. The target groups were included the current and potential car users. Therefore, only those locations were selected for survey where such kinds of travelers were easily available and accessible. These locations included some engineering departments of University of Engineering and Technology and the University of the Punjab, National University of Computer and Emerging Sciences, NESPAK Pvt. Ltd., Transportation Planning Unit (TPU), and some other private organizations. It was assumed that such professional workers and students belonging to engineering fields have more potential to use car.

The questionnaire was equipped with the objectives and details of the conducting authority. The filling guidelines were also mentioned at the start of each part. The respondents were selected randomly at each survey location. The survey was conducted with the help of university graduate students and they were properly trained for this purpose. A pilot survey was conducted before the actual survey in order to assure the clarity of designed questionnaire items. Self-completion approach by respondents was used in this survey. The questionnaires were distributed at selected locations, and instructions were given to the respondents regarding the contents of the questionnaire and the procedure to answer the questions. The respondents were requested to return the completed questionnaire after two weeks, and completed questionnaires were collected with the help of the survey team. An additional one week was given to those respondents who were not able to complete the questionnaire in the initial period.

3. RESULTS AND ANALYSIS

3.1. Distribution of Respondents' Socio-economic Demographics (SEDs)

A total of 550 questionnaires were used in the

survey, and only 372 samples were obtained, which represented a return rate of 67.7%. Eighteen samples were discarded because of incomplete information and double answers on some questions. Therefore, the results of only 354 samples were used in further analysis. The proportions of male and female respondents in the sample were 67.5% and 32.5%, respectively. There were fewer female respondents because they do not ride motorcycles, and the proportion of working women is also lower in Lahore city. Almost 84% of respondents were aged 21–30 years, and only 48% had a driving license. Details of socioeconomic demographics (SEDs) are given in Table 1.

3.2. Average Response on Stated Preferences

Average response was calculated for respondent's behavioral intentions to use public transport under stated conditions. For this purpose, respondents' response was coded on bipolar scale, i.e., -2 (never), -1 (almost never), 0 (sometimes), 1 (almost every time) and 2 (every time).

It can be seen from results presented in Table 2 that respondent's intentions to use public transport vary under different situational constraints. Travelling with family members accounts less average response. It can be said that people feel insecure and less privacy while travelling with family members especially with female. In acceptability of mobility restrictions on use, estimated average response depicts that restriction on car entry in public transport service area has more potential of reducing car use compared to fiscal and parking restrictions. It can be said that improvement in service quality of public transport with car entry restrictions is an effective policy to reduce the traffic congestion in highly congested areas. Parking charges and road tax on car use have almost same influence on car use reduction. In public transport incentives, average response shows that direct access to destination and reliability are the most influencing attributes of public transport along with less travel cost. It looks that sitting has less significance in defining the service quality level of public transport for target group of people.

3.3. Structural Equation Modeling (SEM)

Analyses were conducted using structural equation modeling technique to evaluate influence of public transport incentives and situational constraints on acceptability of car use restrictions. Many studies in the field of transportation research have applied SEM technique to diagnose casual relationship between different factors [16-19]. The SEM is a multivariate statistical analysis tool which can elaborate direct and indirect relationships between

Table 1. Descriptive statistics of respondents' socioeconomic demographics.

Characteristics	Distribution (%)
Marital status	Single (65), Married (35)
Occupation	Students (22.7), private employees (30.6), civil employees (43.1), entrepreneurs (3.6)
Personal income per month (PKR)	< 10,000 (19.5), 11,000–20,000 (13.8), 21,000–30,000 (16.7), 31,000–40,000 (17.2), 41,000–60,000 (17.8), 61,000–80,000 (8.8), > 80,000 (6.2)
Household income per month (PKR)	< 20,000 (4.5), 21,000–30,000 (11.6), 31,000–40,000 (10.5), 41,000–60,000 (24.9), 61,000–80,000 (17.0), > 80,000 (31.2)
Vehicle ownership	None (9.9), Motorcycle (60.2), Car (52.0)
Vehicle driven	None (23.2), Motorcycle (43.2), Car (40.0)
Modal share (usual daily travel mode)	Walk (7.3), Bicycle (1.5), car (31.2), motorcycle (27.6), auto-rickshaw/taxi (12.3), campus/office transport (7.1), Qingqi/wagon (7.2), bus (5.8)
Frequency of usual travel mode	5–7 days a week (86), 3–4 days a week (9), 1–2 days a week (2), a few times a month or less (3)

Table 2. Average response for public transport usage under incentives and restrictions.

Description of items	Mean
Situational Constraints (SC)	
Commuting with family members (SC-1)	-1.083
Travelling with elder family members (SC-2)	-1.232
Commuting with friends (SC-3)	-0.427
Public transport incentives (PTI)	
If public transport is reliable than car (PTI-1)	0.517
When travel cost by public transport is half of car (PTI-2)	0.412
When travel time by public transport is 10 minutes less than car travel time (PTI-3)	0.263
When seat is assured in public transport with same travel time as car (PTI-4)	0.146
When seat is assured in public transport with same travel cost as car (PTI-5)	-0.008
When you can directly access many important places by public transport (PTI-6)	0.576
Acceptability of mobility restrictions on car use (AMR)	
When parking is limited at destination (AMR-1)	0.121
When you need to pay Rs. 100 parking fee at destination (AMR-2)	0.350
When you need to pay road tax Rs.100 for use of car (AMR-3)	0.429
When entry of car is restricted in public transport service area (AMR-4)	0.673

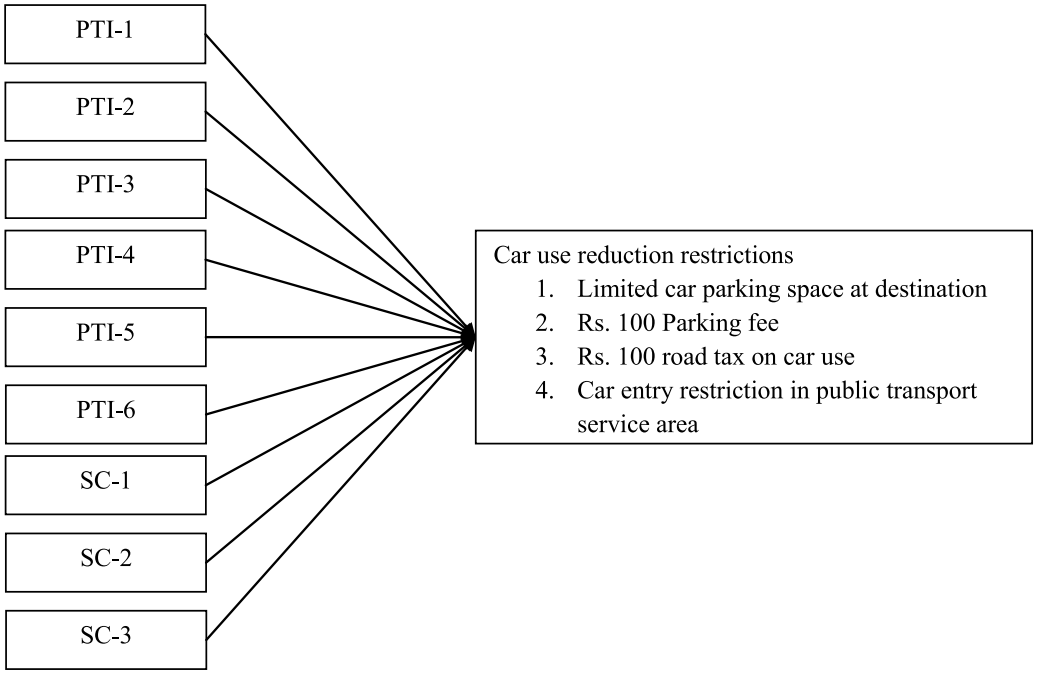

Fig. 1. A typical structural model diagram.

the variables. In a SEM model, it is possible to include latent variables. The SEM technique permits the researcher to interpret the covariance structure without considering the multicollinearity issue. For this purpose various users' friendly software are available such as SPSS AMOS 19.0. A typical structural model diagram for this study is shown in Fig. 1. This diagram shows the influence

Table 3. Results of structural equation modeling.

	Limited parking at destination (AMR-1)	Rs. 100 parking free (AMR-2)	Rs. 100 road tax (AMR-3)	Car entry restriction (AMR-4)
PTI-1	--	.10**	.26***	.32***
PTI-2	.21***	.24***	.24***	.26***
PTI-3	--	.09**	--	--
PTI-4	--	--	-.12***	-.10**
PTI-5	.14***	.07*	.11***	.37***
PTI-6	.12**	.15***	.16***	.12**
SC-1	.24***	--	--	--
SC-2	.29***	--	--	--
SC-3	-.16***	--	--	-.09**

Note: PTI: public transport incentive, SC: social constraints, AMR: acceptability of mobility restrictions, *** significant at 1%, ** Significant at 5%, * Significant at 10%

of public transport incentive (PTI) variables and various situational constraints (SC) variables on a particular car use reduction measures. Table 3 gives the details of significant structural relationships between influencing factors and car use reduction measure. Next sub-sections discuss the results one by one.

3.3.1. Limited Car Parking Space at Destination (AMR-1)

The less travel cost of public transport compared to car has significant and positive relationship with limited parking restriction policy at destination. It implies that limited parking policy has some impact on car use reduction if the public transport travel cost is less. Similarly, in public transport incentives seat assurance and direct access by public transport to most of the destination have positive and significant impact on reduction of car use under limited parking policy. In situational constraints, travelling with family members has positive association with limited parking policy. It means that limited parking policy has significant influence on reduction of car use even when people travelling with family members. The negative relationship between this policy and SC-3 depict that people would prefer to use private car instead of public transport while travelling with friends.

1.3.2. Rs. 100 Parking Fee on Car Use (AMR-2)

The halved travel cost of public transport as compared to car and direct access to important destinations by public transport have very strong association with acceptance of Rs. 100 parking fee on use of private car. It implies that reduced travel cost of public transport along with imposition of parking charges would have significant influence on reduction of private vehicle usage.

3.3.3. Rs. 100 Road Tax Imposition on Car Use (AMR-3)

The provision of public transport incentives has positive influence on acceptability of Rs. 100 road tax on car use. These incentives include reliability, less travel cost compared to car, and higher access of public transport service. The negative relationship of assured seat with same travel time with road tax policy imply that people would prefer to use their private vehicle even if they need to pay Rs. 100 road tax on car use. In situational constraints, none of the relationship is significant with this policy.

3.3.4. Car Entry Restriction in Public Transport Service Area (AMR-4)

The incentives of reliability, less travel cost compared to car and higher access of public transport have positive influence on acceptability of this

policy. However, the incentive of assured seat with same travel time as car has negative relationship with this policy. It depict that this incentive would not help in reducing the use of private vehicle. In situational constraints, people would prefer to use private vehicle while travelling with friends even with the imposition of this policy as relationship is negative.

4. CONCLUSIONS

Reliability of service, less travel cost of public transport and direct access to important destinations by public transport are significant incentives in order to enhance the acceptability of imposed mobility restrictions on car use in Lahore city. It was also revealed that assurance of seat in using public transport with same travel time as private car would not have any impact on reduction of car use even in the presence of mobility restrictions. These findings imply that before imposition of such restrictions on car use we need to enhance the reliability and accessibility of public transport service. It is also required to keep travel cost of public transport on lower side in order to make it attractive for car and non-car users. It was observed that some situational constraints have significant influence on acceptability of car use restrictions such as travelling with friends and family members. People would prefer to use their private vehicle while travelling with friends because they feel better in the society. These findings would be helpful in taking preparatory steps for the improvements of public transport system before imposing above mentioned restrictions on car use.

5. REFERENCES

1. Garling, T., D. Eek, Loukopoulos, S. Fujii, O.J. Stenman, R. Kitamura, R. Pendyala & B. Vilhelmson. A conceptual analysis of the impact of travel demand management on private car use. *Transport Policy* 9: 59-70 (2002).
2. Garling, T. & G. Schuitema. Travel demand management targeting reduced private car use: effectiveness, public acceptability, and political feasibility. *Journal of Social Issues* 63(1): 139-153 (2007).
3. Steg, L. & C. Vlek. The Role of Problem Awareness in Willingness to Change Car Use and Evaluating Relevant Policy Measures. In: *Traffic and Transport Psychology: Theory and Application.* J.A. Rothengatter & E. Carbonell Vaya (Ed.), Elsevier, Oxford, UK, p. 465-475 (1997).
4. Garling, T. & S. Fujii. Travel behaviour modification: theories, methods, and programs. *Resource Paper presented at IATBR Conference*. Kyoto University, Japan (2006).
5. Meyer, M. Demand Management as an Element of Transportation Policy: Using Carrots and Sticks to Influence Travel Behaviour. *Transportation Research Record* 33(7-8): 575-599 (1999).
6. Litman, T. Efficient Vehicles versus Efficient Transportation: Comparing Transportation Energy Conservation Strategies. *Transport Policy* 12(2): 121-129 (2005).
7. Auckland Regional Council. Travel *Demand Management Strategies* (2000). Retrieved from http://www.arc.govt.nz.
8. Faiz, A., K. Sinha, M. Walsh, & A. Varma. Automatic Air Pollution: Issues and Options for Developing Countries. *Working Paper 492, Infrastructure and Urban Development Department.* The World Bank, Washington, DC (1990).
9. J. Schade, & B. Schlag. Acceptability of urban transport pricing strategies. *Transportation Research Part F: Traffic Psychology and Behaviour* 6(1): 45-61 (2003).
10. Schlag, B. & J. Schade. Public acceptability of traffic demand management in Europe. *Traffic Engineering and Control* 41: 314-318 (2000).
11. Bhattacharjee, D., S.W. Haider, & Y. Tanaboriboon. Commuter's attitudes towards travel demand management in Bangkok. *Transport Policy* 4(3): 161-170(1997).
12. Javid, M.A., T. Okamura, F. Nakamura, S. Tanaka & R. Wang. Public perceptions to travel demand management measures in Lahore, Pakistan: Analysis and implications. *Proceedings of the Pakistan Academy of Sciences* 51(1): 17-29 (2014).
13. Thorpe, N., P. Hills & S. Jaensirisak. Public attitudes to TDM measures: a comparative study. *Transport Policy* 7(4): 243-257 (2000).
14. JICA. Lahore Urban Transport Master Plan in the Islamic Republic of Pakistan, Final Report, Vol. I & II, March 2012. Retrieved from JICA online library: http://libopac.jica.go.jp
15. Esmael, M.O., K. Sasaki & K. Nishii. *Road Traffic Accident Trend in Developing Countries – The Policy Implications*. Proceedings of 13th World Conference on Transport Research, Rio De Janeiro, Brazil, July 2014 (2014).
16. Javid, M.A., T. Okamura, F. Nakamura, S. Tanaka & R. Wang. Comparison of commuters' satisfaction

and preferences with public transport: a case of wagon service in Lahore. *Jordon Journal of Civil Engineering* 7(4): 461-474 (2013).

17. Javid, M.A., T. Okamura, F. Nakamura, S. Tanaka & R. Wang. Methodology for evaluating the driver's attitudes towards transportation demand management measures in Lahore, Pakistan. *Journal of Recent Trends in Civil Engineering and Technology* 2(2): 45-59 (2012).
18. Choocharukul, K., H.T. Van & S. Fujii. Psychological determinants of moral obligation of car use reduction and acceptance of car use restriction in Japan and Thailand. *IATSS Research* 30(2): 70-76 (2006).
19. Golob, T. Structural equation modelling for travel behaviour research. *Transportation Research Part B* 37(1): 1–25 (2003).

Proceedings of the Pakistan Academy of Sciences 52 (2): 117–124 (2015)

ISSN: 0377 - 2969 (print), 2306 - 1448 (online)

Pakistan Academy of Sciences

Research Article

A Preliminary Study of *Opuntia stricta* as a Coagulant for Turbidity Removal in Surface Waters

Arslan Mukhtar[1], Waris Ali[2], and Ghulam Hussain[3]*

[1] Environmental and Public Health Engineering Division,
National Engineering Services, Lahore, Pakistan
[2] Institute of Environmental Engineering and Research,
University of Engineering and Technology, Lahore, Pakistan
[3] Institute of Environmental Engineering and Research,
University of Engineering and Technology, Lahore, Pakistan

Abstract: Natural polymers, extracted from plants, can be used as coagulants for water treatment in addition to metal salts and synthetic polymers. Natural materials may offer benefits such as local production, lesser health hazards and affordability for developing world. *Opuntia stricta* plant, a cactus specie native to Mexico, has been explored in this study for its efficacy as coagulant. Efficiency of *Opuntia stricta* was assessed on the basis of turbidity removal from lab prepared and surface water samples. The effect of water pH on its performance was also analyzed. The study results revealed that removal efficiency of *Opuntia stricta* for turbidity removal remains consistent within a wide pH range (pH 5 to 10), in contrast to other coagulants which are pH dependent. Furthermore, pH of the water remains constant during coagulation and pH adjustment may not be required for subsequent treatment processes, which is often needed in case metal coagulants are used. Residual turbidity below 20 NTU is conveniently achieved by using *Opuntia stricta* even when it is used at very low doses. Formation of exceptionally large flocs and their linear configuration reveals the possibility that mechanism of coagulation by *Opuntia stricta* is adsorption and inter-particle bridging.

Keywords: *Opuntia stricta*, cactus, water, treatment, coagulation

1. INTRODUCTION

About 187 million of world population relies on the unimproved surface water sources [1]. Such water use poses high risk of water borne diseases. Turbidity is one of the major problems of surface waters and shallow open wells, as observed in studies in Pakistan [2], Bangladesh [3], Ghana [4, 5], Malawi [6] and Cameroon [7]. Removal of turbidity is necessary to improve its bacteriological quality by subsequent treatment i.e. disinfection. Conventional coagulants, such as aluminum and iron salts, have been successfully used in treatment of turbid waters. Effectiveness of these chemical coagulants is well recognized [8,9]; however, certain disadvantages such as production of large sludge volumes, ineffectiveness in low-temperatures, high procurement costs, and Alzheimer's disease [10, 11] tend to limit their use, particularly in countries of the developing world. Synthetic polymers, such as poly acryl-amide and poly diallyl-dimethyl ammonium chloride, are alternative coagulants used to remove turbidity in water. They can reduce the turbidity of water without increase in sludge volumes;however, health concerns related to the release of carcinogenic oligomer constrain their use [12-15].

In addition to conventional metallic coagulants and synthetic polymers, natural materials like *Moringa oleifera*, *Opuntiaspp*., *Strychnos potatorum* and *Tannin* can also be used for treating

Received, December 2014; Accepted, April 2015
*Corresponding Author: Ghulam Hussain; Email: ghussain@uet.edu.pk

turbidity present in the water through coagulation [12]. These coagulants are not only naturally reproducible but may also offer many other advantages like local availability, adaptability, and lesser health hazards than residual mineral coagulants or synthetic polymers. Among these coagulants, *Opuntia Spp.* are the ones which have been recently deliberated for detailed laboratory investigations to explore its coagulation properties and mechanisms [13].

Opuntiagenus is a group of succulent plants which spreads from Mexico to other parts of the world. *Opuntiaficus-indica* is most common specie of this group which has multiple uses in the industry and everyday life [14].*Opuntia ficus-indica* has been extensively studied for the coagulation of colloidal suspensions by some researchers [13, 15-17]. Mostly, internal part (parenchyma) of *Opuntia cladode* has been used to prepare coagulant solutions after drying and grinding to make a powder. However, Butticeet al. [17] have used chemically extracted mucilage of the *Opuntia cladode* in coagulation studies. Mucilage is the gummy material and a biopolymer found in *Opuntia cladode* [12]. While treating colloidal suspensions with *Opuntia ficus-indica,* as coagulant, zeta potential of colloids and micro-photographs of flocs indicate that potential mechanism of coagulation is absorption and inter-particle bridging [13]. It is found that *Opuntia ficus-indica* has the ability to bring down residual turbidity to around 5 NTU for different initial turbidities of synthetic and natural colloidal samples but the best removal occurs around pH 9-10, and the removal efficiency decrease gradually by lowering the pH to 7 [12-13, 16]. However, the required pH range of the drinking water is 6.5-8.5 according to WHO guidelines for drinking water [18]. Adjustment of pH of natural water to pH 9-10 for optimal coagulation using *Opuntia ficus-indica* requires significant amount of chemicals, which might not be affordable for developing countries.

Opuntia stricta, have not been studied for its coagulation characteristics so far. It is a less common *Opuntia spp.* than *Opuntiaficus-indica*, but is widely spread over South America and Australia. It is also found in Cuba, Haiti and West Indies as well. *Opuntia stricta* has light-green oval to elliptical shaped matured cladodes, which are more often spineless; however, there are widely spaced small glochids on the cladodes. It has seasonal lemon-yellow colored flowers and carmine-red colored elongated club-shaped ripped fruits [19]. Fig. 1 shows cladodes, flowers and fruits of *Opuntia stricta*.

Although actual coagulating agents in *Opuntia* are uncertain;mucilage was found with coagulation properties pertaining to *Opuntia* [12]. Chemically, mucilage of *Opuntia stricta* contains protein, fat, crude fiber, and ash content of about 5.18%, 0.38%, 0.07% and 29.93%, respectively. It has low acute toxicity levels and can be used as additives in the pharmaceutical and food products [20]. Mucilage has complex chemical ingredients, but mostly it is considered to contain polysaccharides abundantly [21]. Mucilage contains varying proportions of l-arabinose, d-galactose, l-rhamnose, and d-xylose, as well as galacturonic acid [22]. The results of a study indicated that turbidity removal of synthetic polysaccharides of mucilage was about 50% only, which suggests the presence of some other active coagulant agents than mucilage in the *Opuntia* [13]. However, analysis of the poly-galacturonic acid, a major constituent of many plants, for coagulation rather than simple galacturonic acid, used by Miller S.M. et al, 2008, may yield a better insight into coagulation ingredients of *Opuntia* [12].

Keeping in view the potential advantages of *Opuntia spp.* as coagulant and constraints of pH adjustment for *Opuntia ficus-Indica*, turbidity removal in surface water using *Opuntia stricta* have been explored in this study.

2. MATERIALS AND METHODS

2.1 Water Sampling

Both natural and synthetic colloidal samples have been used in the study. Natural sample was obtained from River Ravi near Ravi Syphon, District Lahore, Punjab-Pakistan. Samples were stored at room temperature and used for study after

Fig. 1. Cladodes, flowers and fruits of *Opuntia stricta*.

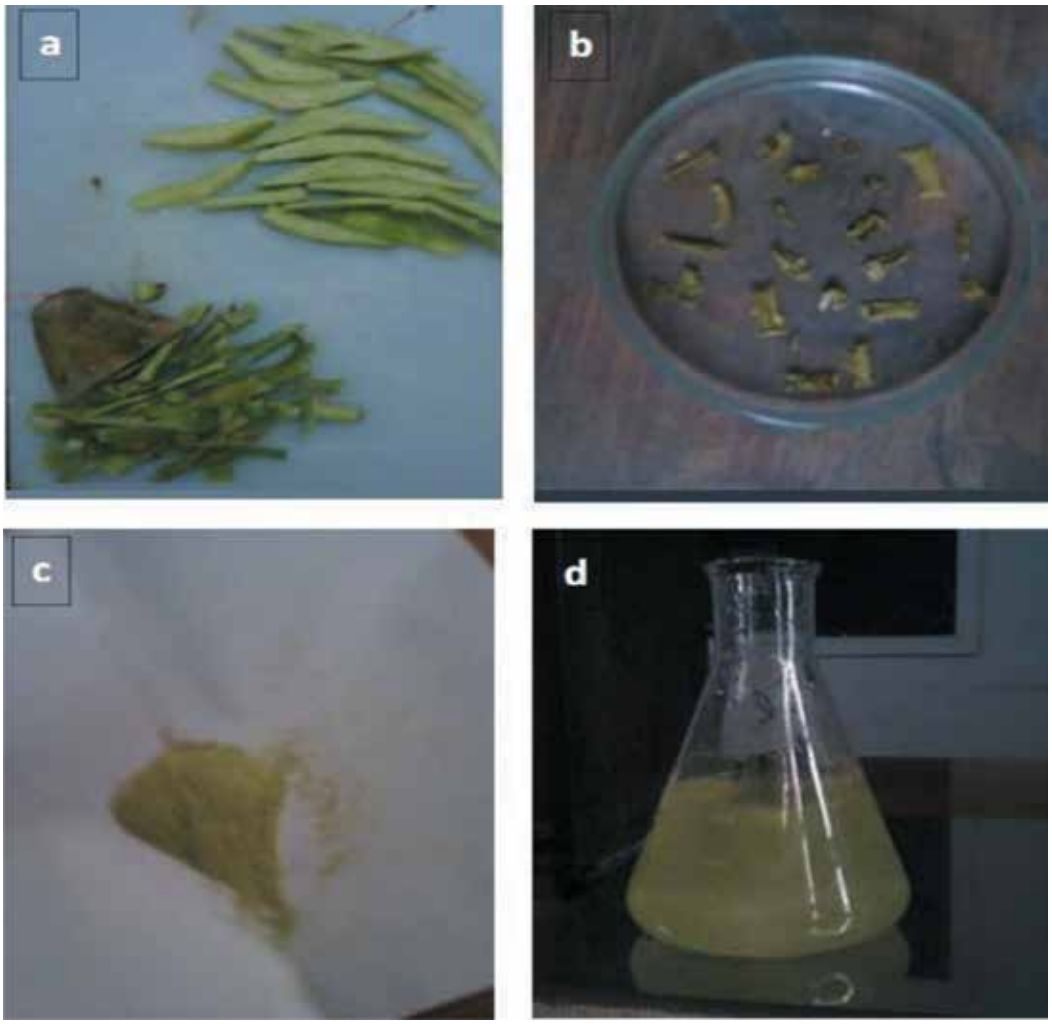

Fig. 2. Extraction and preparation of coagulant solution.

Table 1. Salient physical and chemical characteristics of colloidal samples.

Sr. No.	Parameter	Units	Sample Type	
			River water*	Synthetic water
1	Turbidity	NTU	105	150±10
2	pH	-	7.1	8.0-8.3
3	Electrical Conductivity	µS/cm	238	270±20
4	Alkalinity	mg/L as $CaCO_3$	138	104±10

* Average Values

homogenization through mixing. Synthetic samples were prepared using industrial grade kaolin. Ground kaolin was sieved to get particles less than 75 µm in size and mixed in the blend of distilled and tap water (1:1), settled for 1 hour and supernatant was decanted. The decanted supernatant was used as synthetic colloidal sample for coagulation analysis. Important physical and chemical characteristics of the samples are given in Table 1. Tests were performed according to the "Standard Methods for Examination of Water and Wastewater" [23].

2.2 Preparation of Coagulant Solutions

Opuntia stricta cladodes were obtained from Karachi Golf Club, Karachi, Pakistan. Pads were brought to Lahore and planted in the sandy soil for further natural growth. For preparation of coagulant solution, cladodes were washed with tap water and laterally cut into strips of about 1cm, outer skin was removed manually using knife, and internal parenchyma part was dried in the oven at 65ºC for 24 hours. Dried *Opuntia* was grinded in the Panasonic MJW-176P grinder and sieved to get powder containing particles of sizes ranging from 180 µm to 300 µm. This fine powder was used to make suspension of 1 g/L in distilled water and stirred for 1 hour to liberate active coagulant agents,which was then used as the coagulant solution. The process of coagulant extraction and preparation of coagulant solution is shown in Fig. 2.

2.3 Experimental Procedure

Coagulation experiments were performed using Phipps & Bird BP-900 jar test apparatus. Water samples were poured in 1 liter beakers and varying doses of *Opuntia* were added in different beakers. pH of the Synthetic colloidal suspensions was measured using HACH SensIon3 pH meter and adjusted to desired pH using 1N solutions of NaOH or H_2SO_4. Natural colloidal sample was used without adjustment of its pH. A blank sample was also analyzed in parallel for comparison. Samples were stirred at 100rpm for 2 minutes and slowly mixed at 30 rpm for 20 minutes followed by settling of 30 minutes. Effectiveness of *Opuntia stricta* was evaluated by measuring removal of turbidity at various pH and coagulant doses, both for synthetic and river water. Turbidity of the settled samples was measured using HACH 2100N turbidity meter. All the samples were tested three times and mean values are reported. Flocs formed during coagulation, at optimum dose and pH, were examined with the help of Olympus STM 6 microscope and micro-photographs were taken at appropriate resolution.

3. RESULTS AND DISCUSSION

Coagulation of synthetic water, at *Opuntia* dose of 2 mg/L to 30 mg/L, was carried out at pH 5 to 10. Results of the experiments are presented in Fig. 2. Over the tested pH range, there is insignificant change in residual turbidity for a given coagulant dose. Furthermore, there is a gradual increase in residual turbidity with increasing coagulant dose from 2 mg/L to 30 mg/L. This may be due to destabilization of particles observed at high doses of adsorbed polymers [24].

For initial turbidity of 150 NTU, residual

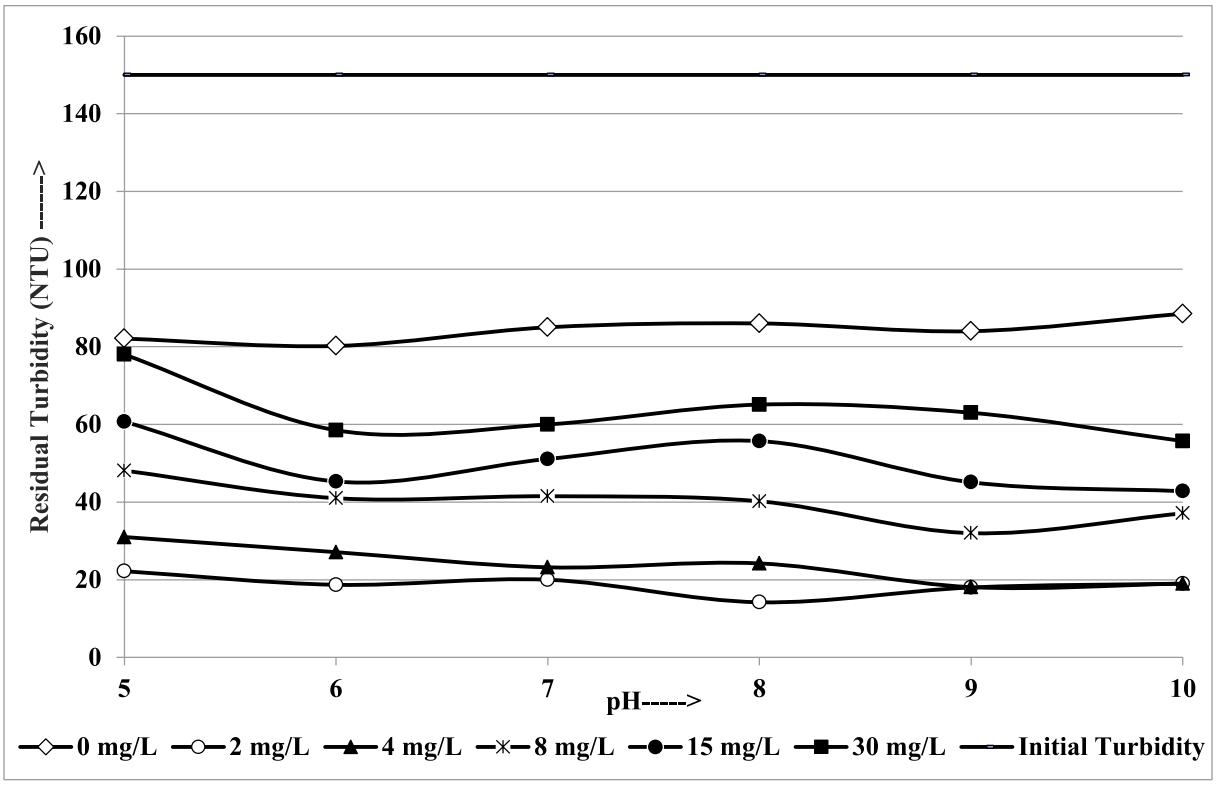

Fig. 3. Initial and residual turbidity in synthetic water sample for different doses of *Opuntia stricta* at varying pH.

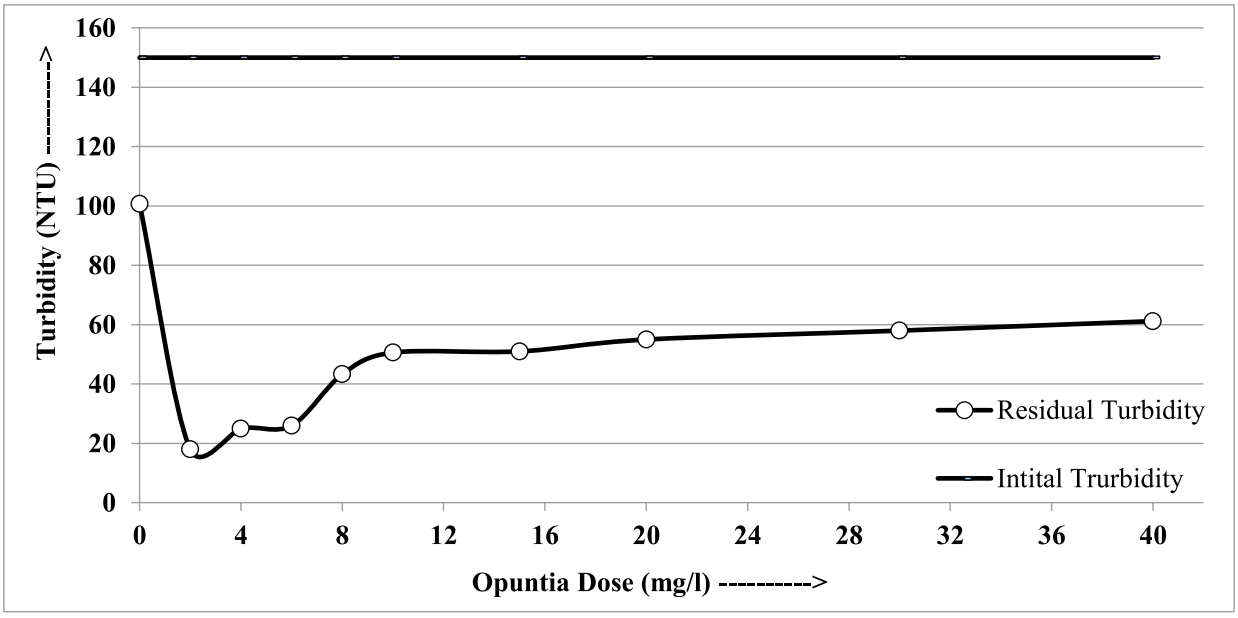

Fig. 4. Initial and residual turbidity of synthetic sample using different doses of *Opuntia stricta* at pH 7.0.

turbidities at pH 9-10 lie between 18 NTU – 63 NTU for different *Opuntia* doses and at pH 5-6, residual turbidities are 18 NTU – 78 NTU. Similarly, residual turbidities in pH range 6-8 lie between 14 NTU – 65 NTU for different *Opuntia* doses. These results indicate that efficiency of the *Opuntia stricta* is not strictly dependent upon the pH of the water; whereas, efficiency of *Opuntia ficus-Indica* and other coagulants is highly pH dependent [13]. It was also observed that there is

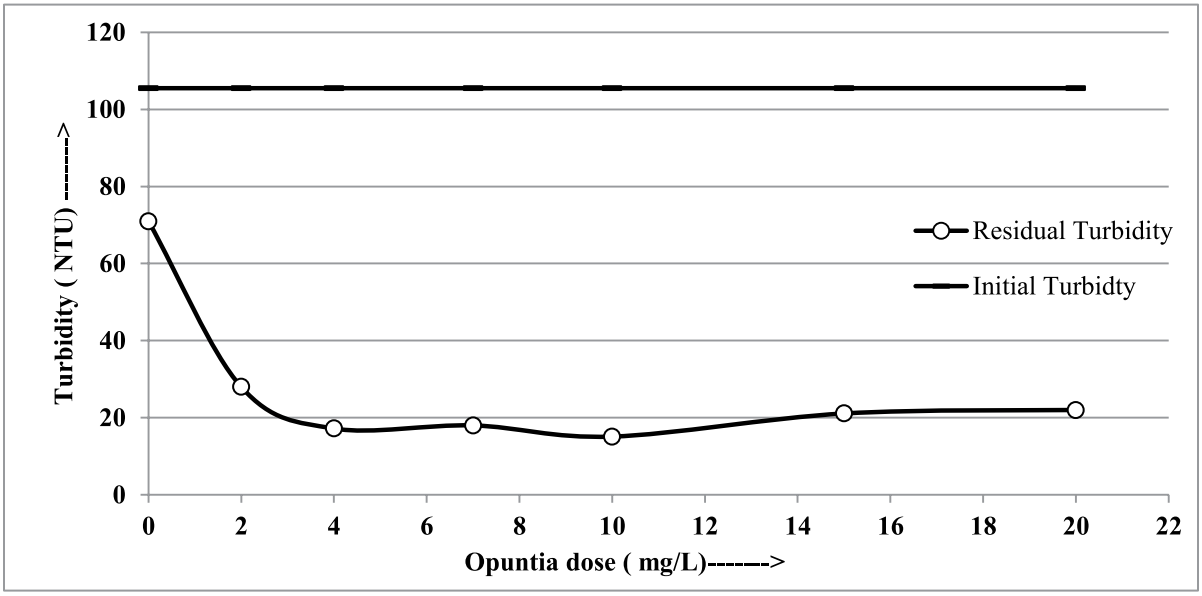

Fig. 5. Initial and residual turbidity of river sample using different doses of *Opuntia stricta* at pH 7.1.

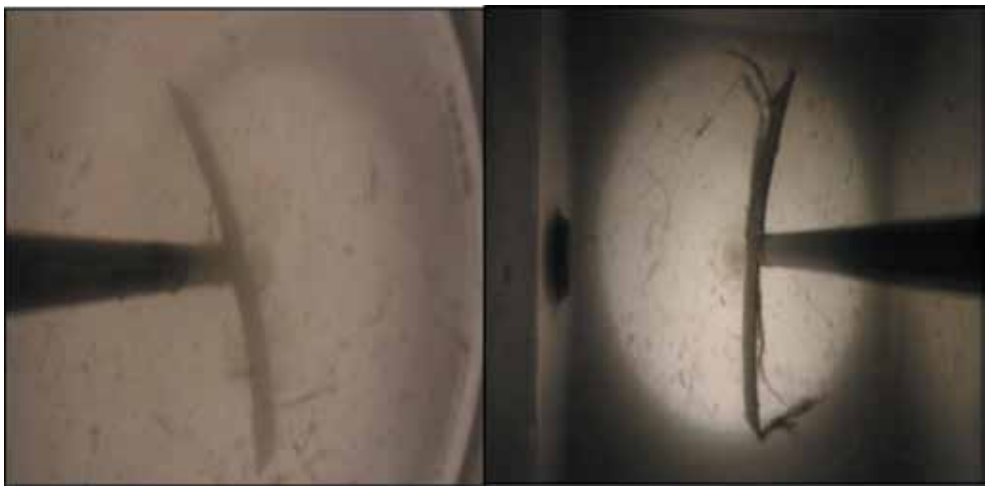

Fig. 6. Flocs formed during coagulation of river water with *Opuntia stricta*.

no significant change in the pH during coagulation process. Insignificant change in the final pH has been reported for *Opuntiaficus-Indica* by Miller et al. and Yang et al. [13, 16].Such performance of *Opuntia stricta* which is independent of water pH along with the least effect on the final pH is unique and favors its practical use.

To explore the effect of *Opuntia stricta* dose on turbidity removal, jar test was performed for both synthetic and natural samples at pH 7.1. Fig. 3 is showing the results of synthetic water, when dose was increased from 2 mg/L to 40 mg/L. It is seen that minimum residual turbidity of 18 NTU was achieved for 2 mg/L dose and the residual turbidity sharply increases by increasing the dose. This implies significant sensitivity of *Opuntia stricta* towards over-dozing. Fig. 4 presents results of coagulation of natural river water sample when *Opuntia* dose is increased from 2 mg/L to 20 mg/L. Turbidity reduced from 105 NTU to minimum of15 NTU for *Opuntia* dose of 10 mg/L. Increased residual turbidity was also observed at high doses for river sample; however, the trend was not as sharp as was in the case of synthetic water.

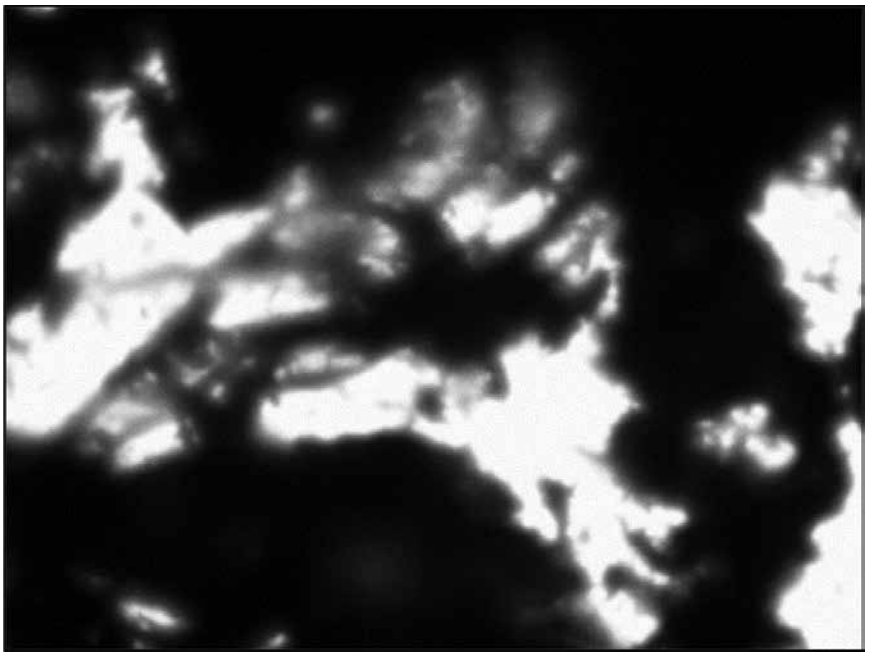

Fig. 7. 50x enlarged view of flocs shown in Fig. 6.

Although, turbidity of the river sample was less than synthetic water, but significant higher requirement of *Opuntia* dose indicates the possible reaction of *Opuntia* with humic substances naturally present in surface waters. Residual turbidities less than 10 NTU were achieved using *Opuntia ficus-Indica* [13, 16]; however *Opuntia stricta* was not able to get such better removal (Fig. 3 to 5). The reason may be the development of a number of smaller flocs which were not able to grow in size or attach with larger flocs,and thereby were unable to settle within 30 minute settling time.

Fig. 6a and Fig. 6b exhibit the floc formation during the coagulation of river water using *Opuntia stricta*. It is observed that large thread like flocs (Fig. 6a) were formed during rapid mix stage, which started diminishing during initial slow mixing but again grew in size (Fig. 6b) as slow mix proceeded. Fig. 7 gives a 50x enlarged view of these flocs under microscope indicating strong binding links within the flocs. Such behavior is only possible with a high molecular-weight polymer with numerous active sites. Linear configuration of the flocs also justifies the inter-particle bridging mechanism of coagulation through *Opuntia* as suggested by Miller et al [13].

4. CONCLUSIONS

Contrary to *Opuntia ficus-Indica*, removal efficiency of *Opuntia stricta* as coagulant for turbidity removal in surface water remains consistent within a wide pH range (pH 5 to 10). Furthermore, pH of the water remains unaffected during coagulation and pH adjustment may not be required for subsequent treatment processes such as filtration or disinfection,which might be needed in case metal coagulants are used. Presence of humic substances in natural surface water may significantly alter *Opuntia*dose for optimal coagulation. *Opuntia stricta* was not able to bring residual turbidity below 10 NTU as achievable through *Opuntia ficus-indica*. However, residual turbidity below 20 NTU is conveniently achieved even at very low doses of *Opuntia stricta*. Therefore, *Opuntia stricta* may prove useful as primary coagulant for subsequent treatment through slow sand filters. However, its efficiency should also be further investigated for water of different qualities in addition to its use as coagulant aid. Analysis of size and nature of flocs achieved through coagulation using *Opuntia stricta*is coherent with the previous suppositions that potential mechanism of coagulation through *Opuntia* is adsorption and inter-particle bridging.

5. ACKNOWLEDGEMENTS

This research publication is based on the post-graduate research conducted at the IEER, UET Lahore. The authors acknowledge the assistance provided by the laboratory staff of IEER.

6. REFERENCES

1. Sorlini, S., D. Palazzini, J.M. Sieliechi & M.B. Ngassoum. Assessment of physical-chemical drinking water quality in the Logone Valley (Chad-Cameroon). *Sustainability* 5(7): 3060-3076 (2013).
2. Memon, M., M.S. Soomro, M.S. Akhtar & K.S. Memon. Drinking water quality assessment in Southern Sindh (Pakistan). *Environmental Monitoring and Assessment* 177: 39–50 (2011).
3. Rahman, I.M.M., M.M. Islam, M.M. Hossain, M.S. Hossain, Z.A. Begum, D.A. Chowdhury, M.K. Chakraborty, M.A. Rahman, M. Nazimuddin & H. Hasegawa. Stagnant surface water bodies (SSWBs) as an alternative water resource for the Chittagong metropolitan area of Bangladesh: physicochemical characterization in terms of water quality indices. *Environmental Monitoring and Assessment* 173: 669–684 (2011).
4. Quagraine, E.K. & C.K. Adokoh. Assessment of dry season surface, ground, and treated water quality in the Cape Coast municipality of Ghana. *Environmental Monitoring and Assessment.* 160:521–539 (2010).
5. Rossiter, H., P.A. Owusu, E. Awuah, A.M. MacDonald & A.I. Schäfer. Chemical drinking water quality in Ghana: Water costs and scope for advanced treatment. *Science of Total Environment* 408: 2378–2386 (2010).
6. Mkandawire, T. Quality of groundwater from shallow wells of selected villages in Blantyre District, Malawi. *Physics and Chemistry of Earth*, Parts A/B/C 33: 807–811 (2008).
7. Tchounwou, P.B., D.M. Lantum, A. Monkiedje, I. Takougang & P. Barbazan. The urgent need for environmental sanitation and a safe drinking water supply in Mbandjock, Cameroon. *Archives of Environmental Contamination and Toxicology* 33: 17–22 (1997).
8. Edzwald, J.K. Coagulation in drinking water treatment: particles, organics and coagulants. *Water Science and Technology* 27: 21–35 (1993).
9. Kang, M.,T. Kamei & Y. Magara. Comparing polyaluminium chloride and ferric chloride for antimony removal. *Water Research* 37: 4171–4179 (2003).
10. Haaroff, J. & J.L. Cleasby. Comparing aluminum and iron coagulants for in-line filtration of cold waters. *Journal of American Water Works Association* 80: 168–175 (1988).
11. Flaten, T.P. Aluminum as a risk factor in Alzheimer's disease, with emphasis on drinking water. *Brain Research Bulletin* 55:187–196 (2001).
12. Yin C.Y. Emerging usage of plant-based coagulants for water and wastewater treatment. *Process Biochemistry 45*(9): 1437-1444 (2010).
13. Miller S.M., E.J. Fugate, V.O. Craver, J.A. Smith & J.B. Zimmerman. Toward understanding the efficacy and mechanism of Opuntia spp. as a natural coagulant for potential application in water treatment. *Environmental Science & Technology* 42(12): 4274-4279, 76 (2008).
14. Jacobo, C.M. & S.P. González. *Castus (Opuntia spp.) as Forage*. FAO Plant Production and Protection Paper 169. Food and Agriculture Organization of the United Nations, Rome (2001).
15. Zhang, J., F. Zhang, Y. Luo & H. Yang. A preliminary study on cactus as coagulant in water treatment. *Process Biochemistry* 41: 122-129 (2006).
16. Yang, Y.C., S.A. Talib, L.Y. Pei, M.S.N. Ismail, S.N.A. Razak & A.M.M. Mohtar. Turbidity removal from surface water and landfill leachate using cactus opuntia. *Institution of Engineers Malaysia (IEM) Journal* 68(1): 61-64 (2007).
17. Buttice, A.L., J.M. Stroot, D.V. Lim, P.G. Stroot & N.A. Alcantar. Removal of sediment and bacteria from water using green chemistry. *Environmental Science & Technology* 44/9: 3514-3519 (2010).
18. WHO. *Guidelines for Drinking Water Quality*, 4th ed. WHO Press, World Health Organization, Switzerland (2011).
19. Weniger, D. *Cacti of Texas and Neighboring States: A Field Guide*, 1st ed. University of Texas Press, Austin, Texas, USA (1984).
20. Gebresamuel, N. & T. Gebre-Mariam. Comparative physico-chemical characterization of the mucilages of two cactus pears (Opuntia spp.) obtained from Mekelle, Northern Ethiopia. *Journal of Biomaterials and Nanobiotechnology* 3(1): 79-86 (2012).
21. Hoffmann, D. *Medical Herbalism: The Science and Practice of Herbal Medicine*. Healing Art Press, Rochester, Vermont, USA (2003).
22. Sáenza, C., E. Sepúlvedaa & B. Matsuhirob. Opuntia spp mucilage's: a functional component with industrial perspectives. *Journal of Arid Environments* 57: 275–290 (2004).
23. Eugene, W.R., B.B. Roger, D.E. Andrew & S.C. Lenore. *Standard Methods for the Examination of Water and Wastewater*, 22nd ed. American Water Works Association/Water Environment Federation, USA (2012).
24. Amirtharajah, A. & C.R. O'Melia. *Water Quality and Treatment*. 4th ed. McGraw Hill Inc, American Water Works Association, New York, USA (1990).

Proceedings of the Pakistan Academy of Sciences 52 (2): 125-134 (2015)

ISSN: 0377 - 2969 (print), 2306 - 1448 (online)

Pakistan Academy of Sciences

Research Article

Evaluating Aquifer Response to Variable Groundwater Pumpage Scenarios in Indus Basin through Finite Element Modeling

Arshad Ashraf[1]*, and Zulfiqar Ahmad[2]

[1]Climate Change, Alternate Energy and Water Resources Institute,
National Agricultural Research Center, Islamabad, Pakistan
[2]Department of Earth Sciences, Quaid-i-Azam University, Islamabad, Pakistan

Abstract: A three-dimensional numerical groundwater flow model was developed using Feflow 5.1 software to investigate the aquifer behavior of Upper Jhelum Canal command under variable scenarios of groundwater pumpage. The results of the study show that the groundwater system is effected by variable conditions of the groundwater pumpage thus influencing the watertable status in the Indus irrigated plain. The groundwater levels indicated sensitivity to both increase in numbers of tubewells and pumpage rates. Although lowering of the watertable due to increase in groundwater pumpage may result in minimizing the negative effects of waterlogging and salinity in the area but other influential factors (physical and management) also need to be investigated in order to reduce future risks of these problems on sustainable basis. A detail investigation of the groundwater system is required in context of increasing number of private/public tubewells and rapidly changing environment in the Indus irrigated plain.

Keywords: Finite element modeling, groundwater system, Indus basin

1. INTRODUCTION

The agriculture production in Pakistan depends on canal irrigation of Indus basin. The canal supplies are not adequate particularly during winter season when rivers discharges are low due to less snowmelt and rainfall. The overall irrigation efficiency is only about 30% [1]. A significant percentage of irrigated area is totally dependent on groundwater alone and the larger part of it is used in conjunction with surface water supplies [2]. The induction of local diesel engines along with subsidized power supply resulted in rapid growth in numbers of private tubewells e.g. increase from 10,000 to about 0.8 million within 1960-2006 period. The total groundwater abstraction from these tubewells is estimated at $51x10^9$ m^3 against a recharge of 40 – $60x10^9m^3$ [3]. Out of this, about $33x10^9m^3$ is extracted through private tubewells whereas the rest $18x10^9$ m^3 comes from large capacity public tubewells [4]. The total estimated recoverable groundwater potential is about 67.84 BCM (55 MAF). This leaves about 8.63 BCM (7 MAF), which remains to be exploited [5]. Although, exploitation of the useable groundwater has provided an opportunity for the farmers to supplement their irrigation requirements but the problem of overdraft of the aquifers has emerged in many areas of the Indus basin due to uncontrolled and unregulated use of groundwater [6]. In some of the central and southern parts of Chaj Doab in Indus basin, waterlogging and salinity have also created a problem mainly due to high seepage from canal system, ineffective water management practices and poor drainage system. The main cause behind some of these groundwater problems might be non-synchronization of the groundwater resource management and its development [7]. Tariq and Latif [8] studied the optimal management

Received, July 2013; Accepted, February 2015
*Corresponding author: Arshad Ashraf; Email: mashr22@yahoo.com

of groundwater and suggested various strategies for management under high watertable areas and declining watertable areas. Alam and Chaudhry [9] studied the environmental issues relative to groundwater management and presented guidelines for its environmental sustainability. There is a need to study the groundwater behavior under different stress conditions of discharge for sustainable management and use of groundwater in the Indus basin area in future.

The technique of groundwater modeling is known as a powerful tool to evaluate groundwater systems quantitatively. The finite element method (FEM) has been adopted as an effective tool to solve groundwater problems in various fields like civil engineering [10] and groundwater hydrology [11]. In this method, the domain is discretized into regular elements where heads/concentrations are computed on each node of the flow domain. In this paper, response of the groundwater aquifer has been studied under different scenarios of groundwater withdrawals for effective water management and coping situation of groundwater depletion in the target Indus basin area.

1.1 Study Area

The study area of Upper Jhelum Canal command lies within longitudes 73° to 74° 5′ E and latitudes 32° to 32° 45′ N in the Indus plain of Punjab, Pakistan (Fig. 1). The area comprises of Mandi Bahauddin and part of Gujrat districts between Jhelum and Chenab Rivers. It is fairly level and slopes towards southwest direction. The elevation ranges within 200-238 meters above sea level (masl). Major landforms in the area include alluvial plain and bar uplands while piedmont plain and sub-mountainous ravines exist over minor area in the north. The area is mainly irrigated by canal system. Under irrigation by water wells, the main crops are wheat, sugarcane, tobacco and fodder [12]. The climate is generally sub-humid to semi-arid. Rainfall is erratic and the mean annual is about 778 mm. About two third of the rains are received during monsoon period i.e. between July and mid September. In summer, the mean maximum temperature is about 39.5°C and mean minimum temperature is about 25.4°C while in winter, the mean maximum and minimum temperatures are about 21.5°C and 5.1°C [13].

1.2 Hydrogeology

The Chaj Doab belongs to Indus plain that form part of Indo-Gangetic Syncline [14] where Quaternary alluvium is deposited over semi-consolidated Tertiary rocks [12]. The area's groundwater reservoir is contained almost exclusively in the alluvial deposits. The general flow of the groundwater is from NE to SW direction. Hydraulic gradient ranges between 0.4-1.35 m/km [15]. There is a vast unconfined aquifer underlying around 6 million ha. The watertable exhibits an annual cycle of rise and fall. It is lowest in the period prior to the monsoon (April-June) and as a result of the Kharif canal supplies and the effect of the rains, it rises and comes closest to the land surface in October before declining again. The watertable of April-June is used as index of waterlogging because it persists throughout the year. There lie three schemes of SCARP-II project of WAPDA namely Sohawa, Phalia and Busal (Fig. 1) where SCARP tubewells were operating to reduce waterlogging in the area. The aquifer data of 10 test holes of WAPDA [16] was used to estimate base conditions for model simulation in this study. According this data, the horizontal hydraulic conductivity ranges from 39.6 m/day to 118.6 m/day while transmissivity (T) values range within 1565.2-4045.6 m^2/day in the study region.

The main recharge sources include seepage from the canal system, precipitation, return flow and seepage from watercourses and fields. Aquifer discharge sources are groundwater pumpage, evapotranspiration, outflows to drains and the rivers, and subsurface flows from the model domain. The groundwater is mainly obtained through hand pumps i.e. from depth of 2.5-8 m and through shallow tubewells i.e. from depth of 32-40 m for domestic and irrigation purpose [13].

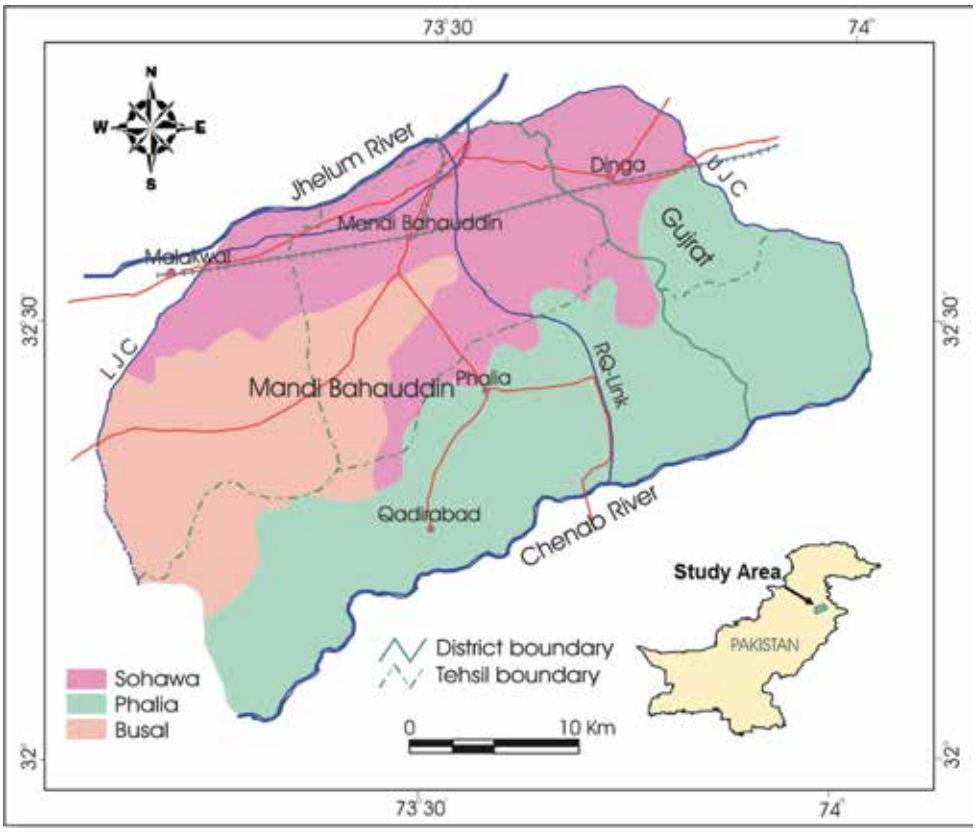

Fig. 1. Location map of the study area.

A large number of electric and diesel tube wells are functioning besides numerous hand pumps in the area. The data of public tubewells is fairly accurate but the pumpage from private tubewells is based on sporadic surveys carried out by various organizations at one time or the other.

2. MATERIALS AND METHODS

2.1 Conceptual Model of Groundwater Flow

A conceptual model represents different aspects of the physical hydrogeological system along with its hydrological behavior in a simplified and an adequate manner [17]. However in developing an adequate conceptual model, sufficient degrees of freedom need to be incorporated in a model to allow simulation of a broad range of responses. Based on the characteristics of subsurface lithology and groundwater pumpage from various tubewells, three layers were defined in the aquifer: 1) The first layer which contains mainly fine material (silt and fine sand) is assumed to have 8 m depth below the average watertable, 2) The second layer extends from 8 m to 40 m depth representing zone of groundwater pumpage from relatively shallow tubewells and, 3) The groundwater zone within 40-107 m depth from where the pumpage from deep tubewells is made.

The first layer was simulated as an unconfined unit, the second layer as convertible from a confined to an unconfined unit depending upon the position of the watertable, while the third layer is treated as a confined unit of the aquifer. Canal seepage has been observed as a major source of recharge in the study area. Groundwater in the irrigated areas is derived mostly from seepage from the conveyance system and fields and as such its renewability is dependent on the availability and use of surface supplies.

2.2 Galerkin's Method

In finite element model (FEM), the major goal is not just to approximate the governing equation but rather is to approximate the solutions [18]. Galerkin

method of weighted residuals is the main function operating behind the FEM that attains the best approximate solution for the finite element mesh by reducing the weighted sum of the residuals for each of the finite elements. Galerkin's method and the finite element technique are combined so frequently in computer solutions of groundwater problems that the two have become practically synonymous. The method is based on a particular weighted residual principle which turns out to be equivalent to a variational principle, if one exists for the problem under consideration [19]. The nodal heads are obtained as the solution of a system of algebraic equations if a particular weighted average of the residual is forced to vanish. The first step is to define an approximate or trial solution, $\hat{h}$ (x,y) expressed as a series summation; each term is a product of a nodal head h_L and an associated nodal basis function N_L(x, y) (Equation a)

$$\hat{h}(x, y) = \sum_{L=1}^{NNODE} h_L N_L(x, y) \quad \text{(a)}$$

The subscript *L* indicates nodal number and *NNODE* is the total number of nodes in the problem domain.

The next step is to require a total of *NNODE* conditions to determine the *NNODE* values of h_L. In the Galerkin's method, the *NNODE* conditions are that the residuals of the governing equation weighted by each of the *NNODE* basis functions be zero when integrated over the entire domain of the problem (Equation b).

$$\iint_D \left(\frac{\partial^2 \hat{h}}{\partial x^2} + \frac{\partial^2 \hat{h}}{\partial y^2} \right) N_L(x, y) dxdy = 0 \quad \text{(b)}$$

Where L = 1, 2,.... , *NNODE*, and *D* signifies that the integration is done over the entire problem domain. The quantity in parentheses is the residual. If the trial solutions $\hat{h}$(x, y) were exact, Laplace's equation would be satisfied throughout the problem domain and the residual would be zero everywhere. In Galerkin's method, the requirement imposed is that *NNODE* weighted average of the residual vanish; the basis function N_L(x, y) are the weighting functions.

2.3 Development of Groundwater Flow Model

A three-layered 3-D numerical groundwater flow model was developed using Feflow 5.1 software [20]. The active area of the model is about 3,417.2 km^2. The finite element model comprised of 5,343 elements and 3,928 nodes was generated from mesh of 5 super elements drawn over the model area. The super elements mesh represents the basic structure of the study domain. The model area with locations of 34 observation wells is shown in Fig. 2. The rivers and main canals are treated as constant head boundaries in the numerical groundwater flow model. In vertical discretization of the grid, topographic surface defines the upper boundary and the alluvium cover up to 107m depth the lower boundary of the aquifer. Ten hydraulic conductivity zones were developed using Thiessen polygon method from the point data of hydraulic conductivity values obtained from pumping tests analysis. Based on the hydrological setup, geomorphology and land capability of the area, 5 recharge zones were developed to estimate the recharge in the model domain (Fig. 2).

The steady-state simulation of groundwater flow was performed, which is fully implicit. The steady-state modeling refers to the arrival of a condition in the groundwater regime when hydraulic heads are no longer changing and the magnitude and direction of the flow velocity becomes constant with time [21]. The model was calibrated for steady-state simulation using initial conditions through Parameter estimation 'PEST' module [22] in Feflow model. Later, the model was rerun for transient-state calibration for a six-month period. The sensitivity analysis was carried out to evaluate performance of various parameters and model assumptions. The flow chart of methodology followed for groundwater modeling modified after [23] is shown in Fig. 3. The steady-state calibrated model was rerun for pre-stress period of variable time steps until 2005. The average watertable values (the spatial average over the whole region) was used

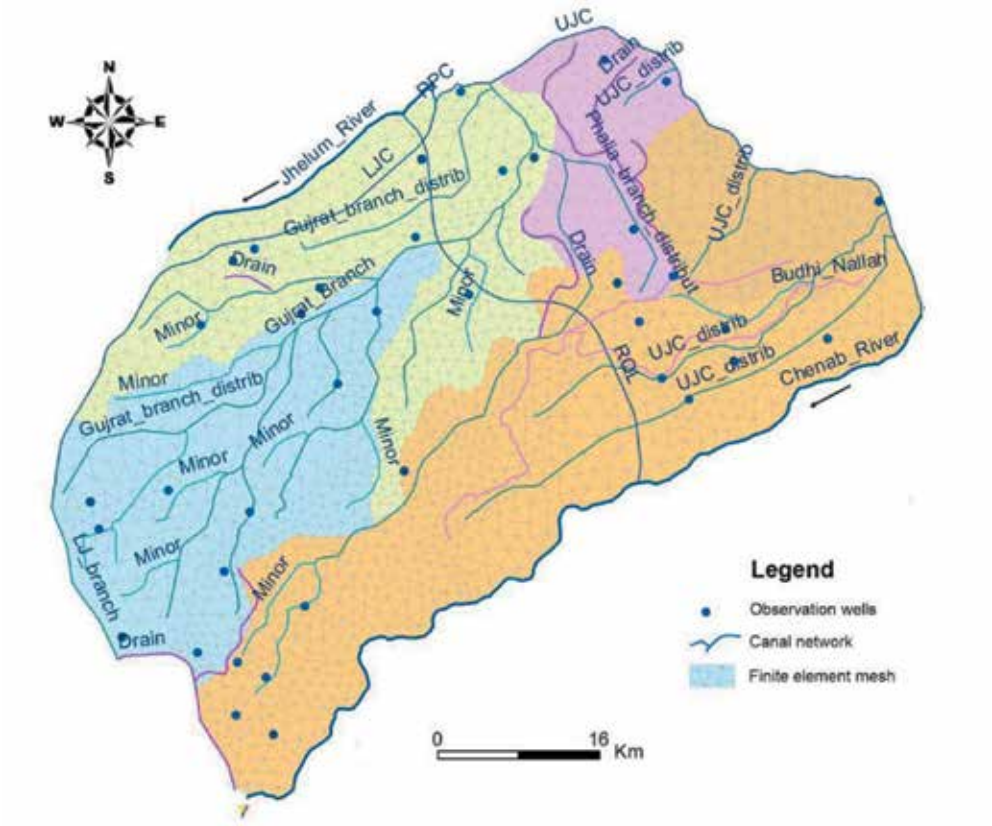

Fig. 2. Location of the observation wells and canal network in various recharge zones of the model domain.

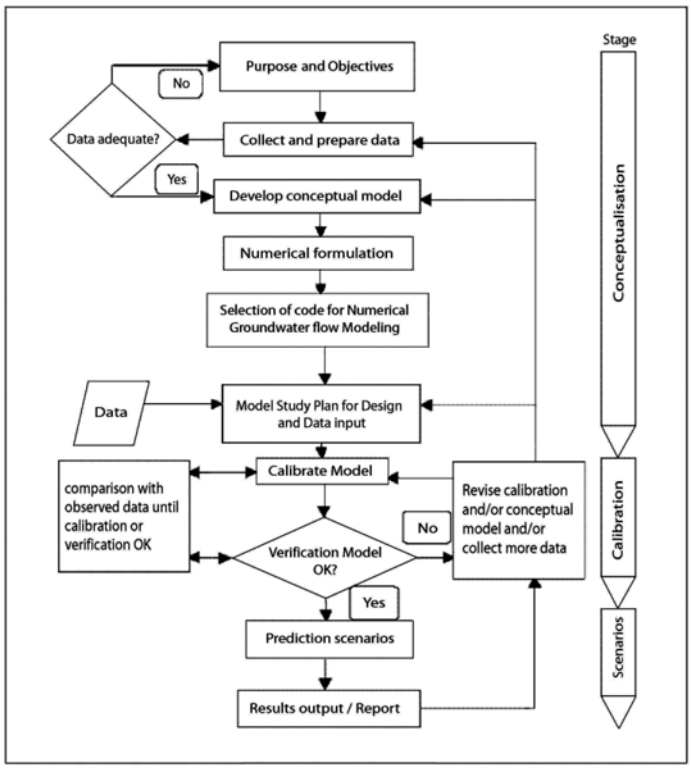

Fig. 3. Flow chart of numerical modeling steps followed in the present study. Modified after [23].

to foresee the overall effect of the watertable in the model domain. Different scenarios of groundwater pumpage were developed to analyze its effect on the groundwater levels of base year 2005.

3. RESULTS AND DISCUSSION

During the calibration phase, the mean residual of 0.06 m and variance of 1.46 m was achieved for observed and calculated heads of the steady-state model. Similarly, the mean residual and variance obtained during transient-state calibration were 0.002 m and 1.86 m respectively. The equipotential surface map of steady-state condition indicated an overall groundwater flow from northeast towards southwest direction following the trend of topographic relief (Fig. 4). The hydraulic conductivity values estimated through calibration of steady-state simulation varied from 2 to 158 m/day for layer 1; 2 to 153 m/day for layer 2; and 0.7 to 168 m/day for layer 3 with mean values of 69.3, 72.2, and 74 m/day, respectively. In layer 1, high velocity of groundwater (>0.12 m/day) was observed near Rasul Barrage. The velocity in the center and southern parts varied between 0.04 m/day and 0.08 m/day. The patches of low velocity zone (<0.02 m/day) were found in northern, northeastern and western parts which extend downward in other layers also. In layer 2, velocity zone 0.02-0.04 m/day dominates in most of the central part while the zone 0.04-0.08 m/day has reduced into a narrow belt in the centre and appears in the southern part of the area. In layer 3, velocity less than 0.02 m/day dominates in most of the northeastern part, 0.02-0.04 m/day in the center and 0.04-0.08 m/day in the southern part of the model area. The variations in the velocity of groundwater flow in each layer of the model domain are shown in Fig. 5. The regional groundwater flow component in the southern part is indicating existence of a potential aquifer zone in this area. The low velocity zone (<0.02 m/day) in the northeastern and western parts exists more or less in all the three layers thus indicating low potential of aquifer here.

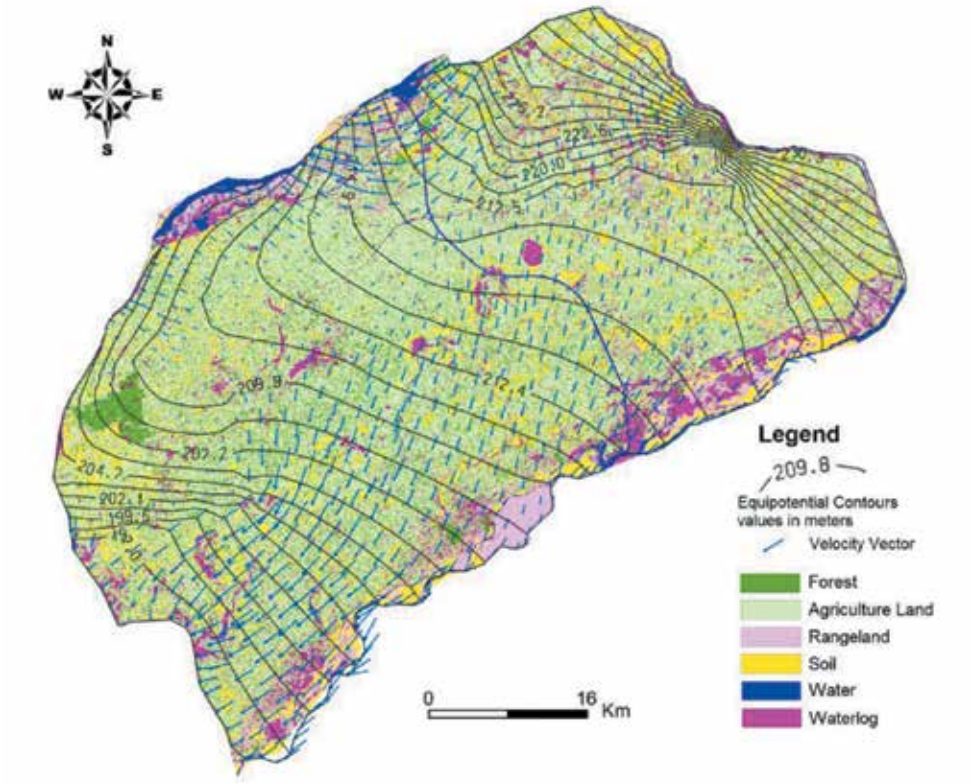

Fig. 4. Velocity vectors and equipotential contours indicating groundwater flow pattern (2005).

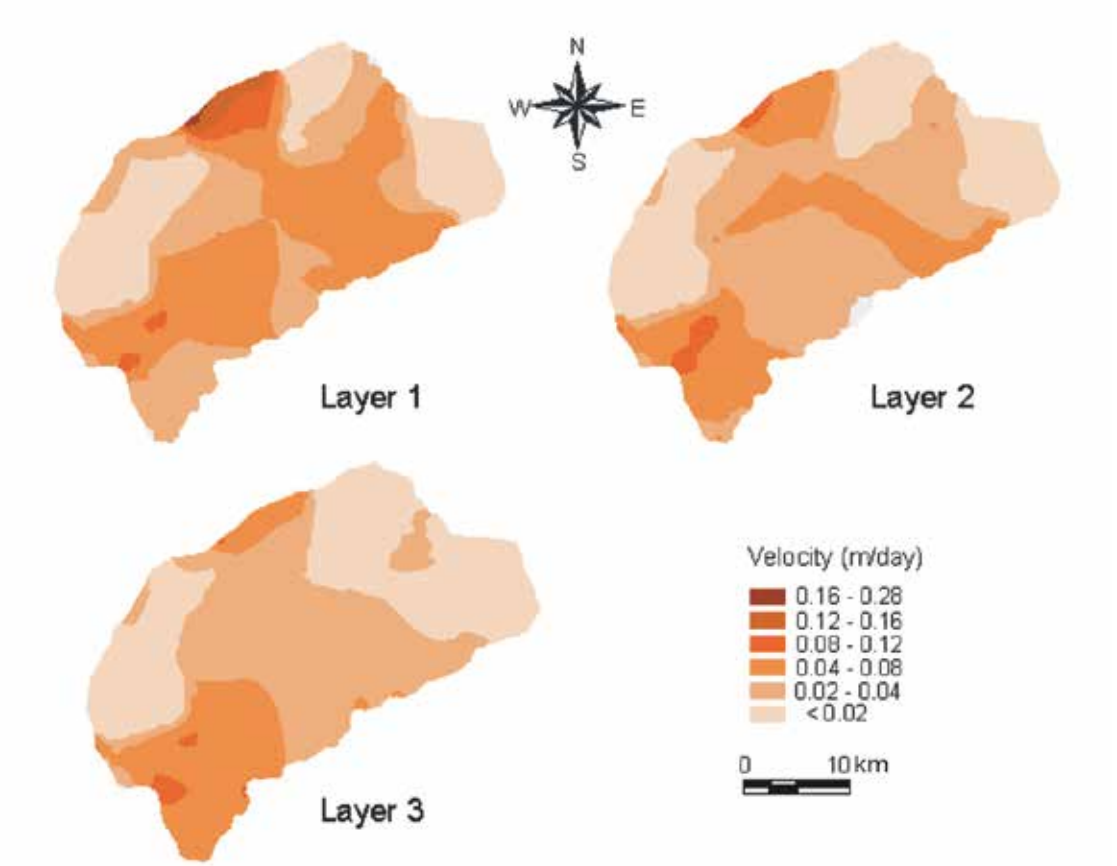

Fig. 5. Groundwater flow velocity during the steady-state condition.

In layer 1, the specific yield values vary between 0.06 - 0.15, in layer 2 between 0.04 - 0.22, and in layer 3 between 0.76 - 0.27. Mean of specific yield values for layer 1 and layer 2 appear to be 0.1 and for layer 3 is 0.15. The lower values in zones 3 and 4 can be attributed to the presence of piedmont deposits containing intercalation of clay and fine silt and sand. Likewise, the higher values of specific yield in zone 6 may represent thick alluvium deposits of medium to coarse sand, and gravels.

3.1 Scenarios of Groundwater Pumpage

The calibrated model of 1985-2005 period were used to predict future changes in average groundwater levels of the target area. The following scenarios were developed to analyze the groundwater behavior under varying tubewell pumpage conditions. The watertable depth of year 2005 was used as base for the analysis.

***Scenario 1*:** In this scenario the pumpage from 33 deep tubewells continued at a constant rate of 5,000 m^3/d from 1 to 3 years period and its impact on the groundwater levels of base year was studied. The groundwater levels indicated an average decline from 0.04m in the 1st year to 0.135m in the 3rd year (Table 1, Fig. 6).

***Scenario 2*:** The pumpage is increased upto 60 percent (at constant rate of 8,000 m^3/d) and continued from 1 to 3 years period. The increase in pumpage rate accelerated the watertable decline process. The average decline in groundwater levels was about 132%, 116% and 87% from that of 1st, 2nd and 3rd year decline values of the scenario-1.

***Scenario 3*:** In this scenario, numbers of tubewells was increased two folds i.e. 66 and pumpage continued at a constant rate of 5,000 m^3/d from 1

Table 1. Summary of different scenarios of watertable variations (Base watertable depth: 2.95 m).

Scenario	Particulars	Year	Change in Watertable depth (m)
1	Groundwater pumpage from 33 TWs	1	-0.044
		2	-0.086
		3	-0.135
2	60% increase in pumpage from 33 TWs	1	-0.102
		2	-0.186
		3	-0.252
3	Groundwater pumpage from 66 TWs	1	-0.158
		2	-0.293
		3	-0.413
4	60% increase in pumpage from 66 TWs	1	-0.285
		2	-0.509
		3	-0.706

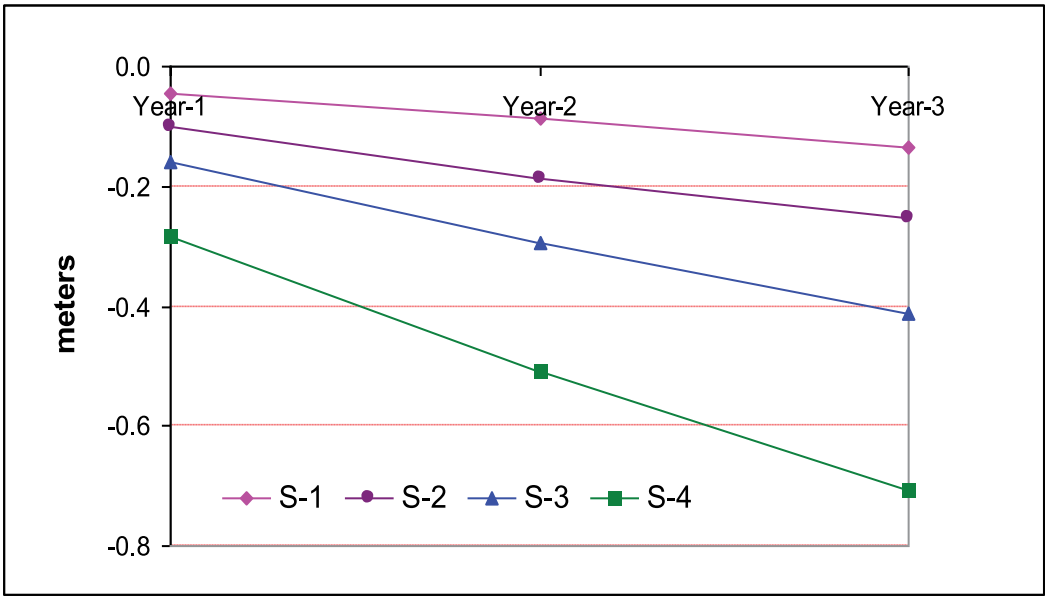

Fig. 6. Watertable response under different scenarios of groundwater pumpage during 3-year period.

to 3 years period. The decline of watertable ranges from 0.158 to 0.413m during 1-3year period from that of base year. This was about 259%, 241% and 206% from that of 1st, 2nd and 3rd year decline values of the first scenario. The situation shows a rapid effect of increase in tubewells use on the groundwater levels in the target area.

***Scenario 4*:** The pumpage increased to 60 percent and continues from 1 to 3 years period. The decline of watertable was observed which ranged from 0.285 to 0.706 m during 1-3 year period from that of base year. The average decline in groundwater levels was about 548%, 492% and 423% from that of 1st, 2nd and 3rd year decline values of the scenario-1.

4. CONCLUSIONS

A 3-dimensional numerical groundwater flow model calibrated for Upper Chaj Doab in Indus basin indicated mean residuals of 0.06 m and

0.002 m between the observed and calculated heads during steady-state and transient-state modeling respectively. The results of the study show that groundwater system is affected by variable conditions of groundwater pumpage thus influencing the groundwater levels in the Indus irrigated area. During the process of groundwater flow modeling, the groundwater levels indicated sensitivity to both increase in numbers of tubewells and pumpage rates. In areas of gradual decline in groundwater due to over exploitation, introduction of water efficient crops and shifting in the cropping pattern can be a few options to increase the water productivity in future. Although lowering of the watertable due to increase in the groundwater pumpage may result in minimizing the high risk of waterlogging and salinity in the area but other influential factors (physical and management) also need to be investigated in order to cope with these problems efficiently in future. A detail investigation of the groundwater system is required to study the impact of growing number of private/public tubewells in the Indus irrigated area. The study findings would help in formulating effective groundwater monitoring and management strategies to ensure sustainable development in the Indus basin in future.

5. ACKNOWLEDMENTS

The data and technical support provided by Water and Power Development Authority (WAPDA) and National Engineering Services Pakistan (NESPAK) are highly appreciated. The valuable input from Prof. Dr. Gulraiz Akhtar. Chairman, Department of Earth Sciences, Quiad-i-Azam University, Islamabad is acknowledged gratefully.

6. REFERENCES

1. Bhutta, M.N. & L.K. Smedema. One hundred years of waterlogging and salinity control in the Indus valley, Pakistan: a historic review. *Irrigation and Drainage* 56: 581-590 (2007).
2. Qureshi, A.S., H.M. Rust & I. Masih. An analytical approach to estimate groundwater punpage. In: *Proceedings of 2nd South Asian Water Forum*, Islamabad, Dec. 2002. pp. 1-11 (2002).
3. World Bank. *Punjab Groundwater Policy- Mission Report*. WB_SA_PK_Punjab GW Mission report, www.worldbank.org/gwmate (2007).
4. Qureshi, A.S., M.A. Gill & A. Sarwar. Challenges and opportunities for sustainable groundwater management in Pakistan. In: *Proceedings of 1st Int. Conf. on Sustainable Water Management in Developing Countries: Challenges and Opportunities*, MUET, Jamshoro, 15-17 Sep. (2010).
5. Lashari, B. & M.N. Mangrio. Sustainability of shallow groundwater tubewells: A case study of Dhoro Naro Minor Command Area of Sindh, Pakistan. In: *Proceedings of 2ns South Asian Water Forum*, Islamabad, Dec. 2002, p. 84 (2002).
6. Kijne, J. W. *Improving the Productivity of Pakistan's Irrigation: The Importance of Management Choices*. International Water Management Institute, Colombo, Sri Lanka (1999).
7. Qureshi, A.S., T. Shah & M. Akhtar. *The groundwater Economy of Pakistan.* Working Paper 64. Lahore, Pakistan: International Water Management Institute (2003).
8. Tariq, A.R. & M. Latif. *Strategies and Optimal Management of Groundwater and Regulation of Groundwater in the Punjab*, Dec 6-7, 1999. Punjab Groundwater Consultant, Lahore, p. 33-50 (1999).
9. Alam, M.M. & M.R. Chaudhry. *Groundwater Management: Environmental Issues*. Proceedings of Workshop, the Management and Regulation of Groundwater in the Punjab. Dec. 6-7, 1999, Punjab Groundwater Consultant, Lahore, pp. 14-32 (1999).
10. Zeinkiewicz, O.C. *The Finite Element Method in Engineering Science*. McGraw-Hill, London (1971).
11. Segerlin, L.J. *Applied Finite Element Analysis*. J. Wiley & Sons, New York (1976).
12. Soil Survey of Pakistan. *Reconnaissance soil survey of Gujrat district.* Directorate of Soil Survey of Pakistan, Lahore (1967).
13. Qureshi, M.K.A. et. al. *Geology and Environmental concerns of the Rasul-Mandi Bahaudin Quadrangle, Punjab, Pakistan*. Ministry of Petroleum and Natural Resources, Geological Survey of Pakistan, Quetta, Pakistan (2003).
14. Wadia, D.N. *Geology of India*. The English Language Book Society and Macmillan & Co., London (1966).
15. PPSGDP Report. *Groundwater Flow and Solute Transport Numerical Models for SCARP II and Shahpur Area of Chaj Doab*. Tech. Rep. No. 39, Punjab Private Sector Groundwater Development Project Consultants, Project Management Unit, Irrigation and Power Department, Govt. of Punjab, Lahore (2000).
16. WASID. *Analysis of Aquifer tests in the Punjab Region of West Pakistan*. Water and & Soils Investigation Division, Water and Power

Development Authority, Lahore (1964).
17. Middlemis. *Groundwater Flow Modeling Guidelines, Murray-Darling Basin Ccommission*. Aquaterra Consulting Pvt, Ltd, S. Perth, Western Australia (2000).
18. Thangarajan, M. *Regional Groundwater Modeling*. Capital Publishing Company, New Delhi, India (2004).
19. Wang, H.F. & M.P. Anderson. *Introduction to Groundwater modeling- Finite Difference and Finite Element Methods*. W.H. Freeman and Company, New York (1982).
20. WASY. *Feflow 5.1 Finite Element Subsurface Flow & Transport Simulation System User's Manual*. WASY Institute for Water Resources Planning and Systems Research Ltd., Berlin, Germany (2004).
21. Freeze R.A. & J.A. Cherry. *Groundwater*. Prentice Hall, (Englewood Cliffs, NJ, USA1979).
22. Doherty, J. *PEST ver. 2.04*. Water mark Computing, Corinda, Australia (1995).
23. Anderson M.P. & W.W. Woessner. *Applied Groundwater Modeling, Simulation of Flow and Advective Transport*. Academic Press, San Diego, California (1992).

Proceedings of the Pakistan Academy of Sciences 52 (2): 135-144 (2015)

ISSN: 0377 - 2969 (print), 2306 - 1448 (online)

Pakistan Academy of Sciences

Research Article

Numerical Solution for Hydromagnetic Viscous Fluids Flow Between Two Horizontal Stretching Sheets

S. Hussain[1, *], M. A. Kamal[2], and F. Ahmad[1]

[1]Department of Mathematics, College of Science Al Zulfi, Majmaah University, Kingdom of Saudi Arabia
[2] Department of Mathematics, Suleman Bin Abdul Aziz University, Al-Kharj, Kingdom of Saudi Arabia

Abstract: The numerical solution has been obtained for the hydromagnetic flow of an incompressible, steady and viscous fluid between two stretching sheets in the presence of variable surface temperature. The governing highly nonlinear partial differential equations are reduced to ordinary differential form by using similarity functions. The resulting equations are solved by using Successive Over Relaxation (SOR) method and Simpson's (1/3) rule. The results have been improved by Richardson extrapolation. The effects of flow parameters namely magnetic parameter M, the Reynolds number R, the suction parameter λ, Prandtl number P_r and temperature index parameter n have been observed on velocity and temperature distribution.

Keywords: Flow between plates, hydromagnetic fluid, Reynolds number, suction parameter, Richardson extrapolation

1. INTRODUCTION

Studies of fluids flow induced by stretching boundaries and heat transfer have relevance to some important applications such as extrusion process and production of plastic sheets. The quality of final product can be improved with proper adjustment of cooling and heat transfer. Hence, for slower rate of solidification, the application of magnetic field is useful because of its easy implementation. The effect of magnetic field in different engineering applications such as the cooling of reactors and many metallurgical processes involve the cooling of continuous tiles has been under more considerable attention. Ganji et al [1] reported the analytical solution of the magneto-hydrodynamic flow over a nonlinearly stretching sheet. Ahmad et al [2] obtained closed form solution for a viscous, incompressible, MHD flow over a porous stretching sheet. Baag et al [3] analyzed MHD flow on a stretching sheet embedded in a porous medium. The fluid flow problems about stretching surface have been studied extensively in various topics such as porous medium, MHD flows, heat transfer and non-Newtonian fluids.

Several engineering processes, such as materials manufactured by extrusion processes and heat-treated materials traveling between a feed roll and a wind-up roll on convey belts possess the characteristics of a moving continuous surface. Sakiadis [4, 5] examined the boundary layer flow on a continuously stretching surface with a constant speed. Erickson et al [6] extended the work of Sakiadis to include blowingorsuction at the stretched sheet surface on a continuous moving surface with constant speed and investigated its effects on the heat and mass transfer in the boundary layer. Crane [7] found an exact solution of two-dimensional Navier-Stokes equation for a stretching plate. Chiam [8] analyzed steady two dimensional oblique stagnation point flow of a viscous fluid. The magneto-hydrodynamic flow

Received, September 2013; Accepted, March 2015
*Corresponding author: S. Hussain; E-mail: sajjad_h96@yahoo.com

over a stretching surface has been studied extensively [9-12] for both permeable and impermeable surfaces. Flow of an electrically conducting non- Newtonian fluid past a stretching surface was studied by Able et al [13], when a uniform magnetic field acts transverse to the surface. Kumaran et al [14] obtained an exact solution for a boundary layer flow of an electrically conducting fluid past a quadratically stretching and linearly permeable sheet. Sheikholeslami et al [15] analyzed hydromagnetic flow between two horizontal plates in a rotating system, where the lower plate is a stretching sheet and the upper is a porous solid plate and studied heat transfer in an electrically conducting fluid bounded by two parallel plates is in the presence of viscous dissipation using Homotopy perturbation method. Pandya [16] considered hydro-magnetic flow between two horizontal plates in a rotating system where the lower plate is a stretching sheet and obtained numerical solution for the governing coupled ordinary differential equations by employing quantic spline collocation method. Chakrabarti and Gupta [17] studied the hydromagnetic flow and heat transfer in a fluid, initially at rest and at uniform temperature, over a stretching sheet at a different uniform temperature. Banerjee [18] studied the effect of rotation on the hydromagnetic flow between two parallel plates where the upper plate is porous and solid, and the lower plate is a stretching sheet. Arthur and Seini [19] investigated the hydromagnetic stagnation point flow of an incompressible viscous electrically conducting fluid towards a stretching sheet in the presence of radiation and viscous dissipation.

In this research paper, hydromagnetic fluid flow between two horizontal stretching plates has been examined. The non linear coupled equations governing the flow and heat transfer have been solved numerically by using a very simple and efficient numerical scheme. The effects of the physical parameters of the study namely M, R, λ, Pr and n have been noticed on velocity and temperature function.

2. MATHEMATICAL ANALYSIS

Consider steady, incompressible fluid flow between two horizontal parallel non-conducting plates, the lower one is a stretching sheet and the upper one is a porous stretching. Cartesian coordinate system is used where the y-axis is perpendicular to the plates located at y=h, y=-h. The fluid with constant velocity V_0 is injected through the upper porous plate. Two equal and opposite forces are introduced to stretch the lower and the upper plates in a way that the position of the points (0, h), (0, -h) remains fixed. A uniform magnetic field of strength B_0 is applied in the positive y-direction normal to the stretching sheet. The external electric field is zero and the electric field due to polarization of charges is negligible. The induced magnetic field is neglected which is valid for small magnetic Reynolds number. The temperature of the fluid at the surface of the lower sheet is $T_w(x) = T_\infty + cx^n$. The heat flux boundary conditions are used and viscous dissipation is neglected. Here c and n are constants with c>0 stands for heated surface and T_∞ is ambient fluid temperature. The geometry of the problem is depicted in Fig. 1.

Under the above assumptions the equations of motion become as:

$$\frac{\partial u}{\partial x} + \frac{\partial v}{\partial y} = 0 \tag{1}$$

$$u\frac{\partial u}{\partial x} + v\frac{\partial u}{\partial y} = -\frac{1}{\rho}\frac{\partial p}{\partial x} + \nu\left(\frac{\partial^2 u}{\partial x^2} + \frac{\partial^2 u}{\partial y^2}\right) - \frac{\sigma B_0^2}{\rho}u \tag{2}$$

$$u\frac{\partial v}{\partial x} + v\frac{\partial v}{\partial y} = -\frac{1}{\rho}\frac{\partial p}{\partial y} + \nu\left(\frac{\partial^2 v}{\partial x^2} + \frac{\partial^2 v}{\partial y^2}\right) \tag{3}$$

$$u\frac{\partial T}{\partial x} + v\frac{\partial T}{\partial y} = \alpha\left(\frac{\partial^2 T}{\partial y^2}\right) \tag{4}$$

where u, v are velocity components and T is fluid temperature, ν and α are kinematic viscosity and thermal diffusivity, respectively and the relation for electromagnetic body force as given by Rossow [20] is $\underline{J} \times \underline{B} = \underline{E}\sigma(\underline{V} \times \underline{B}) \times \underline{B} = -\sigma B^2 \underline{V}$

The boundary conditions are:

$$u = cx, v = 0, \; -\frac{\partial T}{\partial y} = \frac{T_w - T_\infty}{h}$$

at y=-h , $c > 0$

u=cx, v=V_0 , $T = T_\infty$ at y=h , $c > 0$ (5)

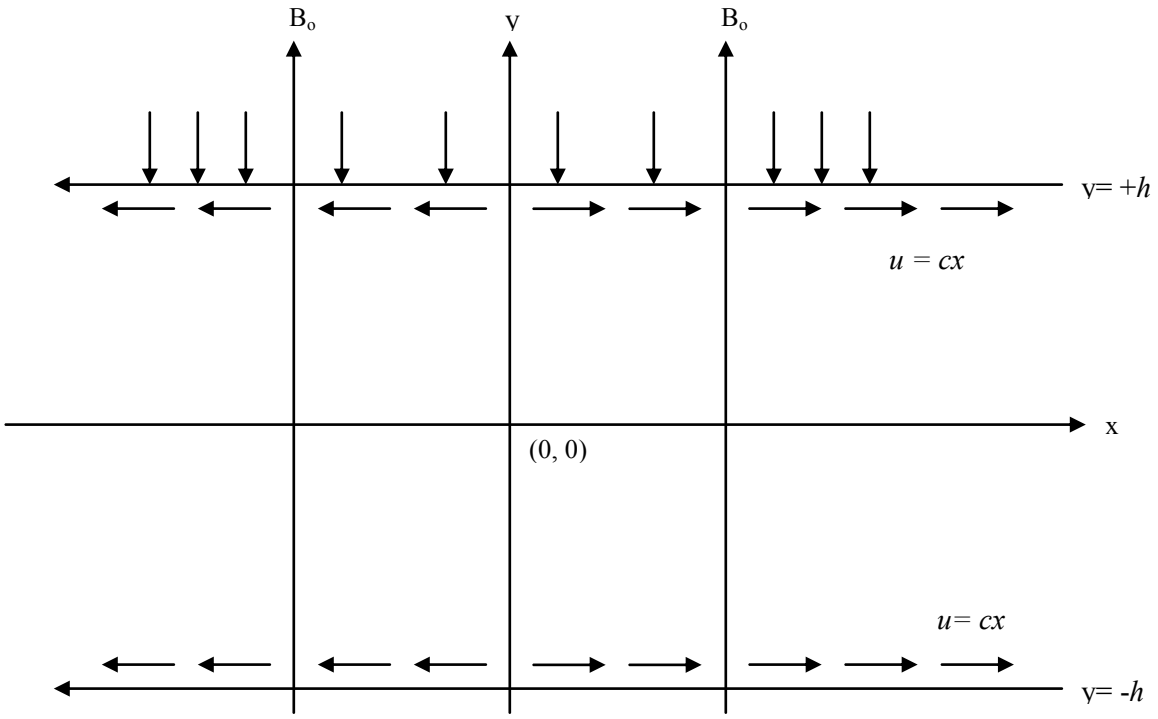

Fig. 1. Geometry of the problem.

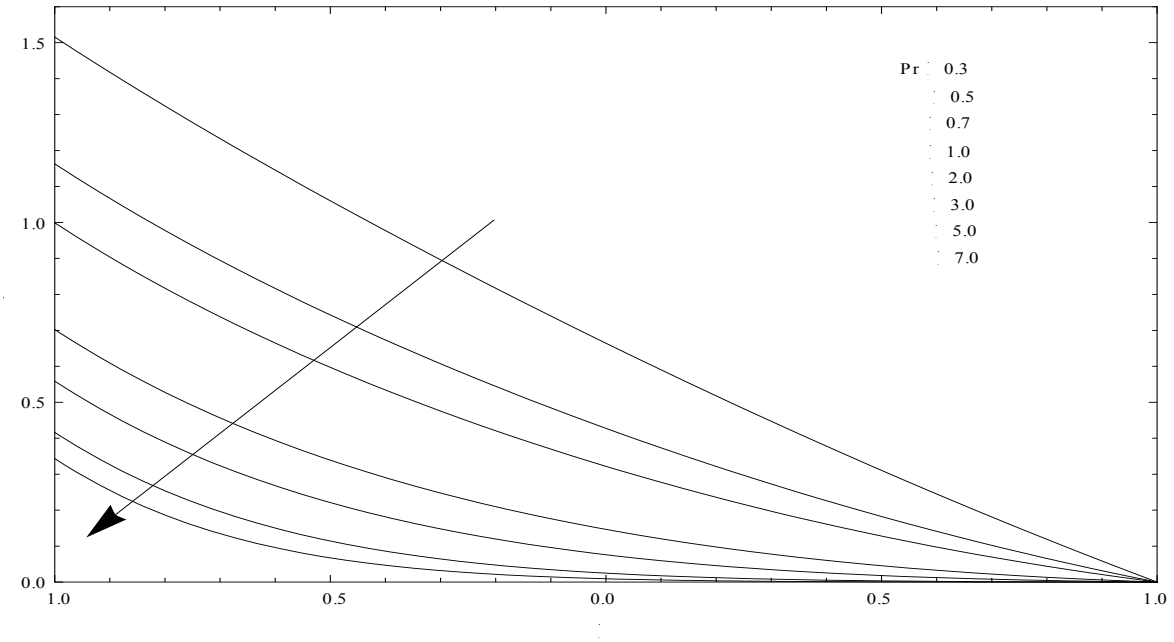

Fig. 2. Graph of θ for different values of *Pr* when *M*=1, *R*=0.05, λ =1, *n*=1.

Using similarity transformations:

$$u = cxf'(\eta), v = -chf(\eta), \eta = \frac{y}{h},$$

$$\theta(\eta) = \frac{T - T_\infty}{T_w - T_\infty} \tag{6}$$

where the primes denote differentiation with respect to η and $u = cx$ represents the velocity of both the plates. Equation of continuity (1) is identically satisfied.

Substituting (6) in to equations (2) and (3), we have

$$-\frac{1}{\rho}\frac{\partial p}{\partial x} = c^2 x(f'^2 - ff'' - \frac{1}{R}f''' + \frac{M^2}{R}f') \tag{7}$$

$$-\frac{1}{\rho h}\frac{\partial p}{\partial \eta} = c^2 h(ff' + \frac{1}{R}f'') \tag{8}$$

Now, differentiating equation (7) with respect to η and equation (8) with respect to *x*, we obtain

$$f^{iv} - R(f'f'' - ff''') - M^2 f'' = 0 \tag{9}$$

The integration of equation(9) yields,

$$f''' - R(f'^2 - ff'') - M^2 f' = A \tag{10}$$

Where *A* is the constant of integration and equation(4) becomes as:

$$\theta'' + \Pr(f\theta' - \eta f'\theta) = 0 \tag{11}$$

The corresponding boundary conditions are:

$$\begin{aligned} &f(-1) = 0, \quad f'(-1) = 1, \quad \theta'(-1) = -1 \\ &f(1) = \lambda, \quad f'(1) = 1, \quad \theta(1) = 0 \end{aligned} \tag{12}$$

3. COMPUTATIONAL PROCEDURE

For numerical purpose, we reduce the order of ODE (10) and let,

$$f' = g \tag{13}$$

The equation(10) becomes:

$$g'' - R(g^2 - fg') - M^2 g = A \tag{14}$$

Equation (14) and equation (11) are discretized by central difference approximation.

The resulting finite difference equations are solved by using SOR method, Smith [21] and the first order ordinary differential equation (13) is solved by Simpson's (1/3) rule, Gerald [22] with the formula given in Milne [23] subject to the appropriate boundary conditions.

The steps for the sequence of iterations are as follows:

1. The corresponding difference equations for the solution of *g* and θ are solved subject to the following boundary conditions:

   $f = 0, g = 1, \theta' = -1$ when $\eta = -1$

   $f = \lambda, g = 1, \ \theta = 0$ when $\eta = 1$.

2. For the solution of f, we use the computed values of *g* from above step in to equations (13) and integrate by Simpson's (1/3) rule.

3. The optimum value of the relaxation parameter ω_{opt} is estimated to accelerate the convergence of the SOR method.

4. The SOR procedure is terminated when the following criterion is satisfied for q:

$$\max_{i=1}^{q} \left| U_i^{q+1} - U_i^q \right| < 10^{-6},$$

Where *q* denotes the number of iterations and *U* stands for *g* and θ.

The above steps 1 to 4 are repeated for higher grid levels *h/2* and *h/4*. The SOR procedure gives the solution of $f' = g$ in the order of accuracy $O(h^2)$ due to second order finite differences used for derivatives and Simpson's (1/3) rule gives the order of accuracy $O(h^5)$ in the solution of *f*. Higher order accuracy $O(h^6)$ in the solution of $f' =$ g is achieved by using Richardson's extrapolation [24].

4. RESULTS AND DISCUSSION

The nonlinear ordinary differential equations (11) and (14) are solved numerically subject to the appropriate boundary conditions. Our numerical scheme is straight forward and very efficient as

Table 1. Results show the effects of the parameters R, M and λ on f' at η =0.

R	M	λ	A	f'
0.05	1.0	1.0	1.093626	0.261939
0.05	3.0	1.0	-2.267975	0.326008
0.20	3.0	3.0	-16.3264	1.675328
0.40	2.0	1.0	-0.16873	0.291429
0.40	4.0	1.0	-5.36558	0.357061
0.40	2.0	3.0	-9.081195	1.709340
0.80	2.0	3.0	-10.33248	1.707032
0.80	4.0	3.0	-29.01695	1.647703

Table 2. Numerical results using Richardson Extrapolation Method.

R=0.25, M =1, λ =1, Pr=0.7, n=1					R=0.05, M =4, λ =3 , Pr=0.7,n=1				
h=0.2	h=0.1	h=0.05	Extrapolated		h=0.2	h=0.1	h=0.05	Extrapolated	
η	f'	f'	f'	f'	η	f'	f'	f'	f'
0.000	1.000000	1.000000	1.000000	1.000000	0.000	1.000000	1.000000	1.000000	1.000000
0.200	0.875013	0.874960	0.874946	0.874941	0.200	1.362455	1.366961	1.368149	1.368550
0.400	0.767668	0.767608	0.767591	0.767586	0.400	1.527394	1.531557	1.532644	1.533010
0.600	0.672598	0.672559	0.672548	0.672544	0.600	1.601332	1.604336	1.605114	1.605376
0.800	0.585113	0.585109	0.585107	0.585105	0.800	1.632242	1.634416	1.634972	1.635159
1.000	0.501016	0.501052	0.501059	0.501061	1.000	1.640323	1.642228	1.642715	1.642878
1.200	0.416443	0.416513	0.416529	0.416534	1.200	1.631037	1.633260	1.633830	1.634021
1.400	0.327717	0.327809	0.327831	0.327838	1.400	1.598749	1.601842	1.602642	1.602911
1.600	0.231219	0.231311	0.231334	0.231341	1.600	1.523363	1.527618	1.528729	1.529104
1.800	0.123266	0.123331	0.123346	0.123352	1.800	1.357970	1.362519	1.363719	1.364125
2.000	0.000000	0.000000	0.000000	0.000000	2.000	1.000000	1.000000	1.000000	1.000000

Table 3. Numerical results using Richardson Extrapolation Method.

R=0.05, M =3, λ =3 , Pr=0.7,n=1					R=0.2, M=3, λ =3 , Pr=0.7,n=1				
h=0.2	h=0.1	h=0.05	Extrapolated		h=0.2	h=0.1	h=0.05	Extrapolated	
η	f'	f'	f'	f'	η	f'	f'	f'	f'
0.000	1.000000	1.000000	1.000000	1.000000	0.000	1.000000	1.000000	1.000000	1.000000
0.200	1.334084	1.336862	1.337578	1.337819	0.200	1.341450	1.344216	1.344923	1.345160
0.400	1.516063	1.519251	1.520069	1.520343	0.400	1.524671	1.527783	1.528582	1.528850
0.600	1.612367	1.615250	1.615985	1.616231	0.600	1.619392	1.622161	1.622871	1.623109
0.800	1.658401	1.660943	1.661589	1.661805	0.800	1.662694	1.665125	1.665747	1.665955
1.000	1.671292	1.673711	1.674324	1.674529	1.000	1.672386	1.674730	1.675328	1.675527
1.200	1.656125	1.658697	1.659351	1.659570	1.200	1.653726	1.656269	1.656920	1.657138
1.400	1.607904	1.610832	1.611580	1.611831	1.400	1.601822	1.604762	1.605511	1.605761
1.600	1.509951	1.513178	1.514006	1.514284	1.600	1.500667	1.503903	1.504732	1.505011
1.800	1.328270	1.331056	1.331774	1.332016	1.800	1.318725	1.321479	1.322189	1.322428
2.000	1.000000	1.000000	1.000000	1.000000	2.000	1.000000	1.000000	1.000000	1.000000

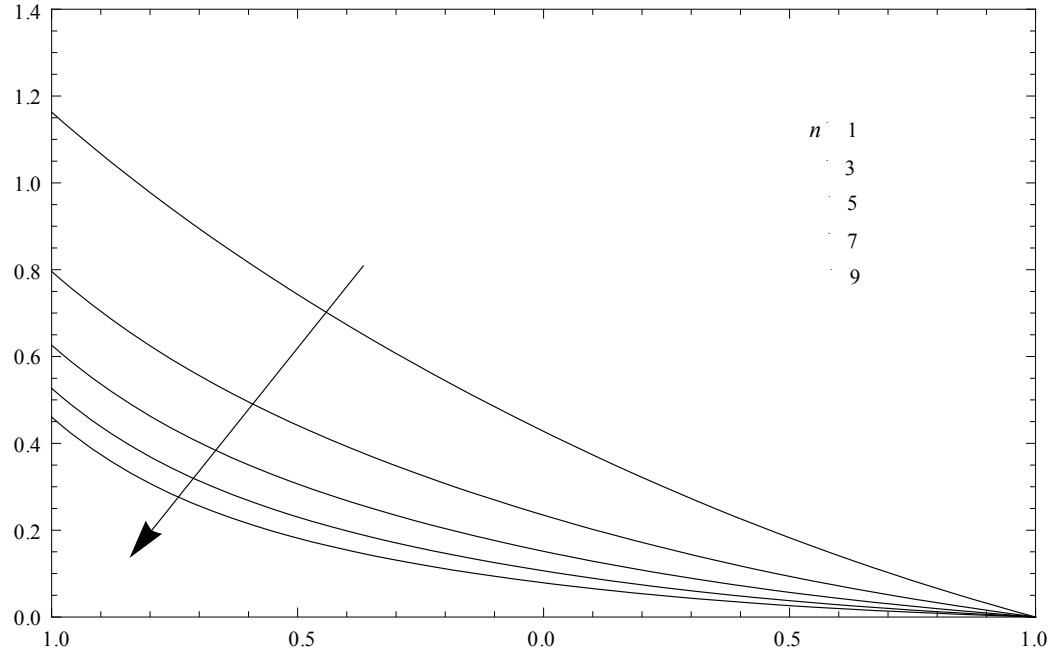

Fig. 3. Graph of θ for different values of n when M=1, R=0.05, λ =1, Pr=0.7.

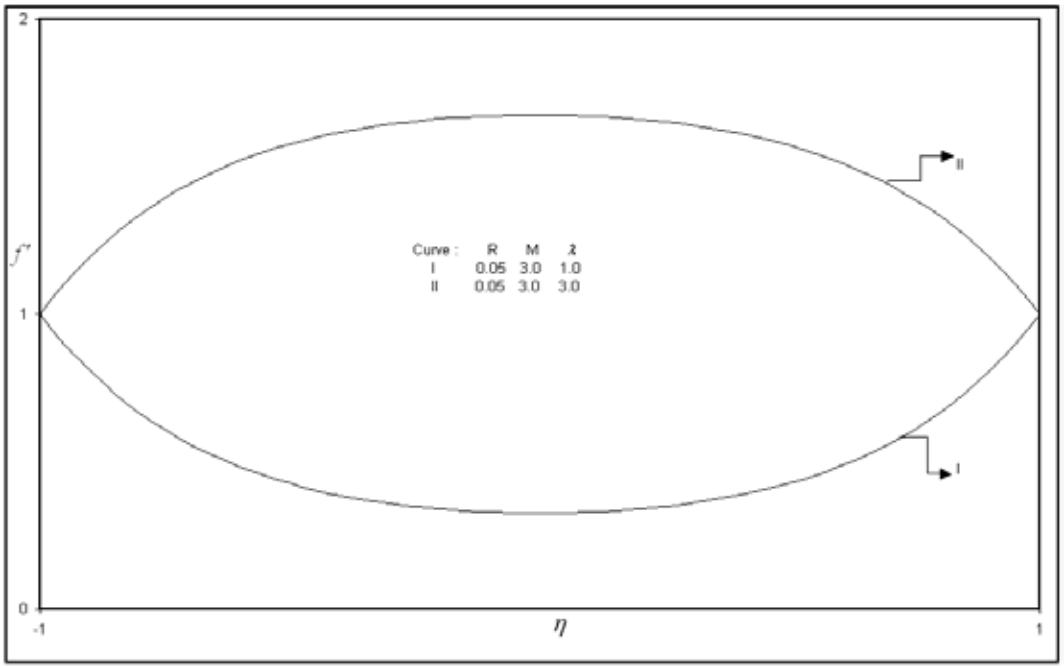

Fig. 4. Graph of f' when both the plates are stretching sheets.

Table 4. Optimum value of relaxation parameter in SOR method and number of iterations when both the plates are being stretching sheets.

M	λ	*R*	NI is Number of Iterations in SOR method with ω_{opt}					
			h=0.1		h=0.05		h=0.25	
			NI	ω_{opt}	NI	ω_{opt}	NI	ω_{opt}
1.0	1.0	0.05	41	1.65	74	1.67	235	1.65
3.0	3.0	0.05	87	1.60	82	1.65	102	1.70
2.0	3.0	0.05	37	1.65	173	1.70	397	1.75
4.0	1.0	0.40	46	1.55	38	1.66	52	1.60
2.0	3.0	0.80	52	1.70	54	1.70	877	1.72
4.0	3.0	0.80	67	1.75	61	1.70	65	1.75

compared to the numerical methods used in previous studies [15, 16]. The results have been computed for different values of the parameters *M*, *R*, λ, Pr and *n* in order to observe their effect on velocity and temperature function. The results are presented in tabular and graphical forms. Table 1 presents the values of the unknown constant *A* are chosen by hit and trial technique to satisfy the boundary conditions. The results for f' in the higher order accuracy $O(h^6)$ are given in Table 2 and Table 3. Table 4 shows that higher order accuracy solution is obtained with very small number of iterations by choosing ω_{opt}.

Fig. 2 and Fig. 3 depict the curves of heat distribution under the effect of Prandtl number P_r and heat index parameter *n,* respectively. The non-dimensional temperature function θ decreases with increase in the values of P_r and *n*.

Fig. 4 and Fig. 5 demonstrate the behavior of horizontal velocity component f', when both the plates are stretched. Fig. 6 depicts f', when the lower plate stretches. It is noticed that f' attains maximum value in the midway of the channel. When the two sheets are stretching there is almost symmetry of the curves of f' about the line $(\eta = 0)$. The magnetic parameter *M* decreases f' around the lower sheet and increases it around the upper sheet for small $\lambda = 1$.

The increase in Reynold number *R* (small *R*<1) decreases f' in the upper half of the channel and increases it in the lower half of the channel. The suction parameter λ has increasing effect on f'. This effect is maximum at the mid of the channel. Fig. 7 shows that the normal velocity component f increases with the increase in the values of λ when *M* is constant.

5. CONCLUSIONS

Numerical solution has been sought for hydromagnetic fluid flow between two horizontal stretching plates with heat flux. Results have been computed to notice the effects of the physical parameters (*M*, *R*, λ, P_r and *n*) on velocity and temperature distributions. The main results of this study are summarized as follows:

- The horizontal velocity f' attains maximum value in the midway of the channel.
- There is almost asymmetry of the curves of f' about the line $(\eta = 0)$, when the two sheets are stretching.
- The magnetic parameter *M* decreases f' around the lower sheet and increases it around the upper sheet for small $\lambda = 1$.
- The increase in Reynolds number *R* (small *R*<1) decreases f' in the upper half of the channel and increases it in the lower half of the channel.
- The suction parameter λ has increasing effect on f'. This effect is maximum at the mid of the channel.
- The normal velocity component f increases with the increase in the values of λ when *M* is constant.

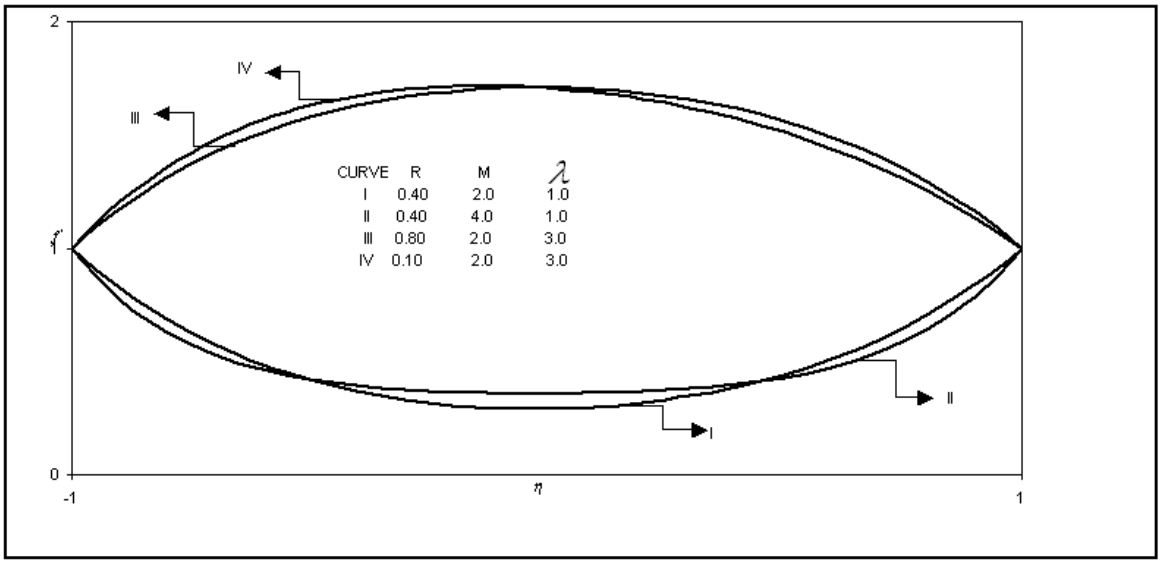

Fig. 5. Graph of f' when both the plates are stretching sheets.

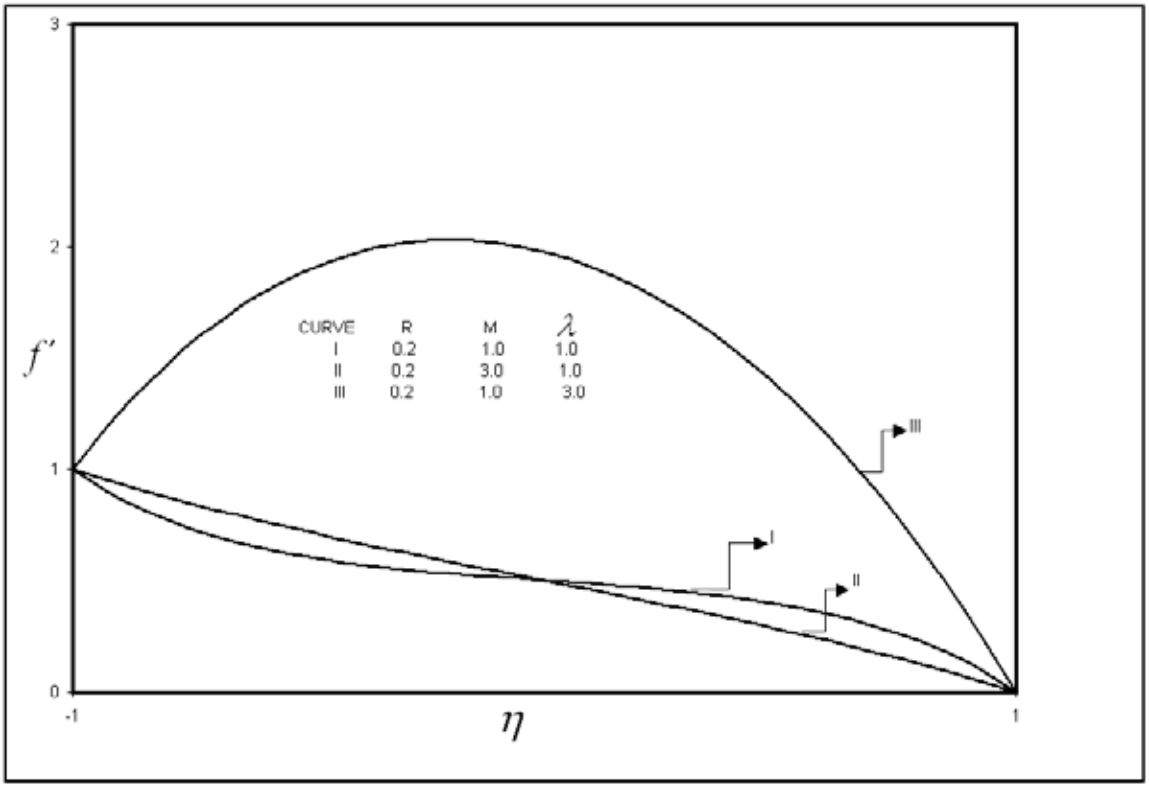

Fig. 6. Graph of f' when lower Plate being a stretching sheet.

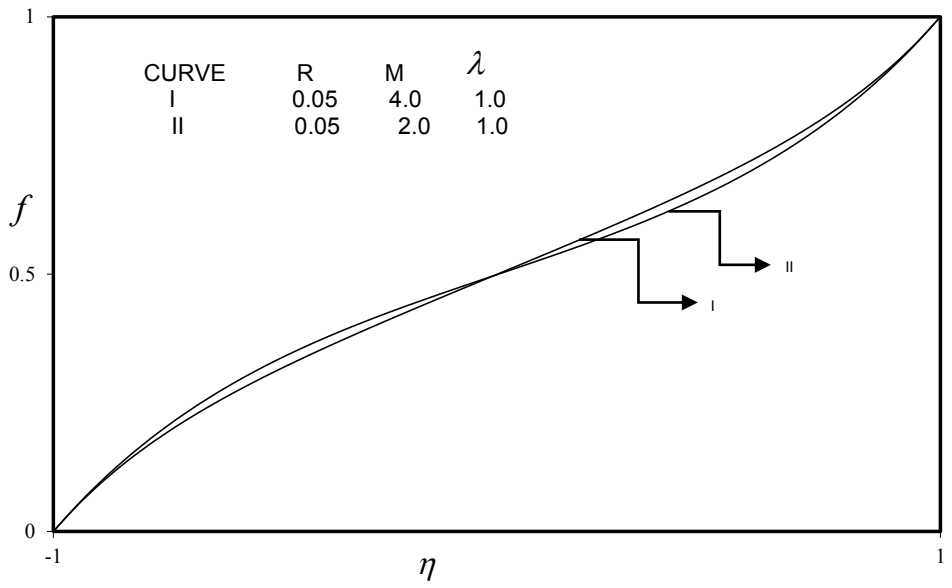

Fig. 7. Graph for different values of *M*, *R* and λ .

Nomenclature

$M^2 = \frac{\sigma}{\rho\nu} B_0^2 h^2$: Magnetic parameter

$\lambda = \frac{V_0}{ch}$: Suction parameter

$R = \frac{ch^2}{\nu}$: Rynold's number:

Pr: Prandtl number

B_0 : Strength of transverse magnetic field

σ : Electrical conductivity

ν : Coefficient of kinematic viscosity

c : Positive constant

ρ : Fluid density

V_0: Injection velocity

u, v : Velocity components along x-,y- axes, respectively

η : Dimensionless variable

- The temperature function θ decreases with increase in the values of Prandtl number P_r and heat index parameter n.

6. REFERENCES

1. Ganji, D.D., H. Bararnia, S. Soleimani & E. Ghasemi. Analytical solution of the magneto-hydrodynamic flow over a nonlinear stretching sheet. *Modern Physics Letters B* 23: 2541–2556 (2009).
2. Farooq, A., S. Hussain & M. Ali. An analytical solution of MHD flow over porous stretching sheet. *Journal of Basic and Applied Scientific Research* 4(3):160-167 (2014).
.3. Baag, S., M.R. Acharya & G.C. Dash. MHD Flow analysis using DTM-Pade' and numerical methods. *American Journal of Fluid Dynamics* 4(1): 6-15 (2014).
4. Sakiadas, B.C. Boundary layer behavior on continuous solid surface: I. Boundary-layer equations for two-dimensional and axisymmetric flow. *Journal AlChe* 7: 221-225 (1961).
5. Sakiadas, B.C. Boundary layer behavior on continuous solid surface: II. Boundary-layer equations for two-dimensional and axisymmetric flow. *Journal AlChe* 7: 226-228 (1961).
6. Erickson , L.E., L.T. Fan & V.G. Fox. Heat and mass transfer on a moving continuous flat plate with suction or injection. *Industrial and Engineering Chemistry Fundamentals* 5(1): 19–25 (1966).
7. Crane, I.J. Flow past a stretching plate. *Zeitschrift für angewandte Mathematik und Physik (Journal of Applied Mathematics and Physics)* 21: 645-647 (1970).
8. Chiam, T.C. Stagnation-point flow towards a stretching plate. *Journal of the Physical Society of Japan* 63: 2443-2444 (1994).
9. Chakrabarti, A. & A.S. Gupta. Hyderomagnetic flow and heat transfer over a stretching sheet. *The Quarterly of Applied Mathematics* 37: 73-78 (1979).
10. Andersson, H.I. An exact solution of Navier-Stokes equations for magneto-hydrodynamic flow. *Acta Mechnica* 113: 241-244 (1995).
11. Pop, I. & T.Y. Na. A note on MHD flow over a stretching permeable surface. *Mechanical Research Communication* 25(3): 263-269 (1998).
12. Liao, S.J. On the analytic solution of magnetohyderodynamic flows of non-Newtonian fluids over a stretching sheet. *Journal of Fluid Mechanics* 488: 189-212 (2003).
13. Able, S., P.H. Veena, K. Rajagopal & V.K. Pravin. Non-Newtonian magnetohydrodynamic flow over a stretching surface with heat and mass transfer. *International Journal of Nonlinear Mechanics* 39: 1067-1078 (2004).
14. Kumaran, V., A.K. Banerjee, A.V. Kumar & K. Vajravelu. MHD flow past a stretching permeable sheet. *Applied Mathematics and Computation* 210:26-32 (2009).
15. Sheikholeslami, M., H.R. Ashorynejad, D.D. Ganji & A. Kolahdooz. Investigation of Rotating MHD viscous flow and heat transfer between stretching and porous surfaces using analytical method. *Mathematical Problems in Engineering* 2011, doi:10.1155/2011/258734 (2011).
16. Pandya, J.U. The solution of a coupled nonlinear system arising in a three-dimensional rotating flow using spline method. *International Journal of Mathematics and Mathematical Sciences* 2012. doi: 10.1155/2012/702458.
17. Chakrabarti & A.S. Gupta. Hydromagnetic flow and heat transfer over a stretching sheet.*Quarterly of Applied Mathematics* 37(1): 73–78 (1979).
18. Banerjee, B. Magneto-hydrodynamic flow between two horizontal plates in a rotating system, the lower plate being a stretched sheet. *Transactions ASME Journal of Applied Mechanics* 50: 470 (1983).
19. Arthur, E.M. & I.Y. Seini. Hydromagnetic stagnation point flow over a porous stretching surface in the presence of radiation and viscous dissipation. *Applied and Computational Mathematics* 3(5): 191-196 (2014).
20. Rossow, V.J. On Flow of Electrically *Conducting Fluids Over a Flat Plate in the Presence of a Transverse Magnetic Field*.Tech Report 1358: NASA (1958).
21. Smith, G.D. *Numerical Solution of Partial Differential Equation*. Clarendon Press, Oxford (1979).
22. Gerald, C.F. *Applied Numerical Analysis*. Addison-Wesley Pub, NY (1989).
23. Milne, W.E. *Numerical Solution of Differential Equation*. Dover Pub (1970).
24. Burden, R.L. *Numerical Analysis*. Prindle, Weber & Schmidt, Boston (1985).

Proceedings of the Pakistan Academy of Sciences 52 (2): 145-149 (2015)

ISSN: 0377 - 2969 (print), 2306 - 1448 (online)

Pakistan Academy of Sciences

Research Article

Appraisal of Solar Activity at Pakistan Atmospheric Regions

Saifuddin Ahmed Jilani[1], and M. Ayub Khan Yousuf Zai[2*]

[1]Department of Physics and Institute of Space & Planetary Astrophysics (ISPA), University of Karachi, Karachi-75270, Pakistan
[2]Department of Applied Physics, Solar- Terrestrial and Atmospherics Research Center and Institute of Space & Planetary Astrophysics (ISPA), University Karachi, Karachi-75270, Pakistan

Abstract: This study presents an indigenous work to investigate periodicity in Solar Flare Duration (SFD) at Pakistan atmospherics region over a period of 1979-2006. The disorderly behavior of solar flare generates solar protons which often associated with gradual flares and Coronal Mass Ejection (CME). Their adverse effects are on space weather and hence orbiting satellites and radio wave communication system. Therefore a better understanding of periodic activities in the sun is useful for the prediction of the effects of solar activity on Earth. We revealed the first peak periodicity in the mixed series of Solar Flare Duration (SFD) and implemented a test of periodic ordinate and confidence interval to substantiate the results. Gradual flares are undesirable to the terrestrial climate so we separate the series of impulsive and gradual flares from the mixed series and revealed their periodic behavior as well. This study intended to propose that periodic behavior in the solar flare duration may be one of the important aspects of solar flare activity.

Keywords: Solar flare duration (SFD), spectral analysis, fast fourier transform (FFT), mixed series of flares, gradual flares, impulsive flares

1. INTRODUCTION

Solar flares were discovered by C. Carrington and R. Hodgson on September 1, 1859. They are closely related to the Sun's magnetic field and occur in the active region of the solar atmosphere that superimposes sunspots [1].

The Sun's turbulent magnetic fields provide the fuel of flares. The swift release of energy in a flare results from a process called reconnection, whereby oppositely directed magnetic field lines come close together and partially annihilate each other [2]. Gradual flares are the long duration flares that lasting more than an hour and are associated with Coronal Mass Ejection (CME) [3]. These are the streams of solar particles and have numerous adverse effects on the terrestrial climate.

Physical origins of solar cycles are not known. They can be the internal property of the Sun as a star and its dynamo action as mostly believed now. Further the planetary influences and interstellar causes may contribute their effects as well [4-5]. The largest flares called CME, pose a potential threat to space travelers and may disrupt Earth communications [6]. CMEs are also the cause of geomagnetic storms that may initiate also in quiet parts of the Sun, without any association of solar flares. But it is misleading to jump to a conclusion, that the flares are not important any more in solar terrestrial relations. Flares are excellent indicators of coronal storms and actually indicate the strongest, fastest and most energetic disturbance coming from Sun [7]. Intense radiation from solar flares can change the electrical properties of our atmosphere; partially or totally black-out of radio wave communication systems. Friction can develop between the expanded atmosphere and satellite travelling in it, altering their orbit that drags them into outer space or down to earth [8].

2. METHODOLOGY

This evaluation based on two aspects of solar flares that are termed as impulsive and gradual

Received, April 2014; Accepted, February 2015
*Corresponding author: M. Ayub Khan Yousuf Zai; Email: ayubzai@yahoo.com

flares in addition to their mixed series. By using spectral techniques, it is possible to look insight into different types of signals that are superimposed with each other. The spectral technique termed as Periodogram has been implemented for detecting the hidden periodicities in terms of their frequency and time contents. The results are analyzed by applying confidence interval to the peaks of these spectral estimates and by a test of periodic ordinates named as Fisher test.

The periodogram was introduced by Shuster in 1898 for studying the periodicities in the sunspot series. Any stationary time series is actually be the random superposition of sines and cosines oscillating at various frequencies and periodogram may be given us an idea of variance components associated with each frequency. This could be used to identify important harmonic components in time series data [9-11].

The period gram is defined by,

$$I(w) = \frac{2}{N}\{(\sum_{t=1}^{N} X_i Coswt)^2 + (\sum_{t=1}^{N} X_i Sinwt)^2\} \quad (1)$$

The function $I(w)$ is then computed for,

$$w_i = \frac{2\pi p}{N} \text{ --- (2); } \quad p = 0,1,2,----(N|2) \quad (2)$$

By searching the squared amplitudes for large values we can thus locate the approximate values of the true frequencies (w_i) [12].

For strong periodic components, the periodogram values corresponding or near to those frequencies will be large whereas the corresponding values of the periodogram will be small for periodic components not present in the data.

The amplitude of the pth harmonic is

$$R_p = \sqrt{a_p^2 + b_p^2} \quad (3)$$

The phase of the pth harmonic is

$$\varphi_p = \tan^{-1}(b_p/a_p) \quad (4)$$

The corresponding time lag for the pth component is

$$t_p = \frac{\theta_p}{2\pi f_p} \quad (5)$$

The Fourier transform determine the energy distribution of a time series so there is need to find its Fourier transform. This determines the coefficients in the Fourier series or evenly the amplitudes and phase lags [13].

An approximate 100(1−α) % confidence interval for the spectral density function would be of the form

$$\frac{v\hat{f}(\omega)}{\chi^2_{v,\alpha/2}} to \frac{v\hat{f}(\omega)}{\chi^2_{v,1-\alpha/2}} \quad (6)$$

The degree of freedom for the Hamming window is 2.50 (N/M) respectively. A useful rough guide is to choose M to be about $2\sqrt{N}$. A window minimize the side-lobes and maximizes (concentrates) the energy near the frequency of interest in the main lobe [12, 14].

3. RESULTS AND DISCUSSION

3.1. Test of Non-stationarity

Spectral analysis is only appropriate for stationary time-series data. In order to detect non-stationary behavior, spectral analysis may perform on the originally observed series. Trend in data may detectable by a peak in the spectral density function at zero frequency [11, 15]. The spectral density function in Fig. 1-3 identified the peak in mixed series of flares at a frequency of 0.0123 whereas for impulsive and gradual flares these are 0.0056 and 0.0068 respectively. As these values are not exactly equal to zero, therefore it may consider that there is no need to implement the methods of removing the trend.

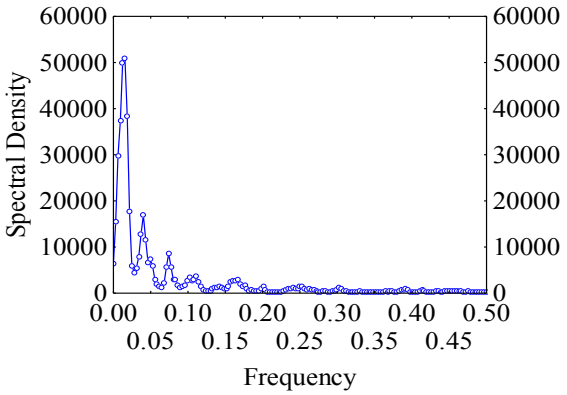

Fig. 1. Spectral Density for mixed series of flares.

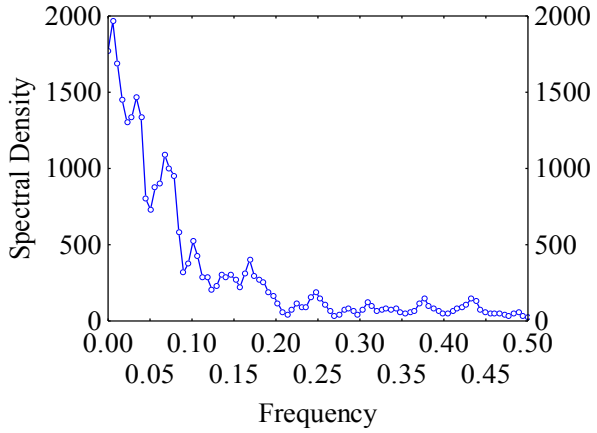

Fig. 2. Spectral Density for impulsive series of flares.

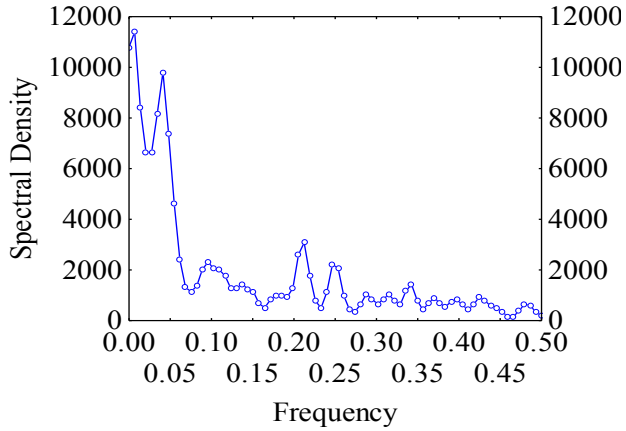

Fig. 3. Spectral Density for gradual series of flares.

3.2. Estimation of Highest Frequency and Corresponding Periods

From periodogram analysis, highest peaks have been detected both in frequency and time domain. Fig. 4-9 depict the periodicities in mixed, impulsive and gradual series of flares. The periodicity in each of the mixed, impulsive and gradual series identified respectively as 81, 178 and 146 months per cycles. In addition to the basic periodicities identified above, there are well-defined peaks corresponding to periods of 54, 162, and 64.8 for the mixed series of flares, 25.4, 14.8, 59.3 for the impulsive phase and 24.3, 48.6, 18.2 for gradual phase.

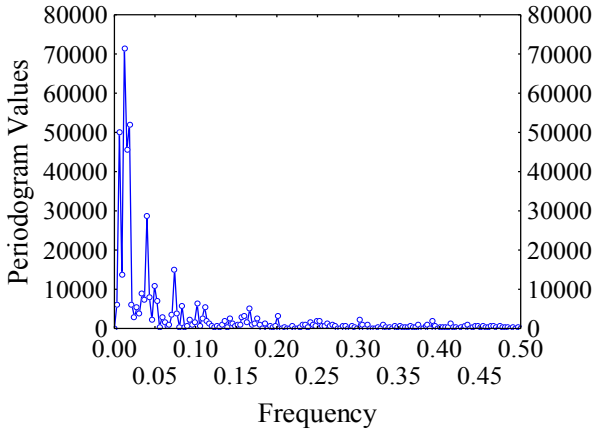

Fig. 4. Periodogram for the mixed series of SFD in frequency domain.

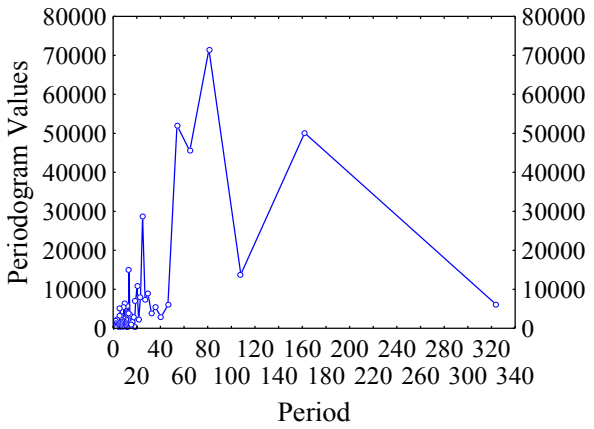

Fig. 5. Periodogram for the mixed series of SFD in time domain.

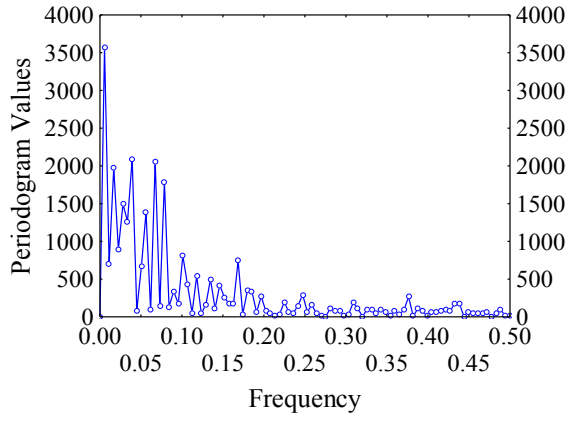

Fig. 6. Periodogram for the series of impulsive flares in frequency domain.

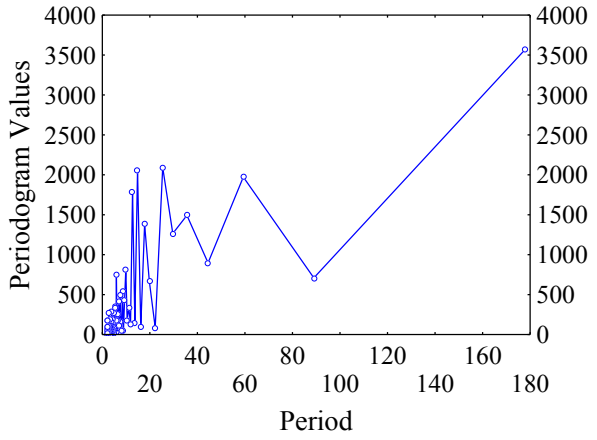

Fig. 7. Periodogram for the series of impulsive flares in time domain.

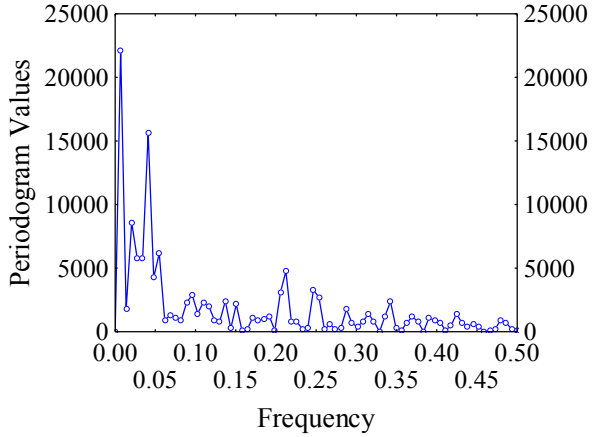

Fig. 8. Periodogram for the series of gradual flares in frequency domain.

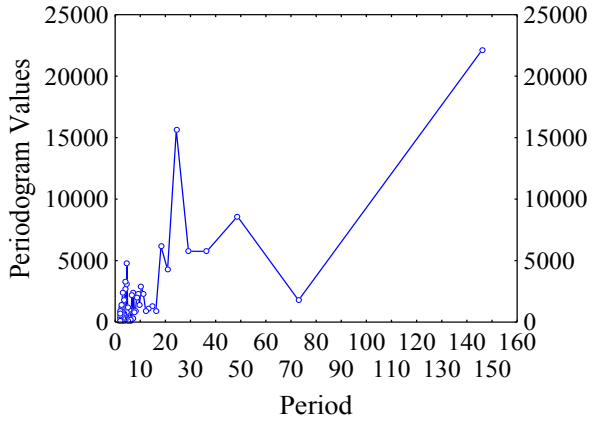

Fig. 9. Periodogram for the series of gradual flares in time domain.

3.3. Confidence Intervals for the Spectrum

A 95% confidence interval for the first highest peaks in the data series of SFD has been evaluated using Hamming window as mentioned in Table 1.

Table 1. First highest peak identified by periodogram.

Data Series	$\hat{f}(\omega)$	T	C.I (H.W)
SFD-Mixed	0.0123	81	0.0074 - 0.0242
SFD-Imp.	0.0056	178	0.0031 - 0.0125
SFD-Grad	0.0068	146	0.0037 - 0.0162

C.I. = Confidence Interval
H.W. = Hamming Window

3.4. Test for Periodic Ordinates

It may possible that peaks in the periodogram may not represent true periodicity in the given data series because of the random fluctuations in the error term. In such cases, it is suitable to apply certain tests to find the stability of the periodogram.

Fisher's Test: Fisher (1929) derived an exact test for max (I_p) based on the test statistic

$$g = \frac{\max(I_p)}{\sum_{p=1}^{N/2} I_p} \quad \text{---------- (7)}$$

known as 'Fisher's g statistic' [8].

The critical values for the Fisher test of significance for periodogram analysis at α = 5 % and N = 160; $g' = 0.08997$; N = 165; $g' = 0.08811$ N = 500; $g' = 0.03368$

For all of the three series the Fisher's g statistic is greater than their critical values, confirms the significance of their peak frequency and therefore the periodicity obtained by the periodogram. The test statistic is illustrated in Table 2.

Table 2. Fisher's g statistic for verifying accuracy of highest peak identified by periodogram.

Data Series	$\max(I_{p})$	$\sum_{p=1}^{N/2} I_p$	*g statistic*
SFD-Mixed	$I_{0.0123} = 71512.9$	$\sum_{p=1}^{162} I_p = 471501.1$	0.1516
SFD-Imp.	$I_{0.0056} = 3572.2$	$\sum_{p=1}^{89} I_p = 28547.6$	0.1251
SFD-Grad	$I_{0.0068} = 22115.2$	$\sum_{p=1}^{73} I_p = 135412.9$	0.1633

3.5. Spectral Energy Estimates

The amplitudes of the Fourier coefficients define a periodogram that give the contribution of each oscillatory component in the total energy of the observed signal [13-15]. The phase angle that gives the relative 'lag' of the component and the corresponding time lag are illustrated in Table 3.

Table 3. Periodogram values with their amplitude, phase and time lag.

Data Series	$I_{p(w)}$	p	R_p	φ_p	t_p
SFD-Mixed	71512.99	4	21.0	0.65	8.44
SFD-Imp.	3572.2	1	6.33	0.197	5.59
SFD-Grad	22115.2	1	17.40	0.165	3.83

R_p = Amplitude φ_p = Phase t_p = time lag

4. CONCLUSIONS

This study of periodic variations in solar activity is sufficient for predicting future activity levels. Strongest amplitude is revealed in solar flare activity according to their duration. Through periodogram we define the highest peak and highest spectral energy at that portion of the time series. The direct impact of solar variability in accordance with the solar flare duration (SFD) becomes more pronounced in mixed series and less pronounced in impulsive and gradual phases of flares may be due to their partially non-stationary behavior. The periodicities identified in these series are more significant by investigating a long-term modulation of solar activity. In addition to the sunspot cycle, the cycles of solar flare duration are also be one of the manifestation of solar activity, is driven by the variations in the magnetic field.

5. ACKNOWLEDGEMENTS

The authors are pleased to acknowledge SUPARCO, HQ for providing the solar flare acquisition data.

6. REFRERENCES

1. Maran, S.P. & C. Sagan. *The Astronomy and Astrophysics Encyclopedia*. Cambridge University Press, Cambridge, UK (1992).
2. Gordon, D.H. The mysterious origins of solar flare. *Scientific American* 294: 38-45 (2006).
3. Bond, P. Haunting Images. Astronomy & Geophysics. *The Journal of the Royal Astronomical Society* 43(2): 2-3 (2002).
4. Dmitriev, A.V., A.V. Suvorova & I.S. Veselovsky. Statistical characteristics of the heliospheric plasma and magnetic field at the earth's orbit during four solar cycles 20-23. In: *Handbook on Solar Wind: Effects, Dynamics and Interactions*. Hans E. Johannson (Ed.), Nova Science Publishers, New York, USA (2009).
5. Juckett, D.A. Solar activity cycles, north/south asymmetries, and differential rotation associated with solar spin-orbit variations. *Solar Physics* 191: 22011-22226 (2000).
6. Hey, N. *Solar System*. Weidenfeld & Nicolson, London (2002).
7. Dwivedi, B.N. & E.N. Parker. *Dynamic Sun*. Cambridge University Press, UK (2003).
8. Lang, K.R. *The Cambridge Encyclopedia of the Sun*. Cambridge University Press, UK (2001).
9. Shumway, R.H. & D.S. Stoffer. *Time Series Analysis and Its Application,* 2nd ed. Springer Science, NY, USA (2006).
10. Gottman, J.M. *Time-Series Analysis*. Cambridge University Press, NY, USA (1981).
11. Diggle, P.J. *Time Series*, Oxford University Press, NY, USA (1990).
12. Rao T.S., M.B. Prriesteley & O. Lessi. *Application of Time Series Analysis in Astronomy and Meteorology*, Chapman & Hall, Great Britain (1997).
13. Emery, W.J. & R.E. Thomson. *Data Analysis Methods in Physical Oceanography*, 2nd ed. Elsevier B.V., Amsterdam, Netherland (2004).
14. Chatfield, C. *Analysis of Time Series*. Chapman & Hall, London (1989).
15. Du Toit, S.H.C., A.G.W. Steyn & R.H., Stumpf. *Graphical Exploratory Data Analysis*. Springer-Verlag, NY, USA (1986).

Proceedings of the Pakistan Academy of Sciences 52 (2): 151-158 (2015)

ISSN: 0377 - 2969 (print), 2306 - 1448 (online)

Pakistan Academy of Sciences

Research Article

Review of Numerical Schemes for Two Point Second Order Non-Linear Boundary Value Problems

Abdul Manaf[1*], Mustafa Habib[1], and M. O. Ahmad[2]

[1]Department of Mathematics, University of Engineering and Technology, Lahore, Pakistan
[2]Department of Mathematics, University of Lahore, Lahore, Pakistan

Abstract: In this paper, numerical solution of two points 2nd order nonlinear boundary-value problems was considered. The numerical solution was reviewed with nonlinear shooting method, finite-difference method and fourth order compact method. The results were compared to check the accuracy of numerical schemes with exact solution. It was found that the nonlinear shooting method is more accurate than finite-difference method and fourth order compact method.

Keywords: BVPs, ODEs, Nonlinear Shooting method, finite-difference method, fourth order compact method

1. INTRODUCTION

Consider a two point 2nd order nonlinear boundary value problem (BVP) of the type

$$y'' = f(x, y, y'), x \in [a,b]; \ a,b \in R \tag{1}$$

jointly among the boundary conditions

$$y(a) = \alpha \ \text{ and } \ y(b) = \beta. \tag{2}$$

Where α and β are constants.

The approach for solving this problem has been projected by a number of researchers such as Roberts and Shipman [1], Malathi [2], Ha [3], Auzinger et al [4] and Attili and Syam [5].

In this research paper, we considered nonlinear shooting method (NLSM), finite-difference method (FDM) and fourth order compact method (FOCM) for the solution of above two points 2nd order nonlinear boundary value problems (BVPs).

2. NONLINEAR SHOOTING METHOD (NLSM)

Consider a two point's 2nd order non-linear boundary-value problem (BVP)

$$y'' = f(x, y, y'), \ y(a) = \alpha, \ y(b) = \beta \tag{3}$$

where $a \le x \le b$ and α, β are constants.

Here, we used the solutions to a sequence of initial value problems (IVPs) of [3, 5, 6]

$$y'' = f(x, y, y'), \ y(a) = \alpha, \ y'(a) = t \tag{4}$$

Concerning a parameter t, and $a \le x \le b$, to approximate the solution to our BVP (3).

By choosing parameters $t = t_k$ in such a way that

$$\lim_{k \to \infty} y(b, t_k) = y(b) = \beta \tag{5}$$

Where $y(x, t_k)$ is the solution to the IVP (4) with $t = t_k$ and y(x) is the solution to the BVP (3).

This procedure is called a Shooting method.

We begin with a parameter t_0 that find out the initial elevation at which the object is excited from the point (a, α) and beside the curve described by the solution to the IVP [6].

$$y'' = f(x, y, y'), \ y(a) = \alpha, \ y'(a) = t_0 \tag{6}$$

Received, November 2014; Accepted, February 2015
*Corresponding author: Abdul Manaf; Email: manaf192@yahoo.com

If $y(b,t_0)$ is not satisfactorily close to β, we try to correct our approximation by choosing another elevation t_1 and so on, until $y(b,t_k)$ is satisfactorily close to striking β [3].

To decide how the parameter t_k can be chosen, suppose a BVP (3) has a single solution. If y(x, t) is the solution to the IVP (4), then we need to determine t so that

$$y(b,t)-\beta = 0 \quad (7)$$

Since this is a nonlinear equation, we use Newton's method

$$x_{n+1} = x_n - \frac{f(x_n)}{f'(x_n)}$$

to solve the problem. We need to choose initial approximation t_0 and then generate sequence by

$$t_k = t_{k-1} - \frac{y(b,t_{k-1})-\beta}{\frac{dy}{dt}(b,t_{k-1})} \quad (8)$$

this requires the knowledge of $\frac{dy}{dt}(b,t_{k-1})$. This presents a complexity, since an explicit illustration for y (b, t) is not identified; we only know the values

$$y(b,t_0),\ y(b,t_1),\ .....,\ y(b,t_{k-1}).$$

Suppose we modify the IVP (4), emphasizing that the solution depends on together x and t.

$$y''(x,t) = f\left(x, y(x,t), y'(x,t)\right), a \le x \le b,$$

$$y(a,t) = \alpha,\ y'(a,t) = t \quad (9)$$

retaining the prime notation to indicate differentiation with respect to x.

Since we need to determine $\frac{dy}{dt}(b,t)$, when $t = t_{k-1}$, we take partial derivative of (9) with respect to t.

$$\frac{\partial y''(x,t)}{\partial t} = \frac{\partial f\left(x, y(x,t), y'(x,t)\right)}{\partial t}$$

$$= \frac{\partial f}{\partial x}\frac{\partial x}{\partial t} + \frac{\partial f}{\partial y}\frac{\partial y(x,t)}{\partial t} + \frac{\partial f}{\partial y'}\frac{\partial y'(x,t)}{\partial t}$$

Since x and t are independent, $\frac{\partial x}{\partial t} = 0$, so

$$\frac{\partial y''}{\partial t}(x,t) = \frac{\partial f}{\partial y}\frac{\partial y(x,t)}{\partial t} + \frac{\partial f}{\partial y'}\frac{\partial y'(x,t)}{\partial t} \quad (10)$$

for $a \le x \le b$. The initial conditions give

$$\frac{\partial y}{\partial t}(a,t) = 0, \text{ and } \frac{\partial y'}{\partial t}(a,t) = 1$$

If we make simpler the notation by using $z(x,t)$ to denote $\frac{\partial y}{\partial t}(x,t)$ and suppose that the order of differentiation of x & t can be reversed, Eq. (10) with initial conditions becomes IVP [6]

$$z''(x,t) = \frac{\partial f}{\partial y}z(x,t) + \frac{\partial f}{\partial y'}z'(x,t),$$

$$a \le x \le b,\ z(a,t) = 0,\ z'(a,t) = 1 \quad (11)$$

Therefore, one requires that two IVPs be solved for each iteration, (4) and (11).

Then from Eq. (8),

$$t_k = t_{k-1} - \frac{y(b,t_{k-1})-\beta}{Z(b,t_{k-1})} \quad (12)$$

In practice, none of these IVPs is solved exactly; instead, the solutions are approximated by one of the IVP solvers [3].

Hence, in shooting method for nonlinear BVPs, we use classical Runge-Kutta fourth-order method to approximate both solutions required by Newton's method.

3. FINITE-DIFFERENCE M ETHOD (FDM)

Methods involving finite differences for solving boundary value problems (BVPs) replace each of the derivatives in the differential equation by an appropriate difference-quotient approximation. The

difference quotient is chosen to maintain a specified order of truncation error [7].

The nonlinear second order BVP of the form (3) requires that difference–quotient approximations be used to approximate both y' *and* y''. First, we take N>0, which is an integer, and break up $[a,b]$ into N+1 equal subintervals, whose end points are mesh points $x_i = a + ih, for\ i = 0,1,2,...,N+1\ where\ h = \frac{b-a}{N+1}$.

At interior mesh points, x_i $for\ i = 0,1,2,...,N$, following differential-equation is to be approximated

$$y''(x_i) = f\left(x_i, y(x_i), y'(x_i)\right) \tag{13}$$

Expanding y, in the third Taylor-polynomial, about x_i evaluated at x_{i+1} and x_{i-1}, we get

$$y(x_{i+1}) = y(x_i) + hy'(x_i) + \frac{h^2}{2!}y''(x_i) + \frac{h^3}{6}y'''(x_i) + \frac{h^4}{24}y^4(\xi_i^+)$$

for some ξ_i^+ in (x_i, x_{i+1}), and

$$y(x_{i-1}) = y(x_i) - hy'(x_i) + \frac{h^2}{2}y''(x_i) - \frac{h^3}{6}y'''(x_i) + \frac{h^4}{24}y^4(\xi_i^-)$$

for some ξ_i^- in (x_{i-1}, x_i), assuming $y \in C^4[x_{i-1}, x_{i+1}]$. By adding the above two equations, we have

$$y''(x_i) = \frac{1}{h^2}\left[y(x_{i+1}) - 2y(x_i) + y(x_{i-1})\right] - \frac{h^2}{24}\left[y^4(\xi_i^+) + y^4(\xi_i^-)\right]$$

Using intermediate value theorem, this can be simplified even further as

$$y''(x_i) = \frac{1}{h^2}\left[y(x_{i+1}) - 2y(x_i) + y(x_{i-1})\right] - \frac{h^2}{12}y^4(\xi_i) \tag{14}$$

for some $\xi_i\ in\ (x_{i-1}, x_{i+1})$. This is called the centered-difference formula for $y''(x_i)$.

A centered difference formula for $y'(x_i)$ is obtained in a related manner resulting in

$$y'(x_i) = \frac{1}{2h}\left[y(x_{i+1}) - 2y(x_{i-1})\right] - \frac{h^2}{6}y'''(\eta_i) \tag{15}$$

for some η_i in (x_{i-1}, x_{i+1}).

The use of the centered difference formulas in equation (13) gives

$$\frac{y(x_{i+1}) - 2y(x_i) + y(x_{i-1})}{h^2}$$
$$= f\left(x_i, y(x_i), \frac{y(x_{i+1}) - 2y(x_{i-1})}{2h} - \frac{h^2}{6}y'''(\eta_i)\right) + \frac{h^2}{12}y^{(4)}(\xi_i)$$

for some $\xi_i\ and\ \eta_i$ in the interval (x_{i-1}, x_{i+1}).

As in linear case, the difference method results when the error terms are deleted and boundary conditions employed [7]:

$w_0 = \alpha,\quad w_{N+1} = \beta,\ and$

$$-\frac{w_{i+1} - 2w_i + w_{i-1}}{h^2} + f\left(x_i, w_i, \frac{w_{i+1} - w_{i-1}}{2h}\right) = 0$$

for each $i = 1,2,...,N$.

The $N \times N$ nonlinear system obtained from this method is

$$2w_1 - w_2 + h^2 f\left(x_1, w_1, \frac{w_2 - \alpha}{2h}\right) - \alpha = 0,$$
$$-w_1 + 2w_2 - w_3 + h^2 f\left(x_2, w_2, \frac{w_3 - w_1}{2h}\right) = 0,$$
.....
.....
$$-w_{N-2} + 2w_{N-1} - w_N + h^2 f\left(x_{N-1}, w_{N-1}, \frac{w_N - w_{N-2}}{2h}\right) = 0,$$
$$-w_{N-1} + 2w_N + h^2 f\left(x_N, w_N, \frac{\beta - w_{N-1}}{2h}\right) - \beta = 0.$$

To approximate the solution to this system, we use Newton's method for nonlinear system. A sequence of iterates $\left(w_1^{(k)}, w_2^{(k)}, ..., w_N^{(k)}\right)^t$ is generated that converges to the solution of system, provided that the initial approximation $\left(w_1^{(0)}, w_2^{(0)}, ..., w_N^{(0)}\right)^t$ is sufficiently close to the solution, $\left(w_1, w_2, ..., w_N\right)^t$, and that the Jacobian matrix for the system is nonsingular. For the system, the Jacobian matrix is tridiagonal.

Newton's method for nonlinear systems requires that at each iteration, the $N \times N$ linear system [8]

$$J(w_1, w_2, ..., w_N)^t (v_1, v_2, ..., v_N)^t$$
$$= -\left(2w_1 - w_2 - \alpha + h^2 f\left(x_1, w_1, \frac{w_2 - \alpha}{2h}\right),\right.$$
$$-w_1 + 2w_2 - w_3 + h^2 f\left(x_2, w_2, \frac{w_3 - w_1}{2h}\right), ...,$$
$$-w_{N-2} + 2w_{N-1} - w_N + h^2 f\left(x_{N-1}, w_{N-1}, \frac{w_N - w_{N-2}}{2h}\right),$$
$$\left.-w_{N-1} + 2w_N + h^2 f\left(x_N, w_N, \frac{\beta - w_{N-1}}{2h}\right) - \beta\right)^t$$

be solved for $v_1, v_2, ..., v_N$, since

$$w_i^{(k)} = w_i^{(k-1)} + v_i, \text{ for each } i = 1, 2, ..., N \quad (16)$$

4. FOURTH ORDER COMPACT METHOD (FOCM)

A fourth order general differencing scheme, proposed by Kreiss [9], is developed and it is applied on the three test problems to confirm accuracy and applicability of this technique. Burger's equation, the Howarth's retarded boundary flow, and the incompressible driven cavity, are the solved test problems [6, 8, 9]. A number of researchers have contributed in this method, some of them are Ahmad [8], Orsazag and Israeli [10], Richard [11], Leventhal and Ciment [12] and Pettigrew and Rasmussen [13]. The detailed work on compact method was done by Ahmad [8]. We follow the procedure of Pettigrew and Rasmussen [13] to derive the compact method for nonlinear ODEs [14, 15].

Consider the nonlinear two point second order BVP of the form (3). Let us denote first and second derivatives with respect to x of y by F and S respectively, i.e.

$$y' = F, \text{ and } y'' = S \quad (17)$$
$$\Rightarrow F' = S$$

Consider $y' = F$

Integrating both sides from x_{i-1} to x_{i+1}, we get

$$y_{i+1} - y_{i-1} = \int_{x_{i-1}}^{x_{i+1}} F(\xi) d\xi \quad (18)$$

$$y_{i+1} = y_{i-1} + \int_{x_{i-1}}^{x_{i+1}} F(\xi) d\xi$$

Approximating integral by Simpson's rule [8]

$$y_{i+1} = y_{i-1} + \frac{h}{3}\left[F_{i-1} + 4F_i + F_{i+1}\right] - \frac{1}{90} h^5 F^4(\xi)$$
$$\Rightarrow \frac{h}{3}\left[F_{i-1} + 4F_i + F_{i+1}\right] + y_{i-1} - y_{i+1} = \frac{1}{90} h^5 F^4(\xi)$$

multiplying both sides by $\frac{3}{h}$, we get

$$F_{i-1} + 4F_i + F_{i+1} + \frac{3}{h}\left[y_{i-1} - y_{i+1}\right] = \frac{1}{30} h^4 F^4(\xi)$$

and to the fourth order, we have

$$F_{i-1} + 4F_i + F_{i+1} + \frac{3}{h}\left[y_{i-1} - y_{i+1}\right] = 0 \quad (19)$$

Thus we have a relationship between y and F and it is the first difference-equation.

Now for the second equation, we start by evaluating equation (eq) (1) at the midpoint i. Thus equation (1) becomes [7]

$$y_i'' = f\left(x_i, y(x_i), y'(x_i)\right)$$

Since $y'' = S$, so we have

$$S_i = f\left(x_i, y(x_i), F_i\right) \quad (20)$$

Now, we require an expression for S_i.

If we expand y in the 5th Taylor's polynomial on x_i evaluated at x_{i+1} and at the x_{i-1}, we get

$$y_{i+1} = y_i + hy_i' + \frac{h^2}{2!}y_i'' + \frac{h^3}{3!}y_i''' + \frac{h^4}{4!}y_i^{(4)} + \frac{h^5}{5!}y_i^{(5)} + \frac{h^6}{6!}y_i^{(6)}(\xi_i^+)$$

for some ξ_i^+ in $\left(x_i, x_{i+1}\right)$, and

$$y_{i-1} = y_i - hy_i' + \frac{h^2}{2!}y_i'' - \frac{h^3}{3!}y_i''' + \frac{h^4}{4!}y_i^{(4)} - \frac{h^5}{5!}y_i^{(5)} + \frac{h^6}{6!}y_i^{(6)}(\xi_i^-)$$

for some ξ_i^- in $\left(x_{i-1}, x_i\right)$, assuming $y \in C^6\left[x_{i-1}, x_{i+1}\right]$. If we add these equations, terms involving y_i', y_i'' and $y_i^{(5)}$ are eliminated and we get

$$y_{i+1} + y_{i-1} = 2y_i + h^2 y_i'' + \frac{h^4}{12}y_i^4 + \frac{h^6}{720}\left[y^{(6)}(\xi_i^+) + y^{(6)}(\xi_i^-)\right]$$
$$\Rightarrow y_{i+1} + y_{i-1} = 2y_i + h^2 S_i + \frac{h^4}{12}y_i^4 + \frac{h^6}{720}\left[y^{(6)}(\xi_i^+) + y^{(6)}(\xi_i^-)\right]$$

Here intermediate-value theorem is used to further simplify this as

$$y_{i+1} + y_{i-1} = 2y_i + h^2 S_i + \frac{h^4}{12}y_i^4 + \frac{h^6}{360}y^{(6)}(\xi_i) \quad (21)$$

for some ξ_i in (x_{i-1}, x_{i+1}).

Now expanding F in Taylor series

$$F_{i+1} = F_i + hF_i' + \frac{h^2}{2!}F_i'' + \frac{h^3}{3!}F_i''' + \frac{h^4}{4!}F_i^{(4)} + \frac{h^{(5)}}{5!}F_i^{(5)}(\xi_i^+) \quad (22)$$

$$F_{i-1} = F_i - hF_i' + \frac{h^2}{2!}F_i'' - \frac{h^3}{3!}F_i''' + \frac{h^4}{4!}F_i^{(4)} - \frac{h^{(5)}}{5!}F_i^{(5)}(\xi_i^+) \quad (23)$$

On subtracting eq(23) from eq(22), we get

$$F_{i+1} - F_{i-1} = 2hF_i' + \frac{h^3}{3}F_i''' + \frac{h^{(5)}}{120}\left[F^{(5)}(\xi_i^+) + F^{(5)}(\xi_i^-)\right]$$

By using intermediate value theorem, we get

$$F_{i+1} - F_{i-1} = 2hF_i' + \frac{h^3}{3}F_i''' + \frac{h^{(5)}}{60}F^{(5)}(\xi_i^+)$$

For a few ξ_i in (x_{i-1}, x_{i+1}).

Since, $F' = S$, $F''' = y^{(4)}$, $F^{(5)} = y^{(6)}$, So,

$$F_{i+1} - F_{i-1} = 2hS_i + \frac{h^3}{3}y_i^{(4)} + \frac{h^{(5)}}{60}y^{(6)}(\xi_i) \quad (24)$$

Eliminating $y^{(4)}$ from eq (21) and (24), we get

$$S_i = \frac{2}{h^2}\left[y_{i-1} - 2y_i + y_{i+1}\right] - \frac{1}{2h}\left[F_{i+1} - F_{i-1}\right] + \frac{h^{(4)}}{360}y^{(6)}(\xi)$$

By a similar procedure, we get

$$S_{i-1} = \frac{1}{2h^2}\left[-23y_{i-1} + 16y_i + 7y_{i+1}\right] - \frac{1}{h}\left[6F_{i-1} + 8F_i + F_{i+1}\right] + \frac{h^{(4)}}{90}y^{(6)}(\xi_i)$$

$$S_{i-1} = \frac{1}{2h^2}\left[7y_{i-1} + 16y_i - 23y_{i+1}\right] + \frac{1}{h}\left[F_{i-1} + 8F_i + 6F_{i+1}\right] + \frac{h^{(4)}}{90}y^{(6)}(\xi_i)$$

and to the fourth order, we have

$$S_i = \frac{2}{h^2}\left[y_{i-1} - 2y_i + y_{i+1}\right] - \frac{1}{2h}\left[F_{i+1} - F_{i-1}\right] \quad (25)$$

$$S_{i-1} = \frac{1}{2h^2}\left[-23y_{i-1} + 16y_i + 7y_{i+1}\right] - \frac{1}{h}\left[6F_{i-1} + 8F_i + F_{i+1}\right] \quad (26)$$

$$S_{i+1} = \frac{1}{2h^2}\left[7y_{i-1} + 16y_i - 23y_{i+1}\right] + \frac{1}{h}\left[F_{i-1} + 8F_i + 6F_{i+1}\right] \quad (27)$$

From eq (25), putting the value of S_i in eq (20), we get

$$\frac{2}{h^2}\left[y_{i-1} - 2y_i + y_{i+1}\right] - \frac{1}{2h}\left[F_{i+1} - F_{i-1}\right] = f\left(x_i, y(x_i), F_i\right) \quad (28)$$

We have replaced now differential equation (3) by two difference-equations (19) and (28).

Now, consider 1st boundary condition i.e. at x=a, and denote the points $x = a,\ a+h,\ a+2h$ *by* $0, 1, 2$. the first difference-equation, we obtain from the boundary condition, is [7]

$$y_0 = \alpha \quad (29)$$

Now to obtain the second equation, we begin with differential equation at points 0 and1.

$$S_0 = f\left(x_0, y_0, F_0\right) \quad (30)$$

$$S_1 = f\left(x_1, y_1, F_1\right) \quad (31)$$

For $i = 1$, eq(26) implies

$$S_0 = \frac{1}{2h^2}\left[-23y_0 + 16y_1 + 7y_2\right] - \frac{1}{h}\left[6F_0 + 8F_1 + F_2\right] \quad (32)$$

Eq (25) implies

$$S_1 = \frac{2}{h^2}\left[y_0 - 2y_1 + y_2\right] - \frac{1}{2h}\left[F_2 - F_0\right] \quad (33)$$

Eq (19) implies

$$F_0 + 4F_1 + F_2 + \frac{3}{h}\left[y_0 - y_2\right] = 0 \quad (34)$$

Now, we have five equations from (30) to (34). We eliminate S_0, S_1, y_2, F_2 from these equations.

From eq (30) and (32), we have

$$f\left(x_0, y_0, F_0\right) = -\frac{23}{2h^2}y_0 + \frac{8}{h^2}y_1 + \frac{7}{2h^2}y_2 - \frac{6}{h}F_0 - \frac{8}{h}F_1 - \frac{1}{h}F_2 \quad (35)$$

From eq (31) and (33), we have

$$f\left(x_1, y_1, F_1\right) = \frac{2}{h^2}y_0 - \frac{4}{h^2}y_1 + \frac{2}{h^2}y_2 - \frac{1}{2h}F_2 + \frac{1}{2h}F_0 \quad (36)$$

From eq (34), we get

$$y_2 = y_0 + \frac{h}{3}F_0 + \frac{4h}{3}F_1 + \frac{h}{3}F_2 \quad (37)$$

Putting this value of y_2 in equations (35) and (36), we get

$$f\left(x_0, y_0, F_0\right) = -\frac{8}{h^2}y_0 + \frac{8}{h^2}y_1 - \frac{29}{6h}F_0 - \frac{10}{3h}F_1 + \frac{1}{6h}F_2 \quad (38)$$

$$f\left(x_1, y_1, F_1\right) = -\frac{4}{h^2}y_0 - \frac{4}{h^2}y_1 + \frac{7}{6h}F_0 + \frac{8}{3h}F_1 + \frac{1}{6h}F_2 \quad (39)$$

Subtracting eq (38) from eq (39), we get

$$f\left(x_1, y_1, F_1\right) - f\left(x_0, y_0, F_0\right) = \frac{12}{h^2}y_0 - \frac{12}{h^2}y_1 + \frac{6}{h}F_0 + \frac{6}{h}F_1 \quad (40)$$

In a similar approach, we derive the following two difference-equations for y and F at x=m. i.e. at the right boundary point [7]

$$y_m = \beta \quad (41)$$

$$f\left(x_m, y_m, F_m\right) - f\left(x_{m-1}, y_{m-1}, F_{m-1}\right) = \frac{12}{h^2}\left(y_{m-1} - y_m\right) + \frac{6}{h}\left(F_{m-1} + F_m\right) \quad (42)$$

Thus for each point we have two difference equations. If we write them all together, we have the following "Fourth Order Compact Scheme".

$$y_0 = \alpha$$
$$\frac{12}{h^2}y_0 - \frac{12}{h^2}y_1 + \frac{6}{h}F_0 + \frac{6}{h}F_1 = f(x_1, y_1, F_1) - f(x_0, y_0, F_0)$$
$$\frac{3}{h}y_{i-1} - \frac{3}{h}y_{i+1} + F_{i-1} + 4F_i + F_{i+1} = 0$$
$$\frac{2}{h^2}y_{i-1} - \frac{4}{h^2}y_i + \frac{2}{h^2}y_{i+1} + \frac{1}{2h}F_{i-1} - \frac{1}{2h}F_{i+1} = f(x_i, y_i, F_i)$$
$$y_m = \beta$$
$$\frac{12}{h^2}y_{m-1} - \frac{12}{h^2}y_m + \frac{6}{h}F_{m-1} + \frac{6}{h}F_m = f(x_m, y_m, F_m) - f(x_{m-1}, y_{m-1}, F_{m-1})$$

5. RESULTS AND DISCUSSION

Test Problem-1:

Consider the two points 2nd order nonlinear BVP of the form

$$y''(x) = 2y^3,\ 1 \le x \le 5,\ y(1) = \frac{1}{4},\ y(5) = \frac{1}{8}$$

and its exact solution is $y(x) = \frac{1}{x+3}$.

Table 1. Comparison of results.

x	Exact values	FDM results	FOCM results	NLSM results
1.00000000	0.25000000	0.25000000	0.25000000	0.25000000
2.00000000	0.20000000	0.15976405	0.20019856	0.20002568
3.00000000	0.16666667	0.12060503	0.16719549	0.16668811
4.00000000	0.14285714	0.11056759	0.14333433	0.14286864
5.00000000	0.12500000	0.12500000	0.12500000	0.12500000

The above Table shows that results of NLSM are more accurate to the exact solution as compared with the results of FDM and FOCM.

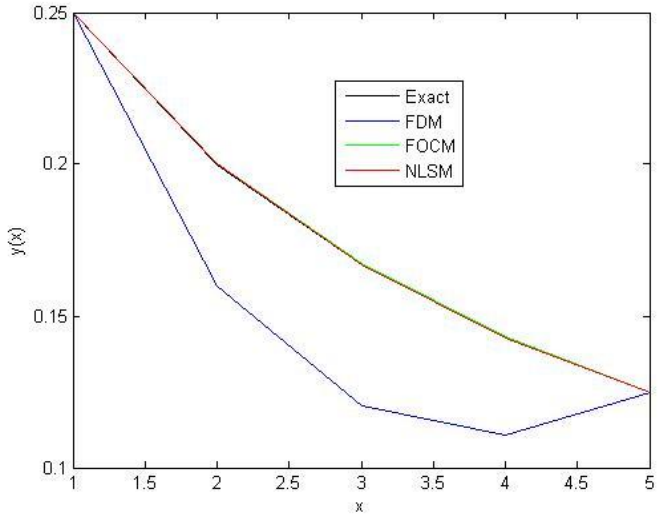

Fig. 1. Comparison of results.

Table 2. Comparison of absolute errors.

x	FDM results	FOCM results	NLSM results
1.00000000	0.00000000	0.00000000	0.00000000
2.00000000	0.04023595	0.00019856	0.00002568
3.00000000	0.04606164	0.00052882	0.00002144
4.00000000	0.03228955	0.00047719	0.00000115
5.00000000	0.00000000	0.00000000	0.00000000

The above table shows the comparison of absolute errors for FDM, FOCM and NLSM. It is found that an absolute error for NLSM is less as compared to the other two methods.

Test Problem-2:

Consider the two points 2nd order nonlinear BVP of the form $y''(x) = \frac{1}{2}y^3$, $1 \le x \le 2,\ y(1) = \frac{-2}{3},\ y(2) = -1$ and its actual solution is $y(x) = \frac{2}{x-4}$.

Table 3. Comparison of results.

x	Exact values	FDM results	FOCM results	NLSM results
1.00000000	-0.66666667	-0.66666667	-0.66666667	-0.66666667
1.25000000	-0.72727272	-0.78365013	-0.72732785	-0.72727455
1.50000000	-0.80000000	-0.88144644	-0.80010259	-0.80000299
1.75000000	-0.88888888	-0.95496986	-0.88999967	-0.88889178
2.00000000	-1.00000000	-1.00000000	-1.00000000	-1.00000000

The above table shows that results of NLSM are more accurate to the exact solution as compared with the results of FDM and FOCM.

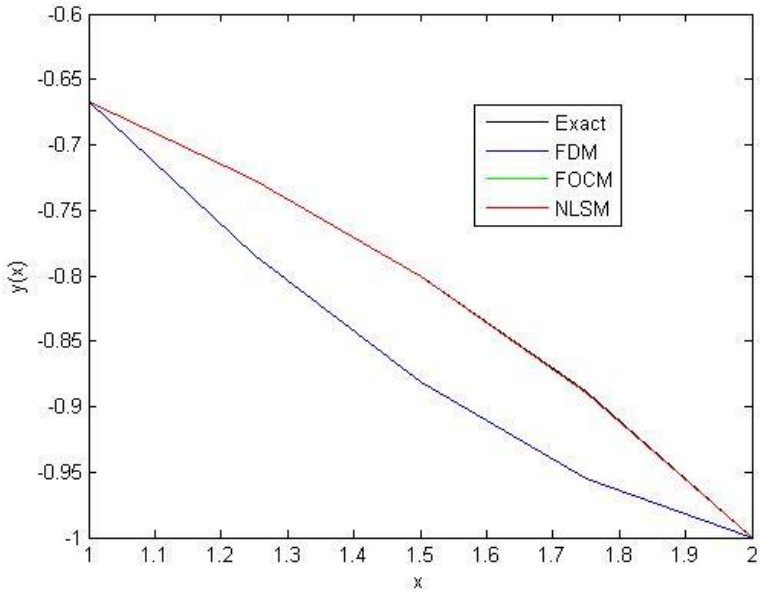

Fig. 2. Comparison of results.

Table 4. Comparison of absolute errors.

x	FDM results	FOCM results	NLSM results
1.00000000	0.00000000	0.00000000	0.00000000
1.25000000	0.05637741	0.00005513	0.00000183
1.50000000	0.08144644	0.00010259	0.00000299
1.75000000	0.06608098	0.00111079	0.00000029
2.00000000	0.00000000	0.00000000	0.00000000

The above table shows the comparison of absolute errors for FDM, FOCM and NLSM. It is found that an absolute error for NLSM is less as compared to the other two methods.

6. CONCLUSION

In this paper, we considered two different nonlinear 2^{nd} order two points BVPs for ordinary differential equations (ODEs) and solved these problems using NLSM, FDM and FOCM. All the above methods are appropriate for solving two points 2^{nd} order nonlinear BVPs, but it was found that NLSM is more accurate than FDM and FOCM.

7. REFERENCES

1. Roberts, S.M, & J.S. Shipman. *Two Point BVPs; Shooting Methods.* American Elsevier, New York, USA (1972).
2. Malathi, V. *Solving Boundary Value Problems for Ordinary Differential Equations Using Direct Integration and Shooting Techniques.* PhD thesis, Universiti Putra Malaysia, Malaysia (1999).
3. Ha, S.N. A nonlinear shooting method for two-point BVPs. *Computer and Mathematics Applications* 42: 1411-1420 (2001).
4. Auzinger. W., G. Kneisl, O. Koch, & E. Weinmuller. A collocation code for boundary value problems in ordinary differential equations. *Numerical Algorithms* 33: 27–39 (2003).
5. Attili, B.S. & M.I. Syam. Efficient shooting method for solving two point BVPs. *Chaos, Solitons and Fractals* 35: 895-903 (2008).
6. Faires, J.D. & R.L. Burden. *Numerical Analysis.* International Thomson Publishing Inc, New York, USA (1998).
7. Mustafa, H. *Fourth Order Compact Method for Nonlinear Second Order BVPs.* M.Phil thesis, University of Engineering and Technology, Lahore, Pakistan (2007).
8. Ahmad, M.O. An *Exploration of Compact Finite Difference-methods for Numerical Solution of PDE.* PhD thesis, University of Western, Ontario, Canada (1997).
9. Kreiss, H.O. *Methods for the Approximate Solution of Time Dependent Problems. GARP* Report No. 13 (1975).
10. Orszag, S.A. & M. Israeli. Numerical simulation of viscous incompressible flows. *Annual Reviews Inc* 6: 281-318 (1974).
11. Richard, S.H. & D.H. Rudy. The role of diagonal dominance and cell Reynolds number in implicit difference methods for fluid mechanics problems. *Journal of Computational Physics* 16: 304-310 (1974).
12. Leventhal, S.H. & M. Ciment. A note on the operator compact implicit method for the wave equation. *Mathematics of Computation* 32(1): 143-147 (1978).
13. Pettigrew, M.F. & H. Rasmussen. A compact method for second order boundary value on neon uniform gaids. *Computer and Mathematics Applications* 31: 1-16 (1996).
14. Schilling, R.J. & S.L. Harries. *Applied Numerical Methods for Engineers.* Thomson Business Information India, Bangalore, India (2006).
15. Sastry, S.S. *Introductory Methods of Numerical Analysis.* Prentice Hall of India, New Delhi, India (2003).

Proceedings of the Pakistan Academy of Sciences 52 (2): 159-168 (2015)

ISSN: 0377 - 2969 (print), 2306 - 1448 (online)

Pakistan Academy of Sciences

Research Article

Awaran, Pakistan, Earthquake of Mw 7.7 in Makran Accretionary Zone, 24 September 2013: Preliminary Seismotectonic Investigations

MonaLisa[1*], and M. Qasim Jan[2, 3]

[1]Department of Earth Sciences, Quaid-i-Azam University, Islamabad, Pakistan
[2]National Centre of Excellence in Geology, University of Peshawar, Peshawar, Pakistan
[3]COMSTECH, Islamabad, Pakistan

Abstract: A large part of Balochistan in southwest Pakistan was devastated by an earthquake of magnitude Mw 7.7 and focal depth of 10 km on 24 September, 2013. Located in the Makran Accretionary Zone, the Awaran Earthquake was followed by a major aftershock of Mw 7.2 that occurred 90 km NNE of Awaran on 28 September, 2013. The earthquake caused widespread destruction in the remote and poorly accessible area, with death toll exceeding 825. An intensity of IIX on MMI scale is assigned to the epicenter of the main shock using the information from the print and electronic media and some field studies. The damage to property and loss of lives occurred due to non-engineered construction of structures within 100 km of the main shock. Fault-plane solutions of both the main event and its largest aftershock, and the distribution of aftershocks suggest that the NNE-SSW-trending left-lateral strike-slip Awaran Fault is currently active. This is also supported by the analysis of more aftershocks fault-plane solutions. The formation of a mud volcano is the probable cause of the emergence of a 200 x 100 m island off the coast of Gawadar a few hours after the main shock. On the one hand, this event has released high seismic energy in NE-SW direction along the Chaman Fault Zone and Makran Subduction Zone, and on the other it has increased the tectonic stresses in the northern and SE directions, which may cause higher seismicity in future.

Keywords: Awaran Earthquake, Makran Accretionary Zone, Awaran Fault, focal mechanism solutions, intensity map, island emergence

1. INTRODUCTION

A devastating earthquake of magnitude Mw 7.7 (according to United Sates Geological Survey (USGS) and Pakistan Meteorological Department (PMD)) took place in the evening (16:29:50 Pakistan Standard Time (PST)) of 24 September 2013 in Balochistan, southwestern Pakistan. Located about 66 km NNE of Awaran this earthquake took the lives of 825 people; several hundred people were injured. The main shock was followed by a major aftershock of Mw 7.2 (PMD) or Mw 6.8 (USGS), which occurred about 90 km NNE of Awaran (Fig. 1, 2) at 12:34:13 PST on 28 September, 2013. This aftershock, along with nine others, increased the death toll by at least 22 people in the epicentral region. The Awaran District was damaged drastically where 80% homes either collapsed or were seriously damaged. Minor damage, including collapse of a few buildings, was reported from Karachi and Hyderabad according to local media reports. The Earthquake was felt in Rawalpindi/ Islamabad, Larkana, Lahore, and also in some parts of India, Oman and United Arab Emirates.

The northward subduction of the Arabian Plate beneath the Eurasian Plate and the northward left-lateral motion of the Indian Plate with respect to Eurasian Plate are the main causes of seismicity in the region. The most active tectonic structure within the area is the Chaman Transform Fault Zone (Fig. 1). This paper does not go into the details of regional tectonics; it describes the seismicity and seismotectonics of the area in the vicinity of the

Received, April 2015; Accepted, May 2015
*Corresponding author: MonaLisa; Email: lisa_qau@yahoo.com

Awaran earthquake. Fault-plane solutions of the main event, its largest aftershock on 28 September, 2013, and the aftershock distribution suggest that the NNE-SSW-trending left-lateral strike-slip Awaran Fault (AF), first identified by Quadri and Quadri [1] and Kazmi [2], as shown in Fig. 2, is currently active. However, this assumption is based on limited seismicity data; more fault-plane solutions are needed to understand better the active tectonics and related seismicity level in the region.

2. SEISMOTECTONICS

The active tectonic features in the southwestern part of Pakistan are referred to by Kazmi and Rana [3] and Kazmi and Jan [4] as the Makran-Accretionary Zone (MAZ). Shallow crustal depths (15-20 km), oblique-strike-slip movement in its northern parts and deepening inland to about 80 km, are indicated by various authors [2-5]. Regionally speaking, the active tectonics in MAZ is due to northward sliding of Indian plate with respect to Eurasian plate in the east and northward subduction of Arabian plate beneath the Eurasian plate in the west (Fig. 1, 2). The structures formed due to these motions are NS to NE-SW-striking, and are initially accommodated along the Chaman Fault System. The southern parts of this fault system, referred to as the Ghazaband and Ornach-Nal Faults [6], are the most active tectonic features in the area. The MAZ is bound by left-lateral Ornach-Nal Transform Fault in its east, together with Nai Rud, Ras Malan and Aghor Faults which strike in NE-SW direction and join the Ornach Fault. According to Lawrence et al [7], these strike-slip faults, parallel or subparallel to the Ornach-Nal Fault, form a dense network of fractures (Fig. 1, 2). Southward this zone widens and undergoes transition from a transform to a convergence regime and the structures gradually swing from north-south to southwest and then towards west [4].

Several smaller faults, e.g., Hudishi and Awaran Faults, with signs of recent activity manifested as fault scarps in Recent to Sub-Recent alluvial deposits, have been mapped earlier [2, 5, 8]. However, detailed work is required to locate the causative fault of the Awaran Earthquake. Seismically, this part of Pakistan is active, but a small number of damaging earthquakes has been documented in the recent past. The most important of these are the 1945 (M 8.0) subduction-zone earthquake [9] and 1947 (M 7.3) earthquake [10] having offshore epicenters. The 1945 event, which severely damaged coastal towns and caused a vertical displacement of 4.5 m on the shore, generated a tsunami, and produced upheaval of the sea floor in the form of a row of small offshore islands or mud volcanoes as happened with the Awaran Earthquake [10]. The limited instrumental documentation of seismicity since 1970 shows that shallow depth earthquakes with magnitude range of 3-7 M (Fig. 3) have occurred inland.

3. SEISMIC OBSERVATIONS FOR THE 24 SEPTEMBER 2013 EARTHQUAKE

The local seismic observatory (PMD) provided the following source parameters of the main shock:

Date:	24.09.2013
Time:	15:29:50 PST
Magnitude:	M_w 7.7
Epicentral location:	27.09° N, 65.61° E
Focal depth:	10 km

According to the location provided by the PMD, the main event occurred in an area of MAZ characterized by complex tectonic features dominated by several active thrust as well as oblique strike-slip faults (Fig. 2, 3). The dominant of these faults are Ornach-Nal, Awaran and Hudishi, which are left-lateral strike-slip, faults trending NNE. The main shock was followed by a major aftershock (6.8 M_w according to USGS, and 7.2 M_w according to PMD), which occurred 30 km NNE of the main shock (the main shock resulted in the death of 359 people in the epicentral area). PMD data show the occurrence of 6 foreshocks and 10 aftershocks till 28 September, 2013. The distribution of these foreshocks and aftershocks (Fig. 3) shows some cluster along the Ornach-Nal Fault. However, they are mostly located between the Awaran and

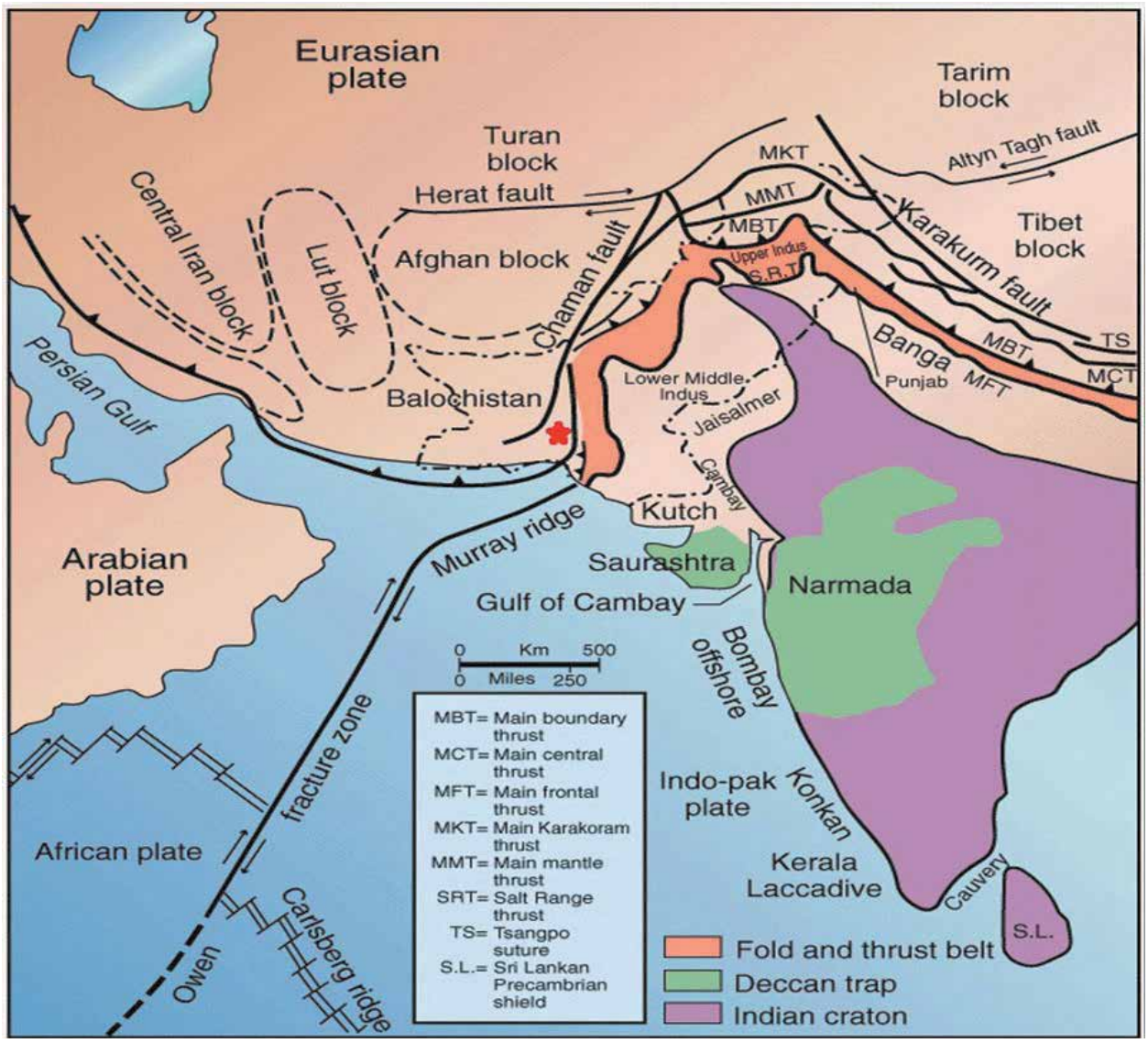

Fig. 1. Tectonic setting of Pakistan and adjacent areas. Location of the 24 September, 2013 Awaran Earthquake and the Chaman Transform Fault are also shown. Modified from Quadri & Quadri [1].

Hudishi faults in a NNE-SSW direction (Fig. 2, 3) suggesting that more than one fault were activated. Most of the foreshocks and aftershocks are at a depth of 10 km. Thus both the aftershocks pattern and depth distribution indicate the activation of shallow surface features, including the Awaran Fault.

4. FOCAL MECHANISM SOLUTIONS (FMS)

The first arrivals of the main event (10 km depth), using the available data of the local as well as international seismic observatories, e.g., PMD, International Seismological Centre and USGS, were used for FMS. The beach ball diagrams were then plotted using the computer programs of AZMTAK and PMAN [11] as shown in Fig. 4. Structurally, this earthquake is surrounded by a number of left-lateral strike-slip faults (Fig. 2). The SSW-NNE-oriented sinistral strike-slip FMS (Table 1) is consistent with the orientation of already existing prominent faults, e.g., the Ornach-Nal Fault, Awaran Fault and Hudishi Fault, along with the major trend of the aftershocks of the main event plotted for the purpose (Fig. 2, 3). Thus, based upon the strike and depth of these faults, the nodal plane striking

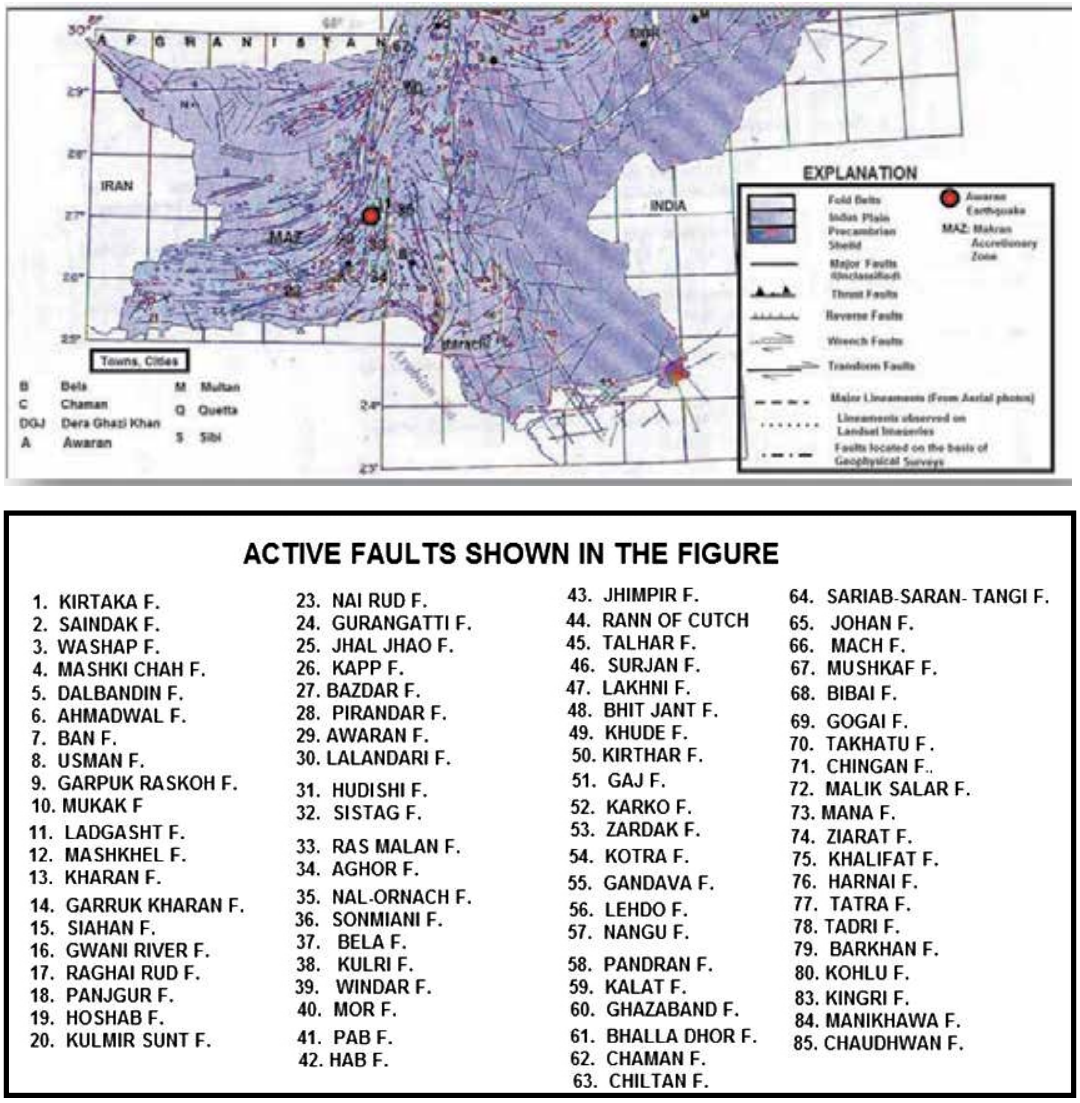

Fig. 2. Active Faults in south-western Pakistan. The 24 September, 2013 Awaran Earthquake and the Chaman (No. 62), Ghazaband (No. 60), Ornach-Nal (No. 35), Aghor (No. 34), Ras Malan (No. 33), Hudishi (No. 31), Awaran (No. 29), NaiRud (No. 23) faults are also shown. Updated from Kazmi and Rana [3].

Table 1. Focal Mechanism Solution (FMS) parameters of 24 September, 2013 Awaran Earthquake.

FMS No.	Type of FMS	Fault Plane (FP)		Auxiliary Plane (AP)		P-Axis		T-Axis	
		Strike	Dip	Strike	Dip	Strike	Plunge	Strike	Plunge
1	LLSS	231°	70°NE	141°0	90°NW	173°	14°	94°	14°

NE-SW and dipping NW is considered to be the rupture plane (Fig. 4, 5). The location and FMS of this earthquake were consistent with rupture within the Eurasian Plate above the Makran Subduction Zone (Fig. 5); yellow filled circles are showing the locations of epicentres of the Awaran Earthquake and its aftershocks, where the Arabian Plate is subducting beneath the Eurasian Plate [12].

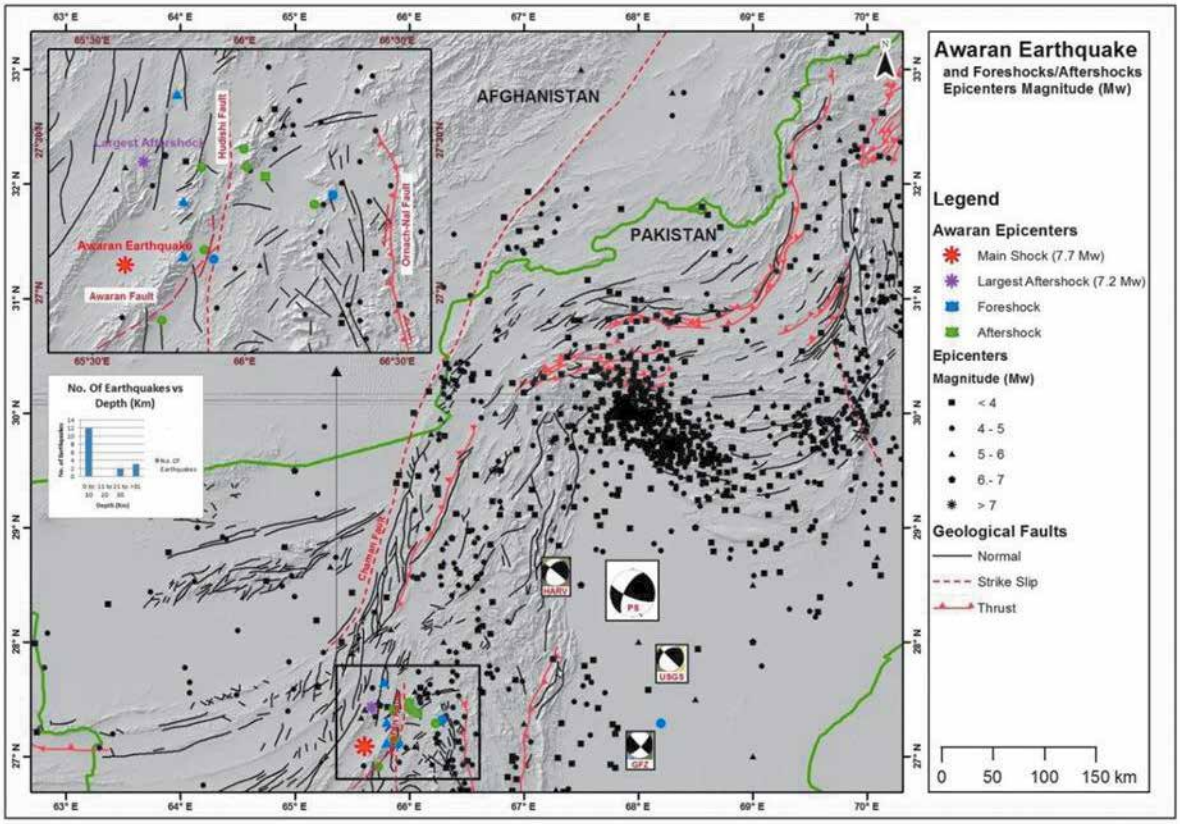

Fig. 3. Map of the study area showing seismicity, active faults, and distribution of foreshocks and aftershocks of the Awaran Earthquake. Focal-mechanism solutions of the main shock from all available sources, i.e., HRV, Harvard, PS, Present Study, USGS, GFZ, Geo Forschungs Zentrum Potsdam, are also shown.

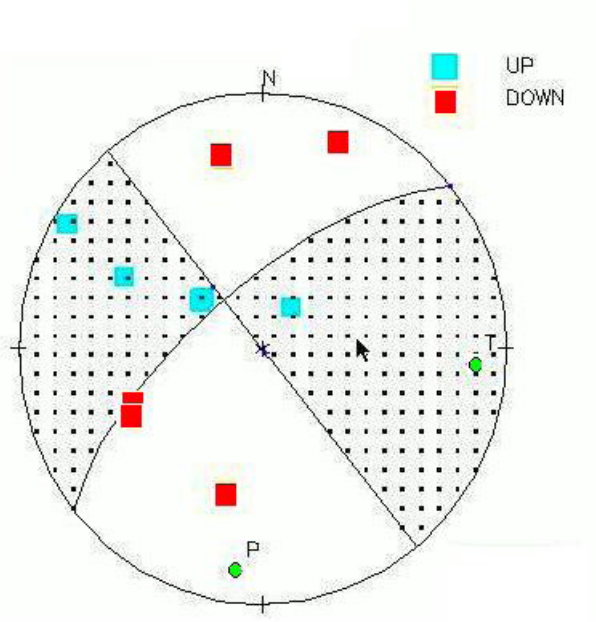

Fig. 4. Focal mechanism solution (FMS) of 24 September, 2013 Awaran Earthquake.

5. INTENSITY AND DAMAGE DISTRIBUTION

The September 24, 2013 Awaran Earthquake was one of the most damaging earthquakes to have occurred in the southwestern part of Pakistan (i.e., Balochistan). Balochistan is the largest but least populous province of Pakistan, with a population of just under eight million. The Balochistan Provincial Disaster Management Authority (PMDA) reported that the main earthquake caused 359 deaths and affected 185,000 people. However, "moderate" to "rather strong" shaking (levels 4 and 5 on the 12-point Mercalli Intensity Scale) were estimated by the USGS across the heavily populated Indus River valley, having a population of some 140 million people. The earthquake was originally rated with a magnitude of Mw 7.4 on the Richter scale, later on upgraded to 7.8, but then revised

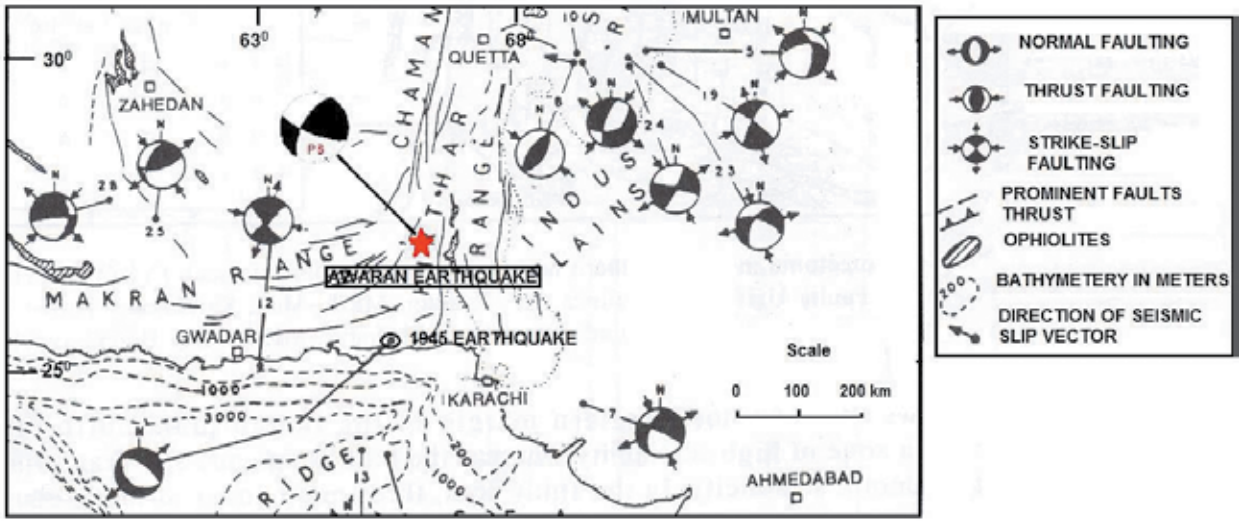

Fig. 5. Map showing the major faults and focal mechanism solutions (FMS) of selected events, including 24 September, 2013 Awaran Earthquake, in the Makran Accretionary Zone and adjacent areas. Dark area in FMS plots shows compression and blank area dilatation [13].

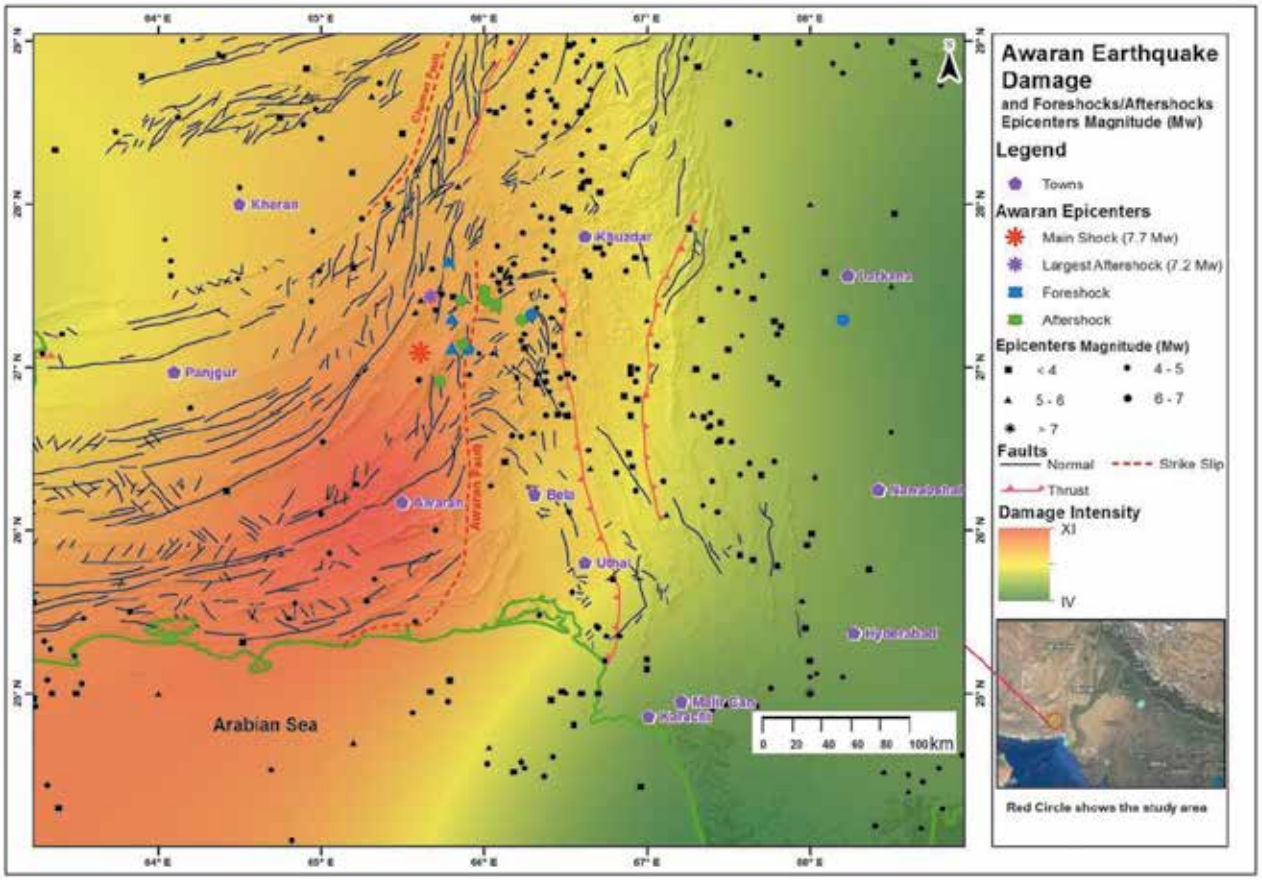

Fig. 6. Intensity map of 24 September, 2013, Awaran Earthquake prepared in the present study.

to 7.7. The destruction caused by this earthquake covered an area of about 100 km radius, but the most severe damage was observed within 30 km of the epicenter. The Awaran Earthquake and its aftershocks, especially its largest aftershock (M_w 7.2 by PMD) of 28 September, 2013 triggered some landslides also which resulted in additional damage. On the basis of information obtained from the print and electronic media, an intensity of MM IIX has been assigned at the epicenter of the main shock.

The intensity map of the Awaran Earthquake, prepared in the current study using the damage/ destruction information from the print media and local sources (Fig. 6), shows the intensity within 100 km area of the main shock. One possibility of this heavy damage is the very shallow focal depth of the main shock: 10 km according to PMD. The Awaran District, where > 60,000 people are living within 50 km of the epicenter, is the worst affected area, with over 80 per cent of mud houses reportedly damaged [14]. Majority of the construction in the district is highly vulnerable to earthquake shaking and there are only a few resistant structures. The vulnerable structures are of adobe block and unreinforced brick masonry construction. Other districts affected by the Earthquake include Kech, Gwadar, Panjgur and Khuzdar. The Government of Balochistan, Federal Government, National Disaster Management Authority, and the armed forces of Pakistan provided rescue and immediate relief services (Fig. 7d). Many NGOs have also supported the relief work, providing health care services, shelter, and food items [14], but their efforts were being hampered by the remoteness of the affected areas and insecurity. Some of the damage in Awaran can be seen in the photographs displayed in Fig. 7a–7d.

6. ISLAND EMERGENCE

Close to Pakistan-Iranian political border, an island, about 200 m long and 100 m wide, emerged near Gawadar [1]. Two smaller islands appeared soon after the first island near Ormara town, with diameters of about 10-13 m and a height of <1 m (Fig. 8a, 8b). These islands are mud volcanoes, which are commonly attributed to seismic activity although a number of other factors may also have contributed to their eruption [15]. Balochistan contains over 70 active mud volcanoes [16]. Along with the ten mud volcanoes near the epicentral location of the Awaran main shock, hundreds of meters below the sea floor, MAZ is rich in gas hydrates (sometimes called frozen methane gas, resembling ice). The seabed near the Makran coast has vast deposits of gas hydrates, or frozen gas having large methane content [17]. These hydrates may be explored for commercial purpose, using several safe and cost-efficient technologies available in many countries, including US, Japan, Canada and India. Therefore a survey of the reserves may be carried out immediately. An island emerges within the water or on the sea surface whenever an earthquake occurs in the nearby area. Such islands also accompanied the 1945 Makran (M 8.1) earthquake but were eroded away within a year (as happened in case of AE). These islands emit flammable gas, according to print media.

7. DISCUSSION

The western part of Pakistan and southeastern Afghanistan are experiencing comparatively high velocity left-lateral strike-slip movement along the Chaman Fault. Shallow and destructives earthquakes are commonly related to strike-slip, reverse-slip and oblique-slip faults. In 1505, a segment of the Chaman Fault system near Kabul, Afghanistan ruptured in an earthquake estimated as Ms 7.3, causing widespread destruction in Kabul city and surrounding villages [18]. In the same region, the more recent 17 April, 2013 Mw 7.8 Khash (Iran) Earthquake (near Pakistan-Iran border; 35 deaths), and 28 October, 2008 Mw 6.4 Ziarat Earthquake [19] and 30 May 1935, M7.6 Quetta earthquake (within the Sulaiman Range) killing 300, and 30,000 - 60,000 people, respectively [18], have been significant events. Off the south coast of Pakistan and southeast coast of Iran, the MSZ is the present-day surface expression of active subduction of the

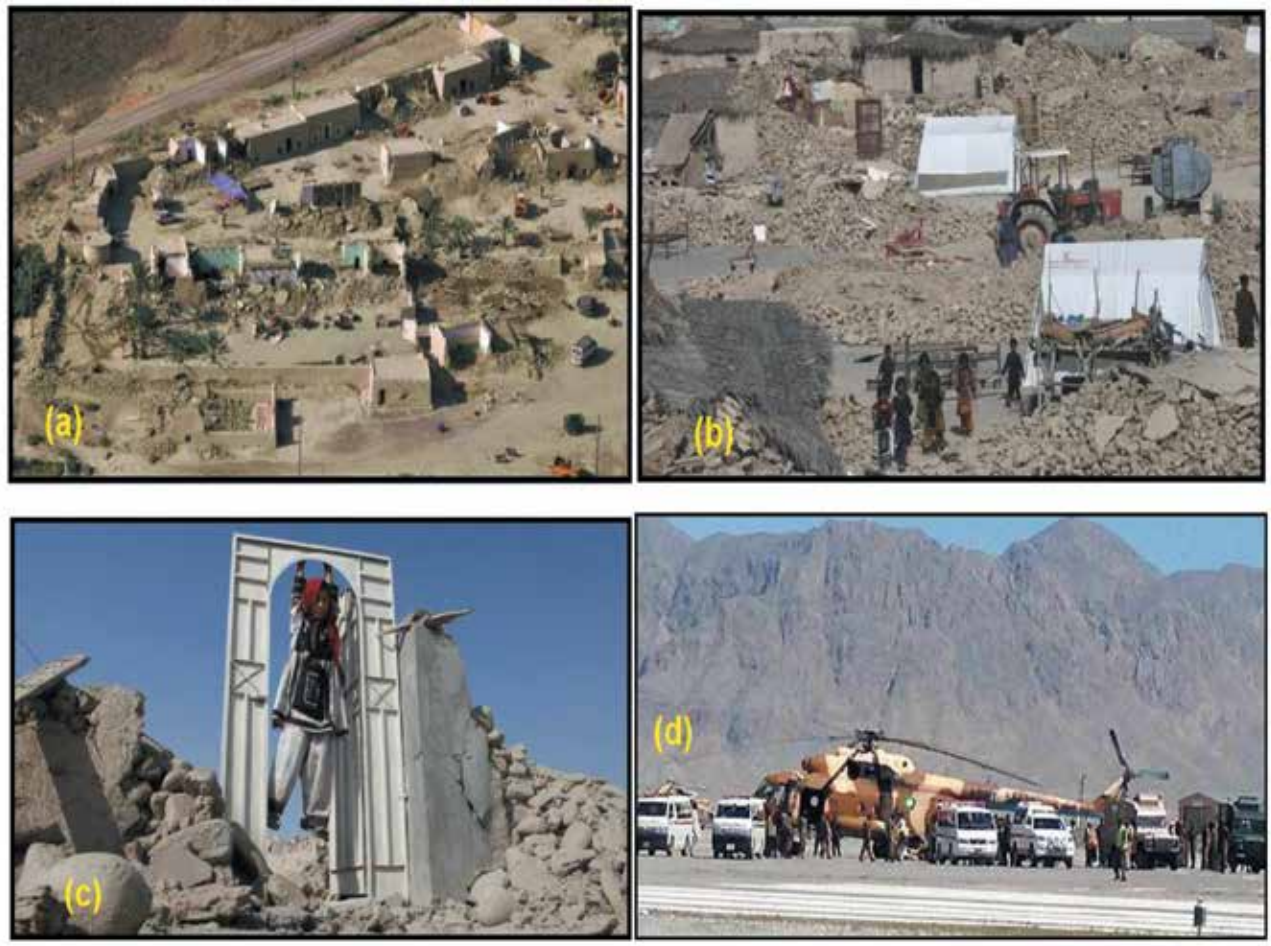

Fig. 7: (a) to (c) Damage and destruction in Awaran, Balochistan; **(d)** Rescue operation by the Pakistan Army.

Fig. 8a and 8b. The Island emerged after 24 September, 2013 Awaran Earthquake (courtesy of NASA and local TV channel). Yellow filled circles in **(a)** represent the location of Awaran Earthquake and its aftershocks, whereas **(b)** shows the offshore island.

oceanic leading edge of the Arabia Plate beneath the continental Eurasia Plate, with a convergence rate of approximately 20 mm/yr [18, 19]. Although the MSZ has a relatively slow convergence rate, it has produced large devastating earthquakes and tsunamis. For example, the November 27, 1945 M 8.1 mega-thrust earthquake produced a tsunami within the Gulf of Oman and Arabia Sea, killing more than 4,000 people. Northwest of this active subduction zone, collision of the Arabia and Eurasia plates forms the approximately 1,500-km long fold and thrust belt of the Zagros Mountains, which crosses the whole of southwestern Iran and extends into northeastern Iraq [20].

Based on this preliminary seismotectonic study of the 24 September, 2013 Awaran Earthquake, it is hypothesized that the MSZ is seismically active, and the Awaran Fault is probably the source of this event. The epicenter of the 1945 earthquake is also located in this region. This 8.1 magnitude earthquake was also of shallow focal depth. We further conclude that the Awaran Fault, which trends NNE-SSW, extends for about 40-50 km from the epicentral location. This is evident by the aftershock pattern, depth distribution and the focal mechanism (Fig. 3, 4, 5). Previous workers, such as [10, 21], have indicated the possibility of a large earthquake in MAZ after 1945 earthquake. A long awaited large earthquake in this area is postulated immediately west of 1945 earthquake site on the basis of recent seismicity pattern. Some parts of this area are also presenting a diffused distribution of earthquakes which cannot be explained at present but can be related with shallow to steeply dipping faults [10]. More detailed integration of the available seismological, geophysical and geological data is required to develop a seismotectonic model for the area.

An intensity of IIX (MMI scale) is observed using the information of damages and destruction from print media (Fig. 6). The damages to construction and loss of lives occurred due to poor construction of structures within 100 km of the main shock (Fig. 7a–7d). Over 80% of Awaran has been completely destroyed, and this damage was escalated by the occurrence of its largest aftershock (M_w 7.2 by PMD) of 28 September, 2013.

The emergence of an off shore island about 200 m long and 100 m wide a few hours after the main shock, is the result of the formation of a mud volcano. Two more, smaller islands appeared soon after the first island. This is basically a combination of mud, sand and water that gushed to the surface after the earthquake. Liquefaction of sand and mud layers may take place after an earthquake, but it takes a strong one to produce an island such as the island off Gawadar [22]. The other possibility can be a rotational landslide, which moves along a rupture surface that is curved or concave (Fig. 8a, 8b). However, more evidence is required to support this assumption. In fact, the causes of the eruption of mud volcanoes, despite their triggering by earthquakes, are yet to be clearly understood [15], Further, the emission of methane gas is not an exception as the energy released by the seismic movement of these faults in MSZ activates inflammable gases in the seabed.

8. CONCLUSIONS

The Awaran Earthquake event has released high seismic energy in NE-SW direction along the Chaman Fault zone and MSZ; however it has increased the tectonic stresses in the northern and SE directions, which may cause high seismicity in future. It is also worth noting that this big event triggered many off shoots and splays of the larger faults (data to be presented separately). Thus, the possibility of large earthquakes, in future, causing serious damage in the cities situated in the area, cannot be excluded. It is, therefore, suggested that an effective National Seismic Hazard Study program should be perused with emphasis on precise delineation of high risk zones.

9. ACKNOWLEDGEMENTS

The manuscript benefited from useful suggestions of three anonymous reviewers and the Editor-in-Chief (Dr. A. Rashid). We would like to thank the Pakistan Academy of Sciences, Pakistan Science Foundation and Higher Education Commission for financial support to our research projects in southeastern and northern Pakistan.

10. REFERENCES

1. Quadri, V.N. & S.M. Quadri. Cretaceous of Pakistan, India should hold more promise. *Oil and Gas Journal* 6: 1-4 (1998).
2. Kazmi, A.H. Active fault systems in Pakistan. In: *Geodynamics of Pakistan*. Farah, A. & K.A. DeJong (Ed.). Geological Survery of Pakistan, Quetta, p. 285-294 (1979).
3. Kazmi, A.H. & R.A. Rana. *Tectonic Map of Pakistan. Scale1:2,000,000*. Geological Survey of Pakistan, Quetta (1982).
4. Kazmi, A.H. & M.Q. Jan. *Geology and Tectonics of Pakistan*. Graphic Publishers, Karachi, Pakistan, 571 pp. (1997).
5. Nakata, T. Active faults of the Himalaya of India and Nepal. In: *Tectonics of the Western Himalayas*. Malinconico, L.L. & R.J. Lilie (Ed.). Geological Society American Special Paper 232, p. 243-264 (1989).
6. Lawrence, R.D., S.H. Khan & T. Nakata. Chaman fault, Pakistan-Afghanistan. *Annales Tectonicae Supplement (VI)*: 196-223 (1992).
7. Qureshi, M.J., M.A. Tariq & Q.Z. Abid. *Geological Map of Pakistan (1:1, 000, 000*). Geological Survey Pakistan, Quetta (1993).
8. Hunting Survey Corporation. *Reconnaissance Geology of Part of West Pakistan: maps 1:250,000. A Colombo Plan Cooperative Project:* Toronto, Ontario, Maracle Press, 550 pp. (1960).
9. Byrne, D.E., L.R. Sykes & D.M. Davis. Great thrust earthquakes and aseismic slip along the pate boundary of the Makran subduction zone. *Journal of Geophysical Research* 97: 449-478 (1992).
10. Quittmeyer, R.C. Seismicity variations in the Makran region of Pakistan and Iran: Relation to great earthquakes. *Pure and Applied Geophysics* 117(6): 1212-1228 (1979).
11. Suetsugu, D. Source mechanism practice. In: *Training Course in Seismology and Earthquake Engineering II.* Japan International Cooperation Agency (JICA), Ibaraki-ken 305, Japan, p. 13-48 (1997).
12. Nowroozi, A.A. Focal mechanism of earthquakes in Persia, Turkey, West Pakistan, and Afghanistan and Plate Tectonics of the Middle East. *Bulletin of the Seismological Society of America* (62): 823-850 (1972).
13. Verma, R.K., M. Mukhopadhyay & A.K. Bhanja. Seismotectonics of Hindukush and Baluchistan arc. *Tectonophysics* 66: 301-322 (1980).
14. www.nrsp.org.pk (30 September 2014)
15. Manga, M., M. Brumm & M.L. Rudolph. Earthquake triggering of mud volcanoes. *Marine & Petroleum Geology* 26: 1785-1798 (2009).
16. Kassi, A.M., S.D. Khan, H. Bayaraktar & A.J. Kasi. Newly discovered mud volcanoes in the Coastal Belt of Makran, Pakistan—tectonic implications. *Arabian Journal of Geosciences* 7(11): 4899-4909 (2013).
17. http://www.bbc.co.uk/news/world-asia (30 September, 2014).
18. Ambraseys, N.N. & R. Bilhalm. Earthquakes and associated deformation in northern Baluchistan 1892-2001. *Bulletin Seismological Society America* 93: 1575-1605 (2003).
19. MonaLisa & M.Q. Jan. Geoseismological study of the Ziarat (Balochistan) Earthquake (Doublet?) of October 28, 2008. *Current Science* 98(1): 50-57 (2010).
20. www.projectdisaster.com
21. Avouac, J.P., F. Ayoub, S. Wei, J.P. Ampuero, L. Meng, S. Leprince., R. Jolivet, Z. Duputel & D. Helmberger. The 2013, Mw 7.7 Balochistan Earthquake, energetic strike-slip reactivation of a thrustfault. *Earth and Planetary Science Letters* 391(1): 128-134 (2014).
22. www.thewatchers.adorraeli.com (30 September 2014).

Proceedings of the Pakistan Academy of Sciences

Instructions for Authors

Aims and Scope: *Proceedings of the Pakistan Academy of Sciences* is official journal of the Academy, published quarterly, in English. This open access journal publishes research papers in *Engineering Sciences & Technology, Life Sciences, Medical Sciences, and Physical Sciences*. State-of-the-art reviews (~20 pages, supported by recent references) summarizing R&D in a particular area of science, especially in the context of Pakistan, and suggesting further R&D are also considered. Manuscripts undergo double-blind review. Authors are not required to be Fellows or Members of the *Pakistan Academy of Sciences* or citizens of Pakistan.

Manuscript Format

Manuscript may contain **Abstract, Keywords, INTRODUCTION, MATERIALS AND METHODS, RESULTS, DISCUSSION (or RESULTS AND DISCUSSION), CONCLUSIONS, ACKNOWLEDGEMENTS and REFERENCES** *and any other information that the author(s) may consider necessary.* The Manuscript sections must be numbered, i.e., **1. INTRODUCTION, 2. MATERIALS AND METHODS,** and so on.

Manuscripts, in *Times New Roman*, 1.5-spaced (but single-space the Tables), with line numbering and one-inch margins on all sides on A-4 size paper, should not exceed 20 pages including Tables and Figures. Number manuscript pages throughout. The text (in **Font Size 11,** except for the sections mentioned in **Font Size 10)** must be typed in a single column across the paper width. All Tables and Figures must be placed after the text, i.e., after REFERENCES section.

Title Page: For Online submission of the manuscript, Title Page should not be included. However, for submitting as an email attachment, the title page must be as under:

(a) **Title** of the article **(**Capitalize initial letter of each main word; font size 16; **bold**), max 160 characters (no abbreviations or acronyms), depicting article's contents; (b) Author' first name, middle initial and last name (font size 12, **bold**), and professional affiliation (i.e., each author's Department, Institution, Mailing address and Email; but no position titles) (font size 12); (c) Indicate the corresponding author with *; (d) **Short running title**, max 50 characters (font size 10).The **next Page** should start with **Title** of the Article, followed by entire manuscript. **Headings and Subheadings** (font size 11): All flush left

LEVEL-1: **ALL CAPITAL LETTERS; bold**

Level-2: **Capitalize each main word; bold**

Level-3: Capitalize each main word; Bold, Italic

Level-4: *Run-in head*; *Italics*, *in the normal paragraph position. Capitalize the initial word only and end in a colon (i.e., **:**)*

Abstract (font size 10; max 250 words)**:** Must be self-explanatory**,** stating rationale, objective(s), methodology, main results and conclusions of the study. Abbreviations, if used, must be defined on first mention in the Abstract as well as in the main text. Abstract of review articles may have variable format.

Keywords (font size 10)**:** Three to eight keywords**,** depicting the article.

For Online submission:

- **Separate submission of Abstract along with Title is required**
- **Author(s)' names and affiliations should not be included in the manuscript or the Abstract**

INTRODUCTION: Provide a clear and concise statement of the problem, citing relevant recent literature, and objectives of the investigation.

MATERIALS AND METHODS: Provide an adequate account of the procedures or experimental details, including statistical tests (if any), in a concise manner but sufficient enough to replicate the study.

RESULTS: Be clear and concise with the help of appropriate Tables, Figures and other illustrations. Data should not be repeated in Tables and Figures, but must be supported with statistics.

DISCUSSION: Provide interpretation of the RESULTS in the light of previous relevant studies, citing published references.

ACKNOWLEDGEMENTS (font size 10)**:** In a brief statement, acknowledge financial support and other assistance.

REFERENCES (font size 10)**:** Cite references in the text **by number only** in **square brackets**, e.g. "Brown et al [2]

reported ..." or "... as previously described [3, 6–8]", and list them in REFERENCES section, in the order of citation in the text, Tables and Figures (not alphabetically). Only published (and accepted for publication) journal articles, books, and book chapters qualify for REFERENCES.

List of REFERENCES must be prepared as under:

a. **Journal Articles** *(Name of journals must be stated in full)*

1. Golding, I. Real time kinetics of gene activity in individual bacteria. *Cell* 123**:** 1025–1036 (2005).
2. Bialek, W. & S. Setayeshgar. Cooperative sensitivity and noise in biochemical signaling. *Physical Review Letters* 100**:** 258–263 (2008).
3. Kay, R.R. & C.R.L. Thompson. Forming patterns in development without morphogen gradients: differentiation and sorting. *Cold Spring Harbor Perspectives in Biology* 1: doi: 10.1101/cshperspect.a001503 (2009).

b. **Books**

4. Luellen, W.R. *Fine-Tuning Your Writing*. Wise Owl Publishing Company, Madison, WI, USA (2001).
5. Alon, U. & D.N. Wegner (Ed.). *An Introduction to Systems Biology: Design Principles of Biological Circuits*. Chapman & Hall/CRC, Boca Raton, FL, USA (2006).

c. **Book Chapters**

6. Sarnthein, M.S. & J.D. Stanford. Basal sauropodomorpha: historical and recent phylogenetic developments. In: *The Northern North Atlantic: A Changing Environment.* Schafer, P.R. & W. Schluter (Ed.), Springer, Berlin, Germany, p. 365–410 (2000).
7. Smolen, J.E. & L.A. Boxer. Functions of Europhiles. In: *Hematology, 4th ed*. Williams, W.J., E. Butler & M.A. Litchman (Ed.), McGraw Hill, New York, USA, p. 103–101 (1991).

Tables, with concise but self-explanatory headings must be numbered according to the order of citation (like **Table 1**, **Table 2**). Round off data to the nearest three significant digits. Provide essential explanatory footnotes, with superscript letters or symbols keyed to the data. Do not use vertical or horizontal lines, except for separating column heads from the data and at end of the Table.

Figures may be printed in two sizes: column width of 8.0 cm or page width of 16.5 cm; number them as **Fig. 1**, **Fig. 2**, … in the order of citation in the text. Captions to Figures must be concise but self-explanatory. Laser printed line drawings are acceptable. Do not use lettering smaller than 9 points or unnecessarily large. Photographs must be of high quality. A scale bar should be provided on all photomicrographs.

Declaration: Provide a declaration that: (i) the results are original; (ii) the same material is neither published nor under consideration elsewhere; (iii) approval of all authors has been obtained; and, (iv) in case the article is accepted for publication, its copyright will be assigned to *Pakistan Academy of Sciences*. Authors must obtain permission to reproduce, where needed, copyrighted material from other sources and ensure that no copyrights are infringed upon.

Reviewers: Authors may suggest four relevant reviewers, two local and two from scientifically advanced countries.

Online Manuscript Submission:

Proceedings of the Pakistan Academy of Sciences is using a web-enabled online manuscript submission and review system, which offers authors the option to track the progress of manuscripts in real time.

For online submission, authors are required to register at website of the Academy (www.paspk.org) by clicking the "Journal and Publications" tab.

Manuscripts must be submitted in Microsoft Word (.doc or .docx format; **pdf** files not acceptable). Figures can be submitted in Word format, TIFF, GIF, JPEG, EPS, PPT.

NOTE: In case of online submission, authors are not required to submit the manuscript as email attachment.

In case of any difficulty while submitting your manuscript, please get in touch with:

Editor-in-Chief
Pakistan Academy of Sciences
3-Constitution Avenue, G-5/2, Islamabad, Pakistan
Email: editor@paspk.org
Tel: +92-51-920 7140
Website: www.paspk.org

Proceedings
OF THE PAKISTAN ACADEMY OF SCIENCES

CONTENTS

Volume 52, No. 2, June 2015 **Page**

Research Articles

Engineering Sciences

Life Sciences

Physical Sciences

PAKISTAN ACADEMY OF SCIENCES, ISLAMABAD, PAKISTAN
HEC Recognized, Category X; PM&DC Recognized